

Greybody Factors Hawking Radiation in Disguise



Jorge Escobedo

Master's thesis

Supervisor: Prof. Dr. Jan de Boer



University of Amsterdam
Institute for Theoretical Physics
Valckenierstraat 65
1018 XE Amsterdam
The Netherlands

August 2, 2008

To my parents, Lucy and Jorge

Abstract

This master's thesis deals with greybody factors of static and spherically symmetric black holes in asymptotically flat spacetimes, with emphasis on the high frequency limit. The first goal is to provide a pedagogical and thorough review of some recent developments in the study of these objects in a semiclassical context. The second goal is to motivate further investigation in this subject as a possible way to gain a better understanding of quantum gravity. We first review an important string theoretical result in the low frequency regime, which gave new insight into the microscopics of black holes. To perform the computations at high frequency, we use the monodromy technique, first introduced in this context by Motl and Neitzke. The results we obtain in this regime are highly suggestive and drawing on the results at low frequency, it has been suggested that they might be telling us something new about the quantum structure of black holes. We conclude by presenting an attempt of using the monodromy technique to compute the greybody factor at high frequency for a stringy black hole. The hope is that the result in this case might be easier to realize in the context of string theory.

Acknowledgments

The past two years have been the most challenging, satisfying and fruitful of my academic life. There are several people that have made this an experience that I will always cherish and I would like to thank them all in these few lines. Here we go, let us hope I do not forget anyone!

First, I would like to thank Professor Jan de Boer for taking me as his student and for inspiring lectures. Jan, I really appreciate the freedom that you gave me, the patience to answer my dumb questions and the help in moments of despair. Also, thanks for the innumerable letters of recommendation and lots of help with the always annoying, but unavoidable burochrtatic stuff. Given that this thesis is my first serious piece of scientific writing, I hope I have been able to grasp some of your amazing physical intuition and that it will be reflected in the way I conduct research from now on. Really, thanks for everything!

Then come my friends: Chris, Pawel, Pierre, Barbara, Alvaro, Hideto, Fernando, Chitrak, Sander, Remik and my officemates. Thank you guys for the parties, dinners, lunches, games, non physics- and physics-related discussions, etc. Without you, this would have been a dull experience! Also, thanks to those of you who proofread parts of my thesis.

I should not forget the people that will most definitely never read or find out about this thesis. To the people of the Huygens Scholarship Program, the Amsterdam Merit Scholarship and the Institute for Theoretical Physics from the University of Amsterdam, thank you for the scholarships that allowed me to study in Holland. To Jan Pieter van der Schaar and Koenraad Schalm: thanks for putting together a nice student seminar and for all the letters of recommendation.

Finally, and most importantly, thanks to my family and girlfriend for all the short- and long-distance love, support and for believing in me. Pa, Ma, Tito, Mina, gracias por todo el apoyo, comprensión y cariño; no hubiera podido lograr esto sin ustedes. Denisse, gracias por enseñarme a soñar despierto y que el amor todo lo puede. Es gracias a ustedes que no existe lugar como casa.

Coco Escobedo
Amsterdam 2008

Conventions

Unless otherwise specified, we work in units where $\hbar = c = k_B = 1$. We do not set Newton's constant to one, but denote it by G_d , indicating that it is its value in d spacetime dimensions.

Any given spacetime metric is of the form $ds^2 = g_{\mu\nu}dx^\mu dx^\nu$, where the signature of $g_{\mu\nu}$ is $(- + + +)$. Spacetime dimensions will be denoted by d , hence, the number of spatial dimensions is $d - 1$.

For simplicity, we use the Gaussian unit system for electromagnetism, in which the electrostatic constant appearing in Coulomb's law is such that: $K = \frac{1}{4\pi\epsilon_0} = 1$.

In d dimensions, the Einstein metric and the string metric are conformally related by

$$g_{\mu\nu}^E = e^{-\frac{4\Phi}{d-2}} g_{\mu\nu}^S,$$

where Φ is the dilaton field.

We use \log to denote either the natural logarithm of a real number or the logarithm of a complex number: the case at hand will be clear from the discussion in the body of the thesis. We will only make a distinction between them when writing the definition of the logarithm of a complex number $z = |z|e^{i\theta}$ as

$$\log z = \ln |z| + i\theta.$$

This convention will prove to be handy when dealing with the analytic continuation of some variables in the computation at high frequency.

Contents

Introduction	1
I Black Holes	5
1 Black holes in classical gravity	7
1.1 Schwarzschild black holes	7
1.2 Reissner-Nordström black holes	10
1.2.1 Extremal Reissner-Nordström black holes	15
2 Black holes thermodynamics	19
2.1 Analogy between black holes and thermodynamics	19
2.2 The holographic principle	21
2.3 Microscopic description of black holes	22
2.4 The information loss paradox	23
3 Black holes in string theory	25
3.1 String theory	25
3.2 Supersymmetry and BPS states	30
3.3 Correspondence between black holes and strings	31
3.4 Constructing black holes in string theory	34
3.5 A five-dimensional black hole with three charges	36
3.5.1 Special cases	39
II Greybody Factors: Hawking Radiation in Disguise	43
4 Klein-Gordon equation in black hole backgrounds	45
4.1 $d = 4$ black hole backgrounds	45
4.1.1 Generalizations	47
4.2 $d = 5$ black hole background with three charges	48
4.3 S-wave approximation	50
5 Greybody factors	53
5.1 Modifying Hawking radiation	53
5.2 Black hole scattering theory	55

5.2.1	Greybody factor = absorption cross section	58
5.3	Frequency regimes: low versus high frequency	58
5.4	Motivating the study of greybody factors	60
III Greybody Factors: Computations		61
6	Greybody factors at low frequency: Semiclassical computation	63
6.1	The wave equation	63
6.2	Computation using simple matching technique	65
7	Greybody factors at low frequency: String theory computation	71
7.1	Statistical mechanics in two dimensions	71
7.2	The long string model	73
7.3	Decay rate of the D-brane bound state	74
7.4	Surprising agreement	76
8	Monodromy technique	79
8.1	Preliminaries	79
8.2	Monodromy of the tortoise coordinate and plane waves	80
9	Greybody factors at high frequency	83
9.1	$d = 4$ Schwarzschild black hole	83
9.1.1	Constructing the Stokes line	83
9.1.2	Asymptotics of the solutions	85
9.1.3	Rotating the tortoise coordinate and the solutions	86
9.1.4	Greybody factor computation	87
9.2	$d = 4$ Reissner-Nordström black hole	92
9.2.1	Constructing the Stokes line	92
9.2.2	Asymptotics of the solutions	94
9.2.3	Rotating the tortoise coordinate and the solutions	94
9.2.4	Greybody factor computation	95
9.3	Suggestive results	100
10	An attempt	101
10.1	Setup	101
10.2	Monodromy of the tortoise coordinate and plane waves	102
10.3	Constructing the Stokes line	102
10.4	Asymptotics of the solutions	104
10.4.1	Solutions as $r \rightarrow +\infty$	104
10.4.2	Solutions as $r \rightarrow 0$	104
11	Conclusions	109

IV	Appendices	113
A	Penrose diagrams	115
B	Euclidean derivation of the Hawking temperature	119
C	Hawking temperature of the five-dimensional black hole	121
D	Klein-Gordon equation in curved spacetime	123
E	Some useful formulas	125
F	Asymptotics of the potential	127
	Bibliography	131

Introduction

Black holes are undoubtedly one of the most fascinating objects in physics. They are predicted by Einstein's theory of general relativity and their existence is now widely supported by observational evidence. A black hole is a part of spacetime with a curvature singularity in the center, where the laws of physics, as we know them, are no longer valid. This singularity is hidden from the rest of the Universe by an event horizon, a surface that can be thought of as the boundary of the black hole. Once an object crosses the event horizon, i.e. falls into the black hole, timelike and spacelike directions switch roles, meaning that the object will be forced to move forward in space, eventually hitting the singularity. This is where black holes get their name from: since not even light can escape from them, they are effectively "black". But how do we properly describe the spacetime singularities inside black holes? Understanding them might give us a clue of how to deal with other important spacetime singularities, such as the Big Bang.

By studying quantum field theory in a black hole background, Hawking showed that this behaves as a thermal system. It has associated thermodynamical quantities such as an entropy and temperature. Furthermore, it emits radiation with a characteristic blackbody spectrum, known as Hawking radiation. Thus, when quantum mechanics is taken into account, black holes are in fact not black and they obey the laws of thermodynamics. The spectrum of the radiation emitted by a black hole is that of a black body exactly at the event horizon. However, as the initial radiation travels away, it will get modified by the non-trivial spacetime geometry that the black hole generates around it. Therefore, an observer located at infinity will measure a spectrum that differs from that of a black body by a so-called *greybody factor*, a frequency- and geometry-dependent quantity that "filters" the initial Hawking radiation. Within a semiclassical approximation, greybody factors can be studied by making use of Schrödinger-like equations to study the scattering of a field by the black hole background. This method allows us to compute the transmission and reflection coefficients of the black hole, in terms of which we can define the corresponding greybody factor.

The thermal nature of black holes raises two deep questions:

- What are the microscopic configurations that a black hole entropy is counting?
- Is information lost once it falls into a black hole?

We will address their nature in the body of the thesis. However, we should point to the fact that in order to solve these two puzzles, we need to go beyond the semiclassical approximation and require a theory of quantum gravity. Roughly speaking, this is due

to the fact that the curvature of spacetime inside a black hole is so large that on very small scales, gravitational effects will be as important as quantum effects.

But, why do we need a theory of quantum gravity? Modern theoretical physics relies on two major theories: quantum field theory and general relativity. The former deals with the world at very small scales and the latter with the world at very large scales. Over the years, the validity of both theories within their respective regimes has been tested beyond any shadow of doubt. However, it would be desirable to have only one theory that describes all known particles and interactions and that, in the appropriate limits, reproduces the predictions made by quantum field theory and general relativity. Such a theory is given the name of quantum gravity and the search for it is one of the most outstanding problems in theoretical physics. Usually, physical systems are studied in regimes when only one of the above mentioned theories is relevant or by using a semiclassical approximation like the one used by Hawking. In order to formulate a theory of quantum gravity, physicists have to look for systems under extreme conditions, in which gravitational and quantum effects are on the same footing. As we just explained above, black holes satisfy this condition!¹ This remarkable feature makes black holes a unique testing ground for ideas and proposals coming from any theory of quantum gravity.

Indeed, black holes have played a crucial role in the development of string theory, nowadays our most promising candidate for a theory of quantum gravity. According to it, the Universe is made up of tiny vibrating strings and higher-dimensional membranes known as p -branes. In 1996, Strominger and Vafa gave a string theoretical derivation of the Bekenstein-Hawking entropy. They constructed a special type of black hole, namely a five-dimensional extremal black hole, using a special type of p -branes known as Dp -branes. Their calculation was later generalized to other cases, showing that string theory successfully accounts for the microscopic degrees of freedom that give rise to the entropy of certain types of black holes.

Diverse studies of black holes in string theory followed the above derivation and one of them was the study of greybody factors of a variety of black holes. In this area, one of the most important results was that of Maldacena and Strominger, who found that in the small frequency regime, the greybody factor of a specific type of black hole could be exactly reproduced by computing the spectrum of a vibrating string and measuring it at infinity. This was a remarkable result, because the greybody factor initially calculated in a semiclassical approximation, could be exactly reproduced by a quantum field theory, which is the one used to study the spectrum of a string. Therefore, we see that one could obtain the same result from a theory with gravity and another one without it! This work was one of the main motivations when Maldacena proposed the AdS/CFT correspondence, a conjectured duality between a string theory defined in $(d+1)$ dimensions and a conformal field theory that lives in d dimensions. This duality has been one of the most important conceptual breakthroughs in theoretical physics in the last years and it is now widely used not only to study the nature of quantum gravity, but also as a computational tool for strongly coupled gauge theories.

¹The other cases that satisfy this condition are the Big Bang and the very first moments after it.

Motivation

We see that by studying greybody factors in a certain frequency regime, great progress was made toward our understanding of string theory. One may ask if by studying greybody factors in a different frequency regime we would be able to learn even more about the quantum structure of black holes and, thus, about quantum gravity. Indeed, motivated by some suggestive results, Motl and Neitzke have proposed that the study of greybody factors at large frequency may reveal new and unexpected features of the quantum nature of black holes. If correct, then greybody factors might help us in resolving the information loss paradox arising from the thermal nature of black holes.

The goal of this thesis is to review the concept of greybody factors in semiclassical gravity and motivate their study in the high frequency regime as a possible way to achieve a better understanding of black holes and quantum gravity. To do so, we will present recent progress made in this area of research and thoroughly explain the techniques used. In the end, we will try to give hints to possible connections of these results to those that have been or can be obtained from string theory.

Outline

This thesis has been written assuming that the target audience is composed of master students of theoretical physics. Hence, anyone with basic knowledge of general relativity and quantum field theory will be able to read it. The outline of the thesis is as follows:

Part I

This part provides the basic background material necessary to understand the main ideas of the thesis. It is included hoping that the thesis is as self-contained as possible and, perhaps, that it can be used as a quick reference for someone who is just starting to learn these subjects. In [chapter 1](#), we start by giving a review of the basics of black holes in four-dimensional Einstein's gravity and present their causal structure schematically by means of Penrose diagrams. In [chapter 2](#), we introduce the analogy between black holes and thermodynamics and explain what puzzles arise from it. Finally, we explain the basics of black hole in string theory in [chapter 3](#), giving an explicit example of a five-dimensional black hole with three charges, first obtained by Horowitz, Maldacena and Strominger.

Part II

In this part, the concept of greybody factors is introduced and we explain the main tools used to compute them explicitly. First, the Klein-Gordon equation is solved in two different black hole backgrounds in [chapter 4](#). This will constitute the backbone of the greybody factor computation. Then, in [chapter 5](#), we explain the concept of greybody factors and give their definition using black holes scattering theory. Finally, we give a detailed explanation of the differences between the low and high frequency regime computation.

Part III

This part contains the computation of greybody factors for different black holes. As a motivation, we show in [chapter 6](#) and [chapter 7](#) the greybody factor computation at low frequency for the five-dimensional black hole mentioned above, both in the semiclassical gravity and string theory context. Remarkably, the two results agree. This was one of the precursors of the AdS/CFT correspondence.

In [chapter 8](#) and [chapter 9](#) we compute the greybody factors at high frequency for the four-dimensional Schwarzschild and Reissner-Nordström black holes in asymptotically flat spacetime. In the latter case, even though the results have been mentioned in the literature, the computation has not been shown explicitly and we fill that gap. The monodromy technique and steps involved in the calculations will be explained in detail.

In [chapter 10](#), we present an attempt of an original computation. We apply the monodromy technique to try to obtain the greybody factor at high frequency for the five-dimensional black hole with three charges. Our motivation to do so is that this black hole has a well-known string theory description; hence, the semiclassical results at high frequency might be more easily realized in this case than in the cases considered in [chapter 9](#).

We conclude by analyzing and discussing our results. Finally, the appendices contain material that may help in clarifying parts of the thesis.

Part I

Black Holes

Chapter 1

Black holes in classical gravity

In this chapter, we review the basics of black holes in four-dimensional classical gravity, including their general properties and causal structure. We include this chapter hoping that the thesis is as self-contained as possible, since these are the type of black holes for which we will be calculating greybody factors in the coming chapters. Excellent references for further details are [1, 2]. For a complete and recent review of higher-dimensional black hole solutions, the reader is referred to [3].

1.1 Schwarzschild black holes

In 1905, with his theory of special relativity, Einstein showed that we must consider space and time on an equal footing. However, and maybe more importantly, in 1915 Einstein published his theory of general relativity, which completely changed our way of looking at the Universe and our understanding of gravity. Using the mathematics of Riemannian geometry, he showed that gravity can be regarded as the curvature of spacetime due to the presence of matter or, equivalently, energy. In order to derive the Einstein's equation of general relativity, we consider the action $S = S_{EH} + S_M$, where

$$S_{EH} = \frac{1}{16\pi G_4} \int d^4x \sqrt{-g} R$$

is the Einstein-Hilbert action, which is the gravitational part of S , and

$$S_M = \int d^4x \sqrt{-g} \mathcal{L}_M$$

is the matter-energy fields term. The Lagrangian density \mathcal{L}_M used to define S_M depends on the problem at hand. Then, the total action we have to consider is

$$S = \frac{1}{16\pi G_4} \int d^4x \sqrt{-g} R + \int d^4x \sqrt{-g} \mathcal{L}_M.$$

By varying this action with respect to the inverse metric $g^{\mu\nu}$ and defining the energy-momentum tensor $T_{\mu\nu}$ as

$$T_{\mu\nu} = \frac{-2}{\sqrt{-g}} \frac{\delta S}{\delta g^{\mu\nu}}, \tag{1.1}$$

we find that Einstein's equation of general relativity is

$$R_{\mu\nu} - \frac{1}{2}Rg_{\mu\nu} = 8\pi G_4 T_{\mu\nu}, \quad (1.2)$$

where $R_{\mu\nu}$ is the Ricci tensor, R is the Ricci scalar (or scalar curvature) and $g_{\mu\nu}$ is the metric tensor of the spacetime under study. G_4 is Newton's gravitational constant in four dimensions; we use this notation for reasons that will become apparent in coming chapters. This equation tells how the geometry of spacetime (left-hand side) reacts to the presence of energy and matter (right-hand side). By taking the trace of (1.2) and rearranging some terms, we can write

$$R_{\mu\nu} = 8\pi G_4 (T_{\mu\nu} - \frac{1}{2}Tg_{\mu\nu}),$$

which is a completely equivalent equation. It is especially useful when finding solutions in the vacuum, i.e. where $T_{\mu\nu} = 0$, since we can readily write the vacuum Einstein's equation in the very convenient form

$$R_{\mu\nu} = 0. \quad (1.3)$$

Soon after the publication of this theory, physicists started working on finding solutions of the equation of general relativity. It was Karl Schwarzschild who found the first analytic solution in the vacuum. He considered a spherically symmetric, stationary body of mass M and found that the metric it generates, in spherical coordinates (t, r, θ, ϕ) , is given by

$$ds^2 = - \left(1 - \frac{2G_4 M}{r}\right) dt^2 + \left(1 - \frac{2G_4 M}{r}\right)^{-1} dr^2 + r^2 d\Omega_2^2, \quad (1.4)$$

where $d\Omega_2^2 = d\theta^2 + \sin^2\theta d\phi^2$ is the metric on a unit 2-sphere S^2 . This solution is known as the Schwarzschild metric and it can be shown that it is the unique vacuum solution with spherical symmetry and that there are no time-dependent solutions of this form. This is known as Birkhoff's theorem (for a proof, the reader is referred to [1]). This metric is asymptotically flat, i.e. far away from the black hole, as $r \rightarrow \infty$, we recover the Minkowski metric.

It is readily seen that the metric (1.4) is singular at $r = 0$ and $r = 2G_4 M$. The former is a true singularity of spacetime, whereas the latter is not and is rather an artifact of the choice of coordinates, as can be checked by computing an invariant quantity (e.g. the curvature invariant scalar) and evaluating it at both points:

$$R_{\mu\nu\rho\sigma} R^{\mu\nu\rho\sigma} = \frac{48G_4^2 M^2}{r^6}.$$

At $r = 0$ this scalar goes to infinity and we regard this point as a true singularity. However, at $r = 2G_4 M$, this scalar has a finite value, as do all other scalars constructed with the Riemann tensor; this suggests that this is not a true singularity and that it appears to be so in (1.4) due to our bad choice of a coordinate system. By the defining

the so-called tortoise coordinate $r^* = r + 2G_4M \ln\left(\frac{r}{2G_4M} - 1\right)$, we can write the metric in a form in which we can clearly see that it is well-behaved at $r = 2G_4M$.¹

The radius $r_0 = 2G_4M$ is called the Schwarzschild radius and the solution of (1.4) for $r < r_0$ is the metric that describes a Schwarzschild black hole. The spherical surface with radius r_0 is known as the *event horizon* and it has the remarkable property of dividing the spacetime in two regions ($r > r_0$ and $r < r_0$) which are causally disconnected. Having introduced this concept, we can give a general definition of a black hole as a region of spacetime separated from infinity by an event horizon. In the Schwarzschild case, objects located outside the event horizon will orbit the black hole as if it was a body of mass M . Nothing too interesting in this region. However, once an object hits and crosses the event horizon, it will never be able to escape the gravitational force of the black hole. Once inside a black hole, timelike directions become spacelike, and viceversa. This means that the lightcone of any object located at $r < r_0$ will be completely tilted and the object will inevitably move toward the singularity at $r = 0$. Therefore, not even light can escape from a black hole and the two spacetime regions defined by the event horizon are causally disconnected.

For ordinary objects, r_0 is much smaller than the physical radius or size of the object; in such cases, we need not worry about the event horizon because the Schwarzschild metric does not apply since we are no longer in empty space. On the other hand, if an object undergoes gravitational collapse, eventually its physical radius will be smaller than r_0 and it will form a black hole; the empty space surrounding it, both inside and outside the event horizon, is correctly described by the Schwarzschild metric. Hence, (1.4) can be used to describe the empty space outside a star, a black hole or a planet, as well as the interior of a black hole. We present below the Penrose diagrams for the full Schwarzschild metric and a realistic Schwarzschild black hole (if the reader is not familiar with Penrose diagrams, see Appendix A).

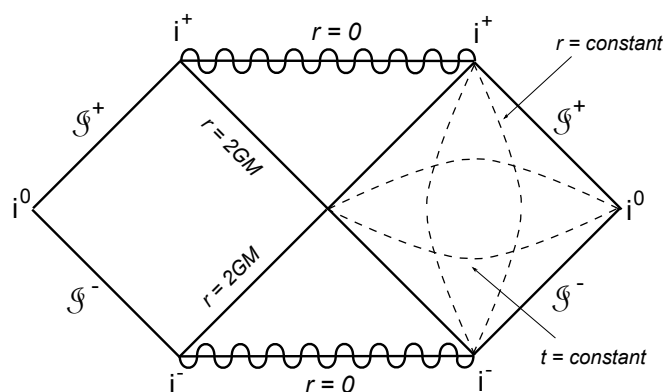


Figure 1.1: Penrose diagram for the full Schwarzschild metric.

¹It is worth mentioning that these still are not the best coordinates to study the full Schwarzschild metric. The appropriate ones are called Kruskal coordinates. See [1].

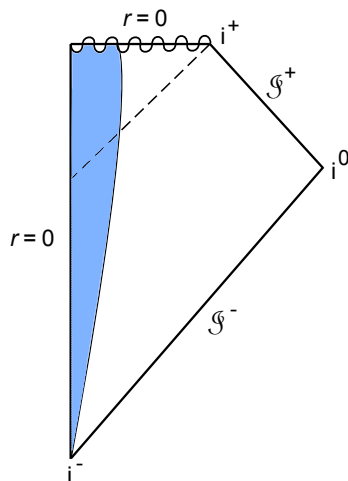


Figure 1.2: Penrose diagram for a realistic Schwarzschild black hole. The shaded region contains the matter of the collapsing star.

Finally, we should mention that the Schwarzschild metric is easily generalized to higher dimensions. More specifically, the Schwarzschild metric in $d = 4 + n$ dimensions is given by

$$ds^2 = - \left[1 - \left(\frac{r_0}{r} \right)^{n+1} \right] dt^2 + \left[1 - \left(\frac{r_0}{r} \right)^{n+1} \right]^{-1} dr^2 + r^2 d\Omega_{n+2}^2, \quad (1.5)$$

where, again, r_0 is the event horizon.

1.2 Reissner-Nordström black holes

The Reissner-Nordström metric is generated by a spherically symmetric, electrically charged object of mass M and charge Q . Such a solution is not extremely relevant to realistic astrophysical situations because in the real world, an electrically charged black hole would quickly discharge via Schwinger pair production, but it is very interesting from a theoretical perspective. In order to find the corresponding solution, we cannot use (1.3), since we are no longer in vacuum. This is due to the fact that Q will generate a nonzero electromagnetic field, which acts as a source of energy-momentum. In order to write the action, we consider the Einstein-Hilbert action plus the action due to energy-matter fields. In this case, the Lagrangian density for the energy-matter fields is that of electromagnetism, namely

$$\mathcal{L}_M = -\frac{1}{4} F_{\mu\nu} F^{\mu\nu},$$

so that

$$S_M = -\frac{1}{4} \int d^4x \sqrt{-g} F_{\mu\nu} F^{\mu\nu}, \quad (1.6)$$

where $F_{\mu\nu}$ is the electromagnetic field strength tensor defined in terms of electromagnetic vector potential A_μ , as

$$F_{\mu\nu} = \partial_\mu A_\nu - \partial_\nu A_\mu. \quad (1.7)$$

Hence, the action to be considered in the Reissner-Nordström case is

$$S_{RN} = \int d^4x \sqrt{-g} \left(\frac{R}{16\pi G_4} - \frac{1}{4} F_{\mu\nu} F^{\mu\nu} \right), \quad (1.8)$$

and using (1.1), we find that the energy-momentum tensor for electromagnetism is

$$T_{\mu\nu} = F_{\mu\rho} F_{\nu}^{\rho} - \frac{1}{4} g_{\mu\nu} F_{\rho\sigma} F^{\rho\sigma}. \quad (1.9)$$

Assuming some general form for the metric and $T_{\mu\nu}$, that take into account the spherical symmetry of the source, it is possible to find the metric $g_{\mu\nu}$. We will not go through the details of the derivation, but only give the final result. The Reissner-Nordström metric is given by

$$ds^2 = -\Delta dt^2 + \Delta^{-1} dr^2 + r^2 d\Omega_2^2, \quad (1.10)$$

where

$$\Delta = 1 - \frac{2G_4 M}{r} + \frac{G_4(Q^2 + P^2)}{r^2}.$$

This metric is also asymptotically flat and if $Q = P = 0$, we recover the Schwarzschild metric. In the last expression, Q is the total electric charge of the black hole and P its total magnetic charge. It is a well-known fact that magnetic monopoles have not been observed in nature, but nothing prevents us from considering them for purely theoretical purposes. However, in what follows, we will set $P = 0$, so that

$$\Delta = 1 - \frac{2G_4 M}{r} + \frac{G_4 Q^2}{r^2}.$$

Since we are only considering electric charge, in this case the electromagnetic vector potential is given by

$$A_{\mu} = \left(-\frac{Q}{r}, 0, 0, 0 \right) \quad (1.11)$$

and the electric field associated with the solution is found using (1.7) as

$$E_r = F_{rt} = \partial_r A_t - \partial_t A_r = \frac{Q}{r^2}.$$

As in the Schwarzschild case, the Reissner-Nordström metric (1.10) has a true singularity at $r = 0$, as can be checked by computing the invariant scalar

$$R_{\mu\nu} R^{\mu\nu} = \frac{4Q}{r^8}.$$

We now want to find the horizon structure; in order to do so, we use the fact that in the chosen coordinates system, the event horizon can be located using the criterion $g^{rr} = 0$. (For a derivation of this criterion, see [1].) By reading off the r - r component of the metric, we see that $g_{rr} = \Delta^{-1}$, so $g^{rr} = \Delta$. Thus, the equation that we have to solve is

$$\Delta = 1 - \frac{2G_4 M}{r} + \frac{G_4 Q^2}{r^2} = 0$$

and the corresponding solutions are

$$r_{\pm} = G_4 M \pm \sqrt{G_4^2 M^2 - G_4 Q^2}. \quad (1.12)$$

By plotting Δ as a function of r in [Figure 1.3](#), we see that depending on the relative values of $G_4 M^2$ and Q^2 , the Reissner-Nordström metric can have one, two or no event horizons at all. Therefore, we will have three possibilities for the metric, each of which corresponds to a specific type of black hole.

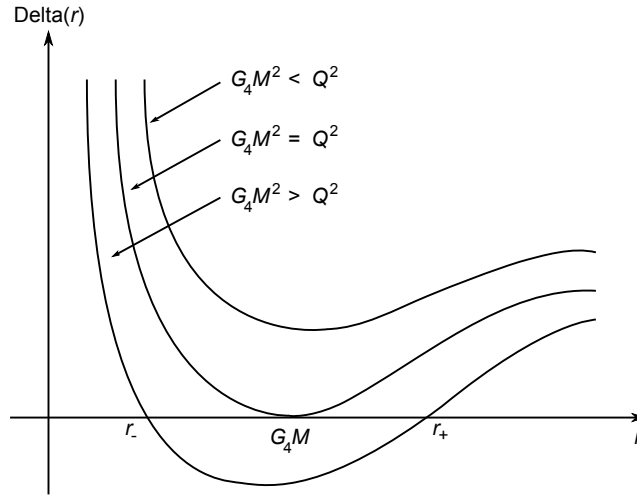


Figure 1.3: Dependence of Δ on the relative values of $G_4 M^2$ and Q^2 .

Let us consider each case separately:

- $G_4 M^2 < Q^2$

In this case, (1.12) does not hold because Δ is always positive. This means that there is no event horizon and therefore the metric is completely regular all the way to $r = 0$, which is still a true singularity. Moreover, the non-existence of an event horizon implies that the singularity at $r = 0$ is not hidden from us; such a singularity is called a *naked singularity*. In 1969, Roger Penrose made a conjecture called *cosmic censorship*, which states that naked singularities, apart from the one at the Big Bang, do not exist. This conjecture is based on the fact that if a naked singularity existed, things happening at the singularity itself would influence our universe. Since the laws of physics (as we know them) break down at the singularity, we would lose predictive power and would not be able to say anything about the future. Although this conjecture has not been proven, several thorough studies of collapsing bodies indicate that naked singularities do not form in such processes (see [2]). Another way of looking at this case is by noticing that the condition $G_4 M^2 < Q^2$ implies, roughly speaking, that the total energy of the black hole is less than the energy contribution from the electric field. Thus, this case is considered to be unphysical and we will not consider it for further analysis. The Penrose diagram for this case is presented in [Figure 1.4](#), from which we readily see that the metric has a naked singularity at the origin.

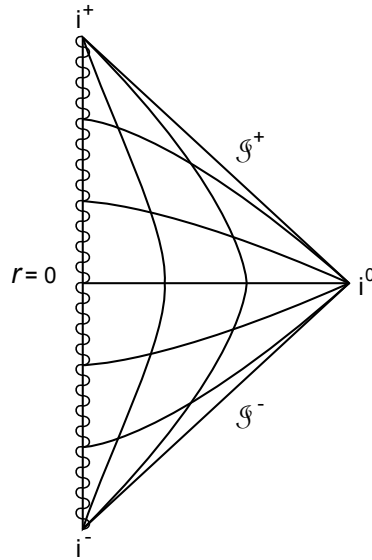


Figure 1.4: Penrose diagram for the case $G_4M^2 < Q^2$.

- $G_4M^2 > Q^2$

In this case, (1.12) holds and we have two horizons located at

$$r_+ = G_4M + \sqrt{G_4^2M^2 - G_4Q^2} \quad (\text{outer horizon})$$

and

$$r_- = G_4M - \sqrt{G_4^2M^2 - G_4Q^2} \quad (\text{inner horizon}).$$

The metric is singular at both these radii and we can see from the figure above that Δ takes negative values inside the two vanishing points r_{\pm} . In order to study the global properties and causal structure of the spacetime generated in this case, we could perform a clever change of coordinates, in which the metric would be related by a conformal transformation $\tilde{d}s^2 = \omega^2 ds^2$ to the original metric, and draw the Penrose diagram. We will skip such steps and merely give the diagram in Figure 1.5. The outer horizon r_+ behaves just like the horizon at r_0 in the Schwarzschild metric: once an object crosses this radius, timelike and spacelike coordinates switch roles and the object will inevitably move in the direction of decreasing r . This means that eventually, the object will hit the radius r_- ; an interesting thing happens there: timelike and spacelike coordinates switch roles again. Therefore, once the object has crossed the inner horizon r_- , it need not hit the singularity at $r = 0$ and can in fact move away from it, in the direction of increasing r .² If this is the case, once it crosses r_- , the direction of increasing r becomes a timelike direction (just as the direction of decreasing r was a timelike direction when going *into* the black hole) and so, eventually, the object will be spit out of the black hole past r_+ . This would be much like emerging from a white

²Hence, strictly speaking, the outer horizon is an event horizon, whereas the inner horizon is a so-called Cauchy horizon.

hole into the rest of our universe. Once outside the black hole, one could choose to move away from it or go back into it; however, this time it would be a different black hole than the first one.

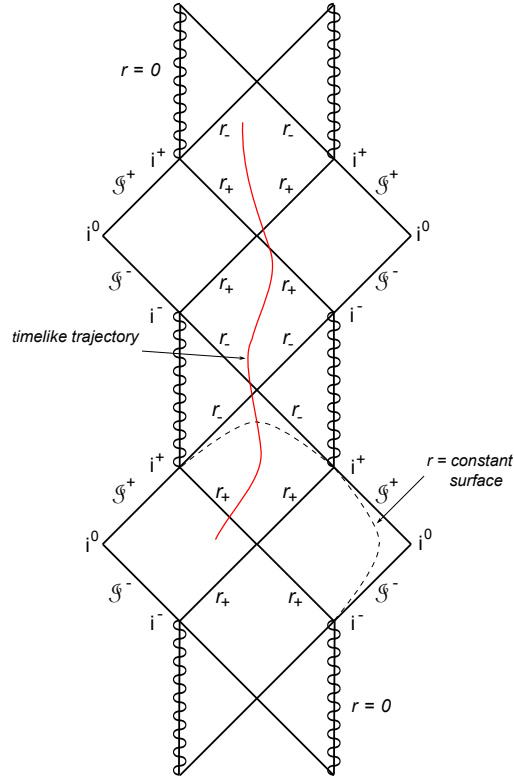


Figure 1.5: Penrose diagram for the case $G_4M^2 > Q^2$.

- $G_4M^2 = Q^2$

This is the case when a black hole has the maximal charge allowed given its mass. Black holes arising from this condition are called *extremal* Reissner-Nordström black holes. This type of black hole plays a crucial role in the context of supergravity and string theory. The reason for this is that in such supersymmetric theories, extremal black holes leave a number of supersymmetries unbroken, which is a helpful feature when doing calculations. It must be noted that this solution is highly unstable, since adding even a very tiny amount of mass to the black hole would bring it to the previous case. As can be seen from (1.12) and Figure 1.3, there is only one event horizon, located at $r = G_4M$. Once an infalling object crosses this horizon, it need not move in the direction of decreasing r and can avoid the singularity, eventually crossing the event horizon in the direction of increasing r . The Penrose diagram is shown below.

Finally, note that the metric (1.10) could also be written as

$$ds^2 = -\Delta dt^2 + \Delta^{-1} dr^2 + r^2 d\Omega_2^2, \quad (1.13)$$

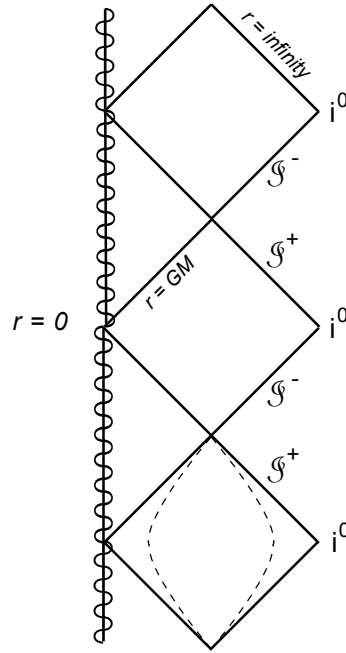


Figure 1.6: Penrose diagram for the case $G_4M^2 = Q^2$.

with

$$\Delta = \left(1 - \frac{r_+}{r}\right) \left(1 - \frac{r_-}{r}\right).$$

This form is more convenient because higher-dimensional Reissner-Nordström solutions are usually written in this fashion. More specifically, the Reissner-Nordström metric in $d = 4 + n$ dimensions is given by

$$ds^2 = -\Delta dt^2 + \Delta^{-1} dr^2 + r^2 d\Omega_{n+2}^2, \quad (1.14)$$

where

$$\Delta = \left[1 - \left(\frac{r_+}{r}\right)^{n+1}\right] \left[1 - \left(\frac{r_-}{r}\right)^{n+1}\right]$$

and r_+ and r_- are again the event horizons.

1.2.1 Extremal Reissner-Nordström black holes

A remarkable feature of these extremal black holes is that we can find exact solutions to the coupled Einstein-Maxwell equations arising after varying the action (1.8). In fact, such solutions can be found for any number of extremal black holes in a stationary configuration, i.e. a multi-extremal-black hole metric. In order to obtain these solutions, let us first rewrite the metric (1.10) in the case at hand. Using the extremality condition $G_4M^2 = Q^2$, it takes the form

$$ds^2 = -\left(1 - \frac{G_4M}{r}\right)^2 dt^2 + \left(1 - \frac{G_4M}{r}\right)^{-2} dr^2 + r^2 d\Omega_2^2.$$

We now shift the radial coordinate and define a new one as

$$\rho = r - G_4 M \quad (1.15)$$

and write the metric in terms of it. It is straightforward to obtain

$$ds^2 = -H^{-2}(\rho) dt^2 + H^2(\rho) (d\rho^2 + \rho^2 d\Omega_2^2), \quad (1.16)$$

where

$$H(\rho) = 1 + \frac{G_4 M}{\rho}. \quad (1.17)$$

This metric is, obviously, also asymptotically flat. It must be noted that in virtue of (1.15), the horizon is now located at $\rho = 0$ and these new coordinates only cover the region outside the horizon. These are called isotropic coordinates and in them, the spatial part of the metric is conformally flat and as such, it has manifest $SO(3)$ symmetry. Hence, we can write (1.16) in the usual Cartesian coordinates as

$$ds^2 = -H^{-2}(\vec{x}) dt^2 + H^2(\vec{x}) (dx^2 + dy^2 + dz^2), \quad (1.18)$$

where H is now

$$H = 1 + \frac{G_4 M}{|\vec{x}|}.$$

Furthermore, using the extremality condition written as $\sqrt{G_4} M = Q$ and the fact that $r = \rho + G_4 M$, we can write the electromagnetic vector potential (1.11) as

$$A_\mu = \left(-\frac{\sqrt{G_4} M}{\rho + G_4 M}, 0, 0, 0 \right)$$

and using (1.17), the timelike component A_0 (which is just the electrostatic potential) and H are related by

$$\sqrt{G_4} A_0 = H^{-1} - 1. \quad (1.19)$$

Let us now forget for a moment that we know that H was defined as in (1.17). If we solve the coupled Einstein-Maxwell equations for the metric (1.18) and the electrostatic potential (1.19), requiring that H is a time-independent function, we find that H obeys Laplace's equation

$$\nabla^2 H = 0,$$

where $\nabla^2 = \partial_x^2 + \partial_y^2 + \partial_z^2$. Therefore, H is a harmonic function and it has the general form

$$H = 1 + \sum_{a=1}^N \frac{G_4 M_a}{|\vec{x} - \vec{x}_a|},$$

for a set of N spatial points defined by the vectors \vec{x}_a , which describe the location of N extremal Reissner-Nordström black holes with masses M_a and charges $Q_a = \sqrt{G_4} M_a$. We have thus checked that the metric at hand in fact describes a stationary configuration of multi-extremal Reissner-Nordström black holes. (The stationary condition is what led us to require that H was a time-independent function.) If we only consider one

black hole located at the origin of our coordinate system, we recover (1.17) and then the metric describes a single Reissner-Nordström black hole (as we had been naively thinking before this analysis).

Finally, let us see what is the geometry of this extremal black hole near the horizon at $\rho = 0$. First, we write the metric (1.16) explicitly in terms of ρ as

$$ds^2 = - \left(\frac{\rho}{\rho + G_4 M} \right)^2 dt^2 + \left(1 + \frac{G_4 M}{\rho} \right)^2 (d\rho^2 + \rho^2 d\Omega_2^2).$$

So, near the horizon ($\rho = 0$), the metric takes the form

$$ds^2 \xrightarrow{\rho \rightarrow 0} - \frac{\rho^2}{G_4^2 M^2} dt^2 + \frac{G_4^2 M^2}{\rho^2} d\rho^2 + G_4^2 M^2 d\Omega_2^2.$$

Now, we define yet another coordinate as

$$\omega = \frac{G_4^2 M^2}{\rho},$$

so that $d\rho^2 = (\rho^2/\omega^2) d\omega^2$. With this new coordinate, we finally obtain the near-horizon metric

$$ds^2 \xrightarrow{\rho \rightarrow 0} \frac{G_4^2 M^2}{\omega^2} (-dt^2 + d\omega^2) + G_4^2 M^2 d\Omega_2^2,$$

which has the form

$$ds^2 = \frac{r_0^2}{r^2} (-dt^2 + dr^2) + r_0^2 d\Omega_2^2.$$

This is known as the Bertotti-Robinson metric and it is readily seen that it consists of two spaces, namely AdS_2 and S^2 . Therefore, we have found that the near-horizon geometry of the extremal Reissner-Nordström black hole is just $AdS_2 \times S^2$, i.e. the direct product of a two-dimensional Anti-de Sitter spacetime and a 2-sphere with radius $G_4 M$.

Chapter 2

Black holes thermodynamics

When quantum field theory is taken into account, black holes are in fact not black and behave as systems with characteristic thermodynamical properties. This remarkable feature raises new and fascinating questions about our understanding black holes. Moreover, the thermal nature of black holes stresses the need for a theory of quantum gravity. In this chapter, we explain how all this comes about.

2.1 Analogy between black holes and thermodynamics

The fact that classically nothing can come out of a black hole poses an apparent problem. Let us make the following thought experiment: imagine we had a system with a given entropy and that somehow we are able to measure the entropy of the entire Universe. We then take such system and throw it into a black hole. The system will vanish from our view and will eventually hit the singularity. This means that if we were to measure the entropy of the Universe again, we would find that it is less than the entropy we measured before throwing the system into the black hole. This would violate the second law of thermodynamics, which is one of the most time-honored laws in physics. In 1973, Bekenstein [4] made the bold conjecture that black holes have an intrinsic entropy. Going back to our situation above, if we associate an entropy S_{bh} to the black hole and label the entropy of the rest of matter and energy in the Universe as S_{ext} , then the total entropy would be non-decreasing

$$\frac{d(S_{bh} + S_{ext})}{dt} \geq 0$$

and hence we would avoid a violation of the second law of thermodynamics. Part of the motivation to make such conjecture came from Hawking's area theorem [5], which states that in any physically allowed process, the total area of all black holes in the Universe cannot decrease. This statement closely resembles that of the second law of thermodynamics for the entropy, which in fact led Bekenstein to propose that the entropy of a black hole should be proportional to its area.

These arguments suggest a close analogy between the laws of thermodynamics and the laws governing the physics of black holes. In 1973 [6], the four laws of black holes mechanics were proposed, which bare a remarkable similarity to the laws of thermody-

namics, if the surface gravity¹ κ and the area A of a black hole (the area of a black hole is the area of its event horizon) are like a temperature and an entropy, respectively. The laws are:

- **Zeroth law:** The surface gravity κ is constant over the horizon of a stationary black hole.
- **First law:** It is stated as

$$dM = \frac{\kappa}{8\pi G_4} dA + \Omega dJ + \Phi dQ, \quad (2.1)$$

where Ω is the angular velocity, J is the angular momentum and Φ is the electrostatic potential.

- **Second law:** The horizon area of the black hole must be nondecreasing in any physically allowed process.

$$dA \geq 0$$

- **Third law:** It is impossible to achieve $\kappa = 0$ via a physical process.

Although the analogy between black holes and thermodynamics looks nice, it was noticed at the time that it was inconsistent. The reason is the following: if black holes had a temperature, we would expect them to radiate with a characteristic Planck spectrum; however, by definition, black holes do not radiate, since nothing can come out of them. This posed an interesting problem and physicists in favor of the analogy argued that quantum mechanical effects had to be taken into account in order to solve it.

In 1975, Hawking [7] made the remarkable discovery that black holes do in fact radiate and made the analogy consistent; thus, the radiation emitted by a black hole is known as Hawking radiation. His semiclassical calculation consisted in studying quantum fields in a classical black hole background, finding that a black hole emits particles with a characteristic blackbody spectrum given by

$$\Gamma(\omega) = \frac{1}{e^{\beta\omega} - 1} \frac{d^3k}{(2\pi)^3}.$$

This result was first derived for massless scalar fields, but it was later generalized to massive and fermionic fields. From the above result, we can directly obtain the black hole temperature (known as the Hawking temperature) as the inverse of β .² The result is

$$T_H = \frac{\kappa}{2\pi} \quad (2.2)$$

(see [Appendix B](#) for a derivation of this result given a quite general metric). Now that we have the temperature associated with the black hole, we can make the analogy complete by replacing (2.2) in (2.1) and recalling that the first law of thermodynamics

¹The surface gravity is defined as the acceleration needed to keep a particle stationary at the horizon.

²Recall that we are working in units where $k_B = 1$, so that $\beta = \frac{1}{T}$.

is $dU = TdS + dW$, from which we find the entropy of the black hole. It is called the Bekenstein-Hawking entropy and it is given by

$$S_{bh} = \frac{A}{4G_4},$$

confirming Bekenstein's early conjecture about the relation between the entropy and the area of a black hole. Although the above result was obtained in four dimensions, it generalizes to any number of dimensions as

$$S_{bh} = \frac{A_d}{4G_d}, \quad (2.3)$$

where G_d is the d -dimensional Newton constant. Furthermore, this result is universal: it is valid for *any* type of black hole.

Therefore, we see that black holes are indeed thermal systems which obey the laws of thermodynamics. However, this realization leads to two profound puzzles: the microscopic description of black holes and the information loss paradox. The search for their resolutions has driven a good part of research in theoretical high energy physics over the last three decades. Since a black hole is a region of spacetime where quantum mechanics and gravity are on equal footing, it seems clear that in order to solve the puzzles, we need a theory of quantum gravity. In the coming sections, we will quickly review their nature and the progress that has been made toward their possible solutions.

2.2 The holographic principle

The reader may have noticed that the entropy of a black hole behaves very differently from that of a normal physical system. More specifically, from the result we just presented, we see that the entropy of a black hole scales with its area, whereas that of a thermodynamical system scales with its volume. That is, in thermodynamics, the entropy is an extensive quantity. To remind the reader why this is the case, let us consider the following example. Consider a system composed of V cubes of unit volume, hence, the total volume of the system is V . Each of the cubes can be in one of two states (spin up or down, for example); therefore, the number of states accessible to each cube is 2. Given that we have V cubes, the total system will have the following number of possible configurations

$$\Omega = 2^V,$$

so that the entropy of the system is given by

$$S = \ln \Omega = V \ln 2.$$

In 1993, 't Hooft [8] investigated this difference and came to a remarkable conclusion, namely, that at Planckian scales, the world is not three-, but two-dimensional. Let us give a simplified version of his arguments. Consider a system with energy E contained in a sphere of volume V and radius R , in which each unit volume has two accessible states (just like in our example above). The energy contained in the sphere is such that the

Schwarzschild radius of the system is smaller than its physical radius, i.e. $2G_4E < R$; this means that the density inside the volume is not allowed to be too large, otherwise it would collapse and form a black hole. 't Hooft showed that the entropy of the system is bounded from above by

$$S \leq \frac{\pi R^2}{G_4} = \frac{A}{4G_4},$$

so that the maximum entropy that it can have is that of a black hole that fills the entire volume V . This result is counterintuitive: it suggests that the entropy of a given system does not scale with its volume, but rather with its area. Why is this so? The field theoretical system that 't Hooft considered is built on two assumptions: that at Planckian scales the degrees of freedom are discrete and that the evolution of the system must be reversible in time. When one tries to calculate the number of accessible states of the system, it seems that we do an over-counting. According to 't Hooft, this is due to the fact that most of the possible states in the field theory have such a high energy, that they would collapse to form a black hole before they can influence the evolution of the system. So, it seems as if when we take into account gravitational physics, the number of degrees of freedom of the system is reduced. Therefore, the number of accessible states of the system grows exponentially with the area instead of the volume. In turn, this explains why the entropy of the system scales with the area. This is known as the *holographic principle*: in order to describe the physics inside a given volume V , it is enough to know the degrees of freedom on its surface A .

The AdS/CFT correspondence [9] in string theory is to date the most successful realization of the holographic principle. It relates string theory in a $(d+1)$ -dimensional space to a conformal field theory in a d -dimensional space. We will explain a little more about it in [chapter 7](#).

2.3 Microscopic description of black holes

As we know from statistical mechanics, the thermodynamical entropy of a system is counting the number of microscopic configurations that give rise to the same macroscopic properties. As one might expect, in order to perform this counting, we need to know what are the microscopic degrees of freedom of the system.

The no-hair theorem in classical gravity states that a black hole solution is uniquely characterized by its three conserved charges: mass, charge and angular momentum. That is, black holes have no hair.³ Physically, this means that once the black hole is formed, external observers cannot retrieve information about the type of matter that collapsed to form it. Therefore, in this context it seems that the black hole has only one state, i.e. its classical phase space is zero dimensional. The entropy we expect it to have is then

$$S = \ln 1 = 0.$$

However, as we saw in the previous section, black holes do have a non-vanishing entropy. Then, the obvious question is: what are the microscopic degrees of freedom

³Strictly speaking, this theorem has not been proven for all types of black holes, but for our discussion this fact is not relevant.

that give rise to the Bekenstein-Hawking entropy?

$$S = \ln \Omega.$$

For example, for a black hole of one solar mass, the entropy is $S \sim 10^{18}$, hence, the number of microscopic configurations goes as $\Omega \sim e^{10^{18}}$. We thus see that the classical and quantum pictures of black holes are extremely different (see Figure 2.1 for a pictorial representation).

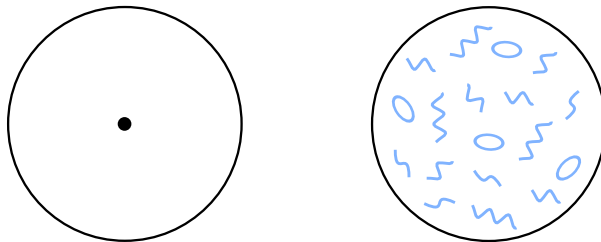


Figure 2.1: Classical and quantum descriptions of a black hole.

String theory is nowadays the most promising candidate for a theory of quantum gravity and, thus, we should expect it to provide an answer to the above question. In 1996, Strominger and Vafa [10] gave a string theoretical derivation of the Bekenstein-Hawking entropy of a certain class of five-dimensional black holes. Starting from such work, many more calculations have been done for other types of black holes and all have found exact agreement with the semiclassical computation of the Bekenstein-Hawking entropy. All these results show that string theory can successfully explain the statistical origin of the gravitational entropy of black holes.

2.4 The information loss paradox

Before explaining the second problem arising from the thermal nature of black holes, let us review some basic quantum mechanics. Let \mathcal{H} be the infinite dimensional Hilbert space spanned by the orthonormal pure quantum states $|\psi_i\rangle$, which are solutions of a quantum mechanical equation. The density matrix for a given pure quantum state $|\psi_a\rangle$ is

$$\rho_{pure} = |\psi_a\rangle\langle\psi_a|.$$

Then, we can naturally introduce mixed quantum states as statistical ensembles of pure states. In this case, the density matrix is given by

$$\rho_{mixed} = \sum_a p_a |\psi_a\rangle\langle\psi_a|,$$

where p_a are the probabilities of each pure state $|\psi_a\rangle$ in the ensemble. The density matrix of mixed states is particularly useful to describe thermal systems. For a system at finite temperature T , the probabilities p_a are proportional to Boltzmann factors

$e^{-\beta E_a}$, so that

$$\rho_{mixed} = \sum_a \frac{e^{-\beta E_a}}{\sum_a e^{-\beta E_a}} |\psi_a\rangle \langle \psi_a|.$$

Consider now an operator U that acts on elements of \mathcal{H} as $|\psi_b\rangle = U|\psi_a\rangle$, such that $\langle \psi_b| = \langle \psi_a|U^\dagger$. Given that $\langle \psi_i|\psi_j\rangle = \delta_{ij}$, we get that

$$1 = \langle \psi_b|\psi_b\rangle = \langle \psi_a|U^\dagger U|\psi_a\rangle \quad \Rightarrow \quad U^\dagger U = \mathbb{1}.$$

Therefore, by demanding orthonormality of the elements of \mathcal{H} , we have come to the conclusion that U has to be a unitary operator. That is, in any physical process consistent with quantum mechanics, we have to require that the evolution be unitary. In terms of the density matrices for pure and mixed states, this statement can be written as

$$\rho_{mixed} \neq U\rho_{pure}U^\dagger,$$

which says that in a theory with unitary operators, a pure state cannot evolve into a mixed state.

Let us now go back to our discussion of the second problem arising from the thermal nature of black holes and make the following thought experiment. Take a pure quantum state and throw it into a black hole; this will infinitesimally increase its mass and will start radiating again. Once the black hole has radiated all its mass, it will have evaporated and all there will remain is thermal radiation, which is described by a mixed quantum state. That is, the black hole acts like a system that transforms pure quantum states into mixed quantum states. As we saw above, this process is not allowed by quantum mechanics because it violates unitary evolution. This is known as the information loss paradox: by studying quantum fields in a classical background, we have obtained a result that is not allowed by one of our starting theories.

Over the years, several attempts have been made to solve the paradox. More recently, Mathur gave a string theoretical proposal that has provided more insight into a possible resolution. It is known as the fuzzball proposal for black holes [11, 12] and it is based on the AdS/CFT correspondence. According to it, one can construct microstate black hole geometries from quantities obtained in a quantum field theory; since any process on the field theory side is unitary, then one would expect that any process in the black hole geometry should also respect unitarity. The problem with this proposal is that it is not clear yet if the above mentioned microstate geometries represent the typical black hole microstates that account for the Bekenstein-Hawking entropy.

Chapter 3

Black holes in string theory

We now give a short introduction to the basic ideas of string theory and the construction of black holes within this framework. Given that this is not the main subject of the thesis, we will only mention the facts that are more relevant to our discussion in coming chapters about the computation of greybody factors of a certain type of black holes in string theory. Excellent and more complete references are [13, 14, 15, 16].

3.1 String theory

The two pillars of modern theoretical physics are quantum field theory and general relativity. The former deals with the world at very small scales and describes all elementary particles and their interactions (electromagnetic, weak and strong force), whereas the latter deals with the world at very large scales and describes how mass and energy deform spacetime (gravitational force). Both theories have been successfully confirmed experimentally within their specific domains of validity, making them universally accepted. However, it would be desirable to have only one theory that, in the appropriate limits, describes all phenomena that the two theories above do. In other words, it is conceptually appealing and elegant to unify quantum field theory and general relativity in a single theory, namely, a theory of quantum gravity. Black holes play a crucial role in the development of such a theory because in them, gravitational and quantum effects are equally important, due to the very large curvature of spacetime. Therefore, they provide an excellent testing ground for ideas and proposals concerning quantum gravity.

String theory is nowadays the most promising candidate for a theory of quantum gravity. The conceptual starting point of the theory is to consider that the fundamental constituents of the Universe are not point-like particles, but fundamental strings. Upon quantization of one of this fundamental strings, it can be shown that all elementary particles of the Standard Model appear as vibrational modes. Moreover, string theory naturally includes a massless spin-2 particle, the graviton, which is the quanta of the gravitational field. Strings can be open or closed and, as they propagate in spacetime, the concept of worldline of a particle is generalized to that of a worldsheet (see figure below). Hence, we can define the worldsheet of a p -dimensional object as the $(p + 1)$ -dimensional worldvolume that it sweeps out as it moves in spacetime. Obviously, in the case of the strings $p = 1$. The points on the worldsheet are parametrized by the

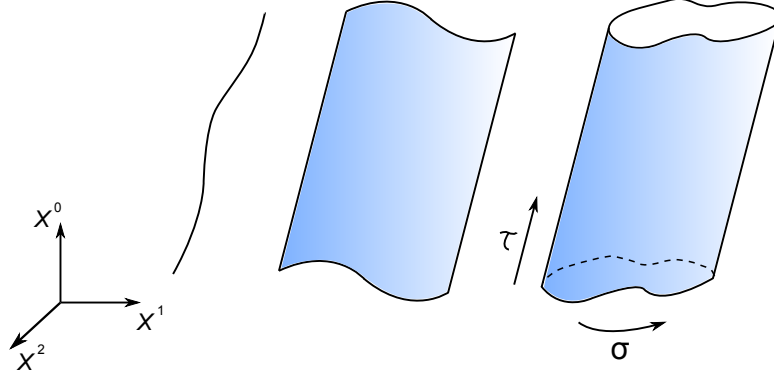


Figure 3.1: From left to right, worksheets of a particle, open string and closed string.

coordinates (τ, σ) , which are timelike and spacelike, respectively. When σ is periodic, it describes a closed string; if it covers a finite interval, it describes an open string.

We use the functions $X^\mu(\tau, \sigma)$ to embed the worldsheet in spacetime; they obey the wave equation $\partial_\alpha \partial^\alpha X^\mu = 0$.¹ In order to solve this equation, we need to specify boundary conditions; the possibilities are:

- Closed string

$$X^\mu(\tau, \sigma) = X^\mu(\tau + \pi, \sigma)$$

- Open string with Neumann boundary conditions

$$\frac{\partial X^\mu}{\partial \sigma} = 0 \quad \text{at} \quad \sigma = 0, \pi$$

- Open string with Dirichlet boundary conditions

$$X^\mu|_{\sigma=0} = X_0^\mu \quad \text{and} \quad X^\mu|_{\sigma=\pi} = X_\pi^\mu$$

With these, the most general solution of the wave equation that satisfies the closed string boundary conditions is given by

$$\begin{aligned} X_R^\mu &= \frac{1}{2}x^\mu + \ell_s^2 p^\mu (\tau - \sigma) + i \frac{\ell_s}{\sqrt{2}} \sum_{n \neq 0} \frac{1}{n} \alpha_n^\mu e^{-2in(\tau - \sigma)} \\ X_L^\mu &= \frac{1}{2}x^\mu + \ell_s^2 p^\mu (\tau + \sigma) + i \frac{\ell_s}{\sqrt{2}} \sum_{n \neq 0} \frac{1}{n} \tilde{\alpha}_n^\mu e^{-2in(\tau + \sigma)}, \end{aligned}$$

for the open string with Neumann boundary conditions

$$X^\mu = x^\mu + 2\ell_s^2 p^\mu \tau + i\sqrt{2}\ell_s \sum_{n \neq 0} \frac{1}{n} \alpha_n^\mu e^{-in\tau} \cos n\sigma$$

¹We have not said what is the range of values of μ . In Figure 3.1, we are only showing three spatial coordinate, i.e. $\mu = 0, 1, 2$, but nothing we are saying restricts us to this choice. Thus, in general $\mu = 0, \dots, d-2$.

and for the open string with Dirichlet boundary conditions

$$X^\mu = x^\mu + 2\ell_s^2 p^\mu \tau + i\sqrt{2}\ell_s \sum_{n \neq 0} \frac{1}{n} \alpha_n^\mu e^{-in\tau} \sin n\sigma.$$

In the previous equations, x^μ is the position of the center of mass of the string and p^μ is its total momentum. We have also introduced the string length ℓ_s , which is related to the string tension T and the open string Regge slope parameter α' by²

$$T = \frac{1}{2\pi\alpha'} \quad \text{and} \quad \ell_s^2 = \alpha'.$$

Note also that the mode expansion of the closed string has right- and left-movers, which appear naturally when solving the wave equation for those boundary conditions. In the case of the open string, right- and left-movers combine to form standing waves.

Upon quantization, the modes α_n^μ are interpreted as creation (for $n < 0$) and annihilation (for $n > 0$) operators that satisfy the commutation relation

$$[\alpha_m^\mu, \alpha_n^\nu] = m\eta^{\mu\nu} \delta_{m+n,0}.$$

They allow us to define a number operator N as

$$N = \sum_{n=1}^{\infty} \alpha_{-n} \cdot \alpha_n,$$

which in turn is used to find the spectrum of the string from the following mass-shell conditions

$$\begin{aligned} \text{Open string} &\rightarrow \alpha' M^2 = N - 1 \\ \text{Closed string} &\rightarrow \alpha' M^2 = 4(N - 1), \end{aligned} \tag{3.1}$$

where M is the mass of the state at level N . Consistency of the theory (namely, that there are no negative-norm states) requires that the number of spacetime dimensions be $d = 26$. It is easy to check that the number of states of a free string grows as $\Omega \sim e^{\sqrt{2\pi}M}$, so that its entropy goes as

$$S_{string} = \ln \Omega = \sqrt{2\pi}M.$$

The above discussion corresponds to the free bosonic string and it has two major drawbacks. The first is that the vacuum is unstable due to the presence of the tachyon, a state of the spectrum with negative mass-squared (corresponding to $N = 0$ in the above mass-shell conditions). The second is that, since the world is also made up of fermions, string theory has to include them in the framework. This is accomplished by using the concept of supersymmetry, or SUSY, a proposed symmetry that relates bosons and fermions. The resulting theory is known as *superstring theory* (usually, when people talk about string theory, they are referring to superstring theory, as we will do in the

²We should note that in part of the literature, a *string length scale* l_s is introduced instead of the string length ℓ_s that we are using in this thesis. The difference is that l_s relates to the Regge slope as $\frac{1}{2}l_s^2 = \alpha'$.

rest of this thesis). There are two basic approaches to incorporate SUSY into string theory

- The Ramond-Neveu-Schwarz (RNS) formalism, which is supersymmetric on the string worldsheet.
- The Green-Schwarz (GS) formalism, which is supersymmetric on the background spacetime geometry.

Once SUSY is taken into account, the number of spacetime dimensions that makes the theory consistent reduces to $d = 10$.

It is well-known that when we try to incorporate gravity into quantum field theory, the result is a theory that is non-renormalizable. String theory successfully deals with this problem by smearing out the interaction points in a Feynman diagram of a quantum field theory process. Schematically, these points are replaced by a surface that is generated by the intersection of the worldsheets of interacting strings (see [Figure 3.2](#)).

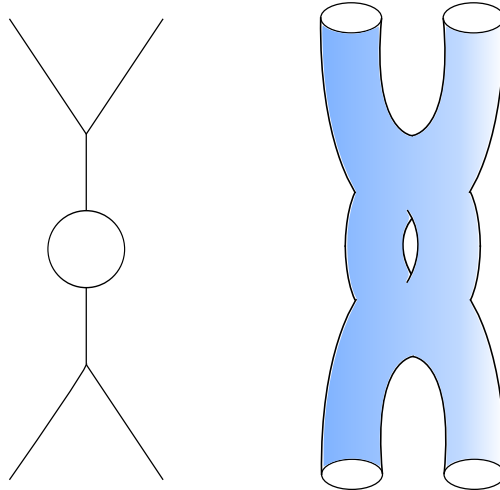


Figure 3.2: The same Feynman diagram in quantum field theory and in string theory

As we have seen, string theory predicts the existence of extra spatial dimensions. This is a radical departure from the classical picture of the world we live in. The extra five spatial dimensions³ are thought of as being curled up at very small scales, so that their existence is not detectable unless we go to extremely high energies. The geometry of these extra dimensions plays a crucial role in string theory; for example, they are responsible for determining the values of the universal physical constants.

Given that string theory predicts extra spatial dimensions, it naturally includes higher-dimensional objects called p -branes. The letter p refers to the number of spatial directions in which the object extends; so, for example, a point is a 0-brane, a string is a 1-brane, the worldsheet of a string is a 2-brane, and so on. As we mentioned previously, a p -brane sweeps out a $(p+1)$ -dimensional worldvolume as it moves in spacetime. What

³They are six when one studies M-theory, an eleven-dimensional theory that limits to the five known ten-dimensional superstring theories, which in turn are related to each other by dualities.

role do these objects play in string theory? Recall that open strings can have either Neumann or Dirichlet boundary conditions. In the first case, there is no momentum flow at either end of the string as can be seen easily from the definition of the boundary conditions. However, in the second case, the ends of the string are fixed in some of the spatial dimensions and this implies that energy can flow from one or both ends of the string. But where does the energy flow to? It turns out that open strings are forced to end in higher-dimensional objects called Dp -branes (D is just short for Dirichlet and p is again the number of spatial dimensions of the object). Then, Dp -branes specify the boundary conditions in each spacetime dimension for the ends of open strings attached to them: they are Dirichlet boundary conditions for directions perpendicular to the Dp -brane (they cannot detach from it) and Neumann boundary conditions for directions parallel to Dp -brane (they are free to move on it).

In 1995, Polchinski [17] showed that Dp -branes are non-perturbative dynamical objects that can fluctuate and move in spacetime. One can study the dynamics of Dp -branes by using the two-dimensional quantum field theory defined on the open string. This is physically easy to understand because, since open strings are attached to Dp -branes, any fluctuation on the latter should be somewhat reflected on the former. In this way, it is possible to understand non-perturbative phenomena (brane) by making use of well-known perturbative techniques (string). Moreover, Dp -branes also interact with closed strings, for example gravitons, meaning that they also interact gravitationally (see Figure 3.3).

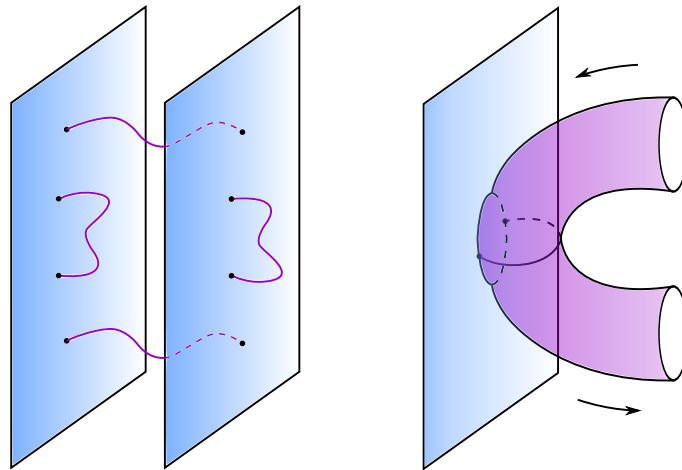


Figure 3.3: On the left, open strings with ends on the same or on different D2-branes. On the right, a graviton interacting with a D2-brane.

Finally, let us give a set of relations between different classical constants and the ones that appear in string theory. The string coupling constant g_s that appears in perturbative expansions in string theory is uniquely determined by the value of the dilaton field Φ by the relation

$$g_s = e^{\Phi}.$$

This coupling constant plays the same role as the different coupling constants in ordinary quantum field theory, i.e. they determine the strength of the interaction between strings. The ten-dimensional Newton constant is related to the string coupling constant and the string length by

$$16\pi G_{10} = (2\pi)^7 g_s^2 \ell_s^8, \quad (3.2)$$

in terms of which we can compute any d -dimensional (for $d < 10$) Newton constant as

$$G_d = \frac{G_{10}}{(2\pi)^{10-d} V_{10-d}}, \quad (3.3)$$

where $(2\pi)^{10-d} V_{10-d}$ is the volume of the compactified extra dimensions (the factors of 2π are included for unit convenience). We can now define the d -dimensional Planck length ℓ_d as

$$16\pi G_d = (2\pi)^{d-3} \ell_d^{d-2}. \quad (3.4)$$

Moreover, we see that the string length and the Planck length in d dimensions are related by

$$V_{10-d} \ell_d^{d-2} = g_s^2 \ell_s^8. \quad (3.5)$$

3.2 Supersymmetry and BPS states

As we explained in the previous section, string theory is a supersymmetric theory. For completeness, let us quickly review some basic supersymmetry concepts. Supersymmetry, or SUSY, is a proposed symmetry that relates bosons to fermions. In 1975, Haag, Lopuszański and Sohnius [18] proved that it is the only possible extension of the known spacetime symmetries of particle physics. Supersymmetry is the extension of the Poincaré symmetry algebra by introduction of anticommuting symmetry generators Q which transform under spinor representations of the Lorentz group, i.e. these new generators are spinors and carry half-integer spin. Hence, supersymmetric theories have conserved spinorial currents, which are generated by the supercharges Q_α .

We will focus on supersymmetry in $d = 4$ dimensions, where, in general, we can consider a theory with \mathcal{N} supersymmetries, which give a total of $4\mathcal{N}$ supercharges.⁴ Thus, the supersymmetry generators Q_α^I carry two indices: $I = 1, \dots, \mathcal{N}$ labels the supersymmetry and $\alpha = 1, 2, 3, 4$ labels the four components of each spinor supercharge. The most general \mathcal{N} -extended SUSY algebra allowed by Lorentz invariance is

$$\begin{aligned} \{Q_\alpha^I, \bar{Q}_\beta^J\} &= -2\delta^{IJ} P_\mu \Gamma_{\alpha\beta}^\mu - 2i Z^{IJ} \delta_{\alpha\beta} \\ \{P^\mu, Q_\alpha^I\} &= [Z^{IJ}, Q_\alpha^K] = [Z^{IJ}, P_\mu] = [Z^{IJ}, Z^{KL}] = 0 \end{aligned}$$

where P_μ is the four-momentum, Γ^μ are the usual Dirac matrices, which represent the Clifford algebra

$$\{\Gamma^\mu, \Gamma^\nu\} = 2\eta^{\mu\nu},$$

⁴In any number of dimensions the ratio of the number of supercharges to the smallest spinor representation gives the number of supersymmetries \mathcal{N} .

$\bar{Q} \equiv Q^\dagger \Gamma^0$ (with Q^\dagger the hermitean conjugate of Q) and Z is the antisymmetric central-charge matrix. As we can see from the above algebra, the central charges Z^{IJ} are conserved quantities (electric and magnetic charges) that commute with all the other generators. They only appear in theories with extended supersymmetry, i.e. theories with more supersymmetry than the minimal $\mathcal{N} = 1$ case.

To see the effect of the central-charge matrix, let us restrict the algebra to the space of particles with mass $M > 0$ in their rest frames. Then, the algebra takes the form

$$\{Q_\alpha^I, Q_\beta^{\dagger J}\} = 2M\delta^{IJ}\delta_{\alpha\beta} + 2iZ^{IJ}\Gamma_{\alpha\beta}^0.$$

By a transformation of the form $Z \rightarrow U^T Z U$, where U is a unitary matrix, we can bring Z to the canonical form

$$Z = \begin{pmatrix} 0 & Z_1 & 0 & 0 & \\ -Z_1 & 0 & 0 & 0 & \dots \\ 0 & 0 & 0 & Z_2 & \\ 0 & 0 & -Z_2 & 0 & \\ \vdots & & & & \ddots \end{pmatrix}$$

with $|Z_1| \geq |Z_2| \geq \dots \geq 0$. The structure of implies that the $2\mathcal{N} \times 2\mathcal{N}$ matrix

$$\begin{pmatrix} M & Z \\ Z^\dagger & M \end{pmatrix}$$

should be positive semidefinite. This implies in turn that the eigenvalues of the matrix have to be nonnegative, i.e. $M \pm |Z_i| \geq 0$. Therefore, the mass is bounded from below by the central charges

$$M \geq |Z_i|.$$

This is known as the Bogomolny-Prasad-Sommerfeld (BPS) bound. As a consequence of it, we see that massless states must be neutral. States that satisfy $M = |Z_i|$ are called BPS states and they belong to a short supermultiplet or BPS representation. These states are important because, due to energy and charge conservation, they are stable at any point in the moduli space of a theory. This means that when one changes the value of a modulus in the theory, the density of BPS states will remain the same.

3.3 Correspondence between black holes and strings

In 1993, Susskind [19] proposed an interesting approach to study black holes in string theory. Let us explain the line of reasoning using a four-dimensional Schwarzschild black hole. In string theory, the string coupling g_s is not a constant but a variable quantity. Then, let us consider a highly excited, free string state ($g_s = 0$); if we increase the string coupling, gravity will come into play because Newton's constant grows as $G_4 \sim g_s^2 \ell_s^2$

and the string will decrease in size.⁵ If the mass M_s of the string is sufficiently large, we should expect that as we keep increasing the coupling, eventually the length of the string will decrease below its Schwarzschild radius; we could then effectively think of the string as a black hole. Conversely, if we start with a black hole ($g_s \gg 1$) and decrease the coupling, the radius of the black hole $r_0 = 2G_4 M_{bh}$ will also decrease and eventually become smaller than the length of a string. Susskind suggested that we should think of this final state as a highly excited string state.

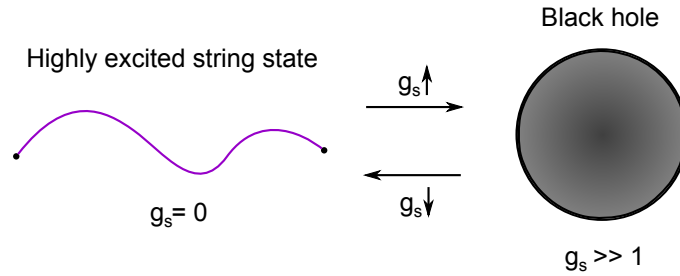


Figure 3.4: Correspondence between a highly excited string state and a black hole. We see that the transition from one picture to the other occurs as we vary the string coupling g_s

The above proposal seems to be perfectly consistent. However, there is a problem. If we compute the entropy of a single string (weak coupling) and the Bekenstein-Hawking entropy of a black hole (strong coupling), we will find that they both grow as different powers of the mass. Namely, in d spacetime dimensions, we have that

$$\begin{aligned} S_{string} &\sim M_s \sim \sqrt{N} \\ S_{bh} &\sim M_{bh}^{\frac{d-2}{d-3}}, \end{aligned} \quad (3.6)$$

where N is again the excitation level of the string introduced in the previous section. The result for S_{string} can be derived by computing the number of states of a free string and taking its logarithm, whereas S_{bh} can be obtained from purely geometrical arguments.

The resolution to the above problem was given by Horowitz and Polchinski [20]. The idea is the following: as the transition from a highly excited string state to a black hole, and viceversa, occurs, the masses M_s and M_{bh} should obviously be the same. Let us consider a free ($g_s = 0$), highly excited string state; as we said above, the mass M_s of the string should be large so that it eventually forms a black hole. Equivalently, this means that we need to look at a string state for large N (also obvious because we are dealing with a highly excited state of the string). Therefore, from (3.1), we have that

$$M_s \sim \frac{\sqrt{N}}{\ell_s}.$$

Now, let us turn our attention to the black hole picture. Again, we will use a four-

⁵From (3.2) and (3.3), we see that the four-dimensional Newton constant goes as $G_4 \sim g_s^2 \ell_s^2$, because the volume of the compactified spatial dimensions V_6 is proportional to ℓ_s^6 .

dimensional Schwarzschild black hole. Hence, the mass of the black hole goes as

$$M_{bh} \sim \frac{r_0}{G_4}.$$

So, we see that the ratio of the masses depends on g_s

$$\frac{M_s}{M_{bh}} \sim g_s^2.$$

This means that the masses of the string and the black hole cannot be equal for all values of the string coupling. Therefore, in order to match the two masses, we have to choose a value of g_s at which they should be equal. The natural choice is the value of the string coupling at which the transition occurs, i.e. the string forms a black hole, or viceversa. Obviously, this happens when the horizon of the black hole is of order of the string length (or viceversa, depending on what was our initial picture). So, when $r_0 \sim \ell_s$, we have that the mass of the black hole is equal to that of the string and, from the above equations, we get

$$M_{bh} = M_s \sim \frac{\ell_s}{G_4} \sim \frac{\sqrt{N}}{\ell_s}.$$

This last equation is the solution to the mismatch of the entropies in (3.6). Indeed, now that we have the mass of the black hole, it is straightforward to see that as the transition occurs, the entropy of the black hole will go as

$$S_{bh} \sim \frac{r_0^2}{G_4} \sim \frac{\ell_s^2}{G_4} \sim M_{bh} \sim \sqrt{N}.$$

So, the Bekenstein-Hawking entropy of the black hole is comparable to the string entropy given in (3.6).

Although we have used a Schwarzschild black hole to explain the resolution of the problem, all we have said is easily generalized to Reissner-Nordström black holes [20]. The main difference is that in the charged case, some of the charges that appear in the black hole solution are not carried by single strings. Instead, they are carried by D-branes. Therefore, in the case of Reissner-Nordström black holes, the free string state ($g_s = 0$) is replaced by a state of strings and D-branes ($g_s \ll 1$). The reasoning goes as follow. Given that string theory predicts extra dimensions of space, we have to compactify $10 - d$ of them in order to obtain a d -dimensional black hole. When we do that, the resulting black hole will have charges coming from three sources: internal momentum in a given compact direction, strings winding around the compact directions and D-branes winding around the compact directions. However, even in that case, the size of the black hole becomes smaller when the string coupling decreases, so that we can still match entropy of the black hole picture ($g_s \gg 1$) to that of a typical state of strings and D-branes ($g_s \ll 1$). Again, the transition happens when the size of the black hole is of the order of the string length.

We are finally in a position to give a more precise statement of the correspondence principle between black holes and strings:

1. Given a black hole, if the curvature at its horizon becomes greater than scale set by the string length, the typical black hole state becomes a typical state of strings and D-branes with the same conserved charges.
2. As the transition from one picture to the other occurs, the mass changes by at most a factor of order unity.

The above black hole-string correspondence proposed by Susskind and refined by Horowitz and Polchinski gives the correct dependence of the entropies on the excitation level N or, equivalently, on the mass $M = M_s = M_{bh}$. However, it does not allow us to compute and compare the coefficients of the entropies, because that requires knowing when exactly the transition from one picture to the other occurs (recall that we gave the *estimate* that it happens when $r_0 \sim \ell_s$). Nevertheless, this correspondence principle shows that strings have enough states to account for the Bekenstein-Hawking entropy of black holes.

3.4 Constructing black holes in string theory

It should be clear by now that in order to have a full understanding of black holes and the physical processes that take place in them, we need a theory of quantum gravity. Therefore, we should hope that string theory correctly reproduces the semiclassical features of black holes and that it could also elucidate the problems related to their thermal nature (see [chapter 2](#)). Indeed, starting with the work of Strominger and Vafa [10], string theoretical derivations of the Bekenstein-Hawking entropy of a variety of black holes have been given. The method they introduced not only gives the correct dependence of the entropy on some of the black hole parameters, but correctly reproduces the exact coefficients appearing in the entropy formulas. Let us now explain concisely how all this comes about.

The discrepancy between the entropies of a string and a black hole in (3.6) was solved in the previous section, where we explained the correspondence principle between black holes and strings. However, that method does not allow us to compute the exact coefficients appearing in the entropy formulas. In order to do so, we would need to know the exact value of the string coupling at which the transition from one picture to the other occurs. Imagine now that we could find states (on either side of the correspondence) that move together as we change g_s . Were we able to do so, we would not need to worry about knowing the precise value of the coupling at which the transition occurs: the density of states would not vary as we change the coupling and this, in turn, would make the entropies on both sides of the correspondence match. This is where BPS states come in. We have seen that the mass of a BPS saturated state is determined by its charge and the moduli of the theory ($M = Q$ in suitable units). When constructing black holes in string theory, the charge of a state will be just given by its winding number around the compact directions. Thus, for BPS states, we may calculate the number of states at weak coupling and compare it with the result at strong coupling, because all BPS states of mass M will move together as we change g_s : they will be uniquely determined by their charges, which are not coupling-dependent. The corresponding

black holes that we expect at strong coupling are supergravity⁶ solutions and, as the name of the theory implies, they are supersymmetric. These black holes are extremal in the sense that they have the minimal mass allowed by their charge in order to avoid a naked singularity.

In short, the strategy is the following. We start at strong coupling with a supersymmetric black hole, whose Bekenstein-Hawking entropy is known from geometrical arguments. We then decrease the coupling and count the number of BPS states at weak coupling that have the same charge as that of the black hole. The result is that the number of BPS states at weak coupling is exactly the exponential of the Bekenstein-Hawking entropy of the black hole at strong coupling (for a well-written and pedagogical review, see [13]).

Since we are interested in black holes with non-vanishing entropy in the supergravity limit, we want them to have finite horizon area. It turns out that in order to obtain this type of black hole in four and five spacetime dimensions, we need to add four and three charges, respectively. Otherwise, the resulting black hole will have zero horizon area. Some of these extra charges are not carried by fundamental strings, but rather by D-branes. Therefore, we will construct black holes using both strings and D-branes. For clarity, let us explain how to construct a prototypical example: a five-dimensional black hole with three charges. Since string theory lives in ten dimensions and we want a five-dimensional black hole, we need to compactify five spatial directions. The simplest case is that in which the compactified space is a five-torus $T^5 = T^4 \times S^1$. We now take Q_5 D5-branes wrapped around T^5 , Q_1 D1-branes (fundamental strings) wrapped around S^1 and finally, we add Q_p units of momentum in the S^1 direction. From the point of view of the non-compact five-dimensional spacetime, all these objects lie on the same point; therefore the configuration that we just gave describes a localized object in five spacetime dimensions.

In the strong coupling regime (black hole picture), the D-branes used in our construction do not appear in the usual sense of higher-dimensional membranes; rather, only the D-brane charges are the ones taken into account to write the supergravity black hole solution with finite horizon area. The Bekenstein-Hawking entropy and other quantities are computed in terms of these charges and other parameters that appear in the supergravity solution.

In the weak coupling regime (string-D-brane picture), the D-branes used in our construction do appear as higher-dimensional membranes on which strings end. They form a D-brane bound state, whose dynamics are described by a two-dimensional supersymmetric gauge theory, in which we can count the number of states that have the appropriate charges. This will allow us to compute the entropy of the system and see that it matches with the entropy computed in the strong coupling regime. We should stress that the D-brane bound state computation is done in ten-dimensional Minkowski spacetime, which is the spacetime predicted by string theory when the interactions in the theory are sufficiently weak.

Before concluding our present discussion and giving an explicit example in the next section, we would like mention an important point. We have said previously that the

⁶The low energy limit of string theory is a supergravity theory.

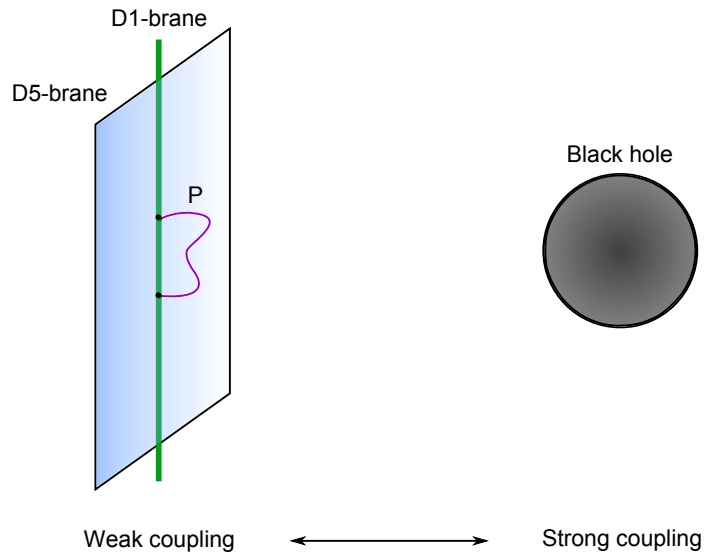


Figure 3.5: D-brane construction of a five-dimensional black hole. In the weak coupling regime, we have a D1-D5-P bound state. In the strong coupling regime, we have a black hole with three charges corresponding to those of the D-branes.

type of black hole resulting from the string theory construction is supersymmetric. This, in turn, implies that they have zero temperature and thus do not radiate. One may wonder why are we interested in studying these type of black holes at all. The reason is twofold. Firstly, extremal black holes were the first for which a precise agreement was found between the entropy in the strong coupling regime and that in the weak coupling regime. Secondly, it turns out that using the same construction explained above, we can obtain black holes that are non-extremal with nonzero temperature. The process of Hawking radiation should then be somehow realized in the D-brane bound state picture. This is indeed the case and we will explain it in [chapter 7](#).

3.5 A five-dimensional black hole with three charges

In [21], Horowitz, Maldacena and Strominger found a general metric for a five-dimensional black hole with three charges, like the one obtained from our D-brane construction. They considered the low-energy action for ten-dimensional type-IIB string theory (known as type-IIB supergravity) and compactified five spatial dimensions on $T^5 = T^4 \times S^1$, adding momentum p in the S^1 direction. The noncompact directions are labeled by coordinates x^μ , $\mu = 0, \dots, 4$, the compact directions of T^4 are labeled by x^i , $i = 6, \dots, 9$ and we choose the S^1 to be in the direction of x^5 . The length of the S^1 is $2\pi R$ and the volume of the T^4 is $(2\pi)^4 V$.

The authors found a six parameter family of solutions to the equations of motion corresponding to the ten-dimensional action mentioned above. In the Einstein frame,

this solution is given by

$$\begin{aligned}
ds_{10}^2 = & \left(1 + \frac{r_0^2 \sinh^2 \alpha_1}{r^2}\right)^{-3/4} \left(1 + \frac{r_0^2 \sinh^2 \alpha_5}{r^2}\right)^{-1/4} \left[-dt^2 + dx_5^2 + \right. \\
& \left. + \frac{r_0^2}{r^2} (\cosh \alpha_p dt + \sinh \alpha_p dx_5)^2 + \left(1 + \frac{r_0^2 \sinh^2 \alpha_1}{r^2}\right) dx_i dx^i \right] + \\
& + \left(1 + \frac{r_0^2 \sinh^2 \alpha_1}{r^2}\right)^{1/4} \left(1 + \frac{r_0^2 \sinh^2 \alpha_5}{r^2}\right)^{3/4} \left[\left(1 - \frac{r_0^2}{r^2}\right)^{-1} dr^2 + r^2 d\Omega_3^2 \right],
\end{aligned} \tag{3.7}$$

where

$$r^2 = x_1^2 + x_2^2 + x_3^2 + x_4^2$$

and $d\Omega_3^2$ is the metric on a 3-sphere. If we wanted the solution in the string frame, we would simply make use of the equation given in our conventions that conformally relates the Einstein and string metrics. With $d = 10$, we would have $g_{\mu\nu}^S = e^{\frac{\Phi}{2}} g_{\mu\nu}^E$, where in this case

$$e^{-2\Phi} = \left(1 + \frac{r_0^2 \sinh^2 \alpha_5}{r^2}\right) \left(1 + \frac{r_0^2 \sinh^2 \alpha_1}{r^2}\right)^{-1}.$$

As we see, the above ten-dimensional solution is parametrized by six quantities: α_1 , α_5 , α_p , r_0 , R and V . The role played by α_i and r_0 will be explained below. We can define three charges (normalized to be integers) in terms of the previous six parameters as

$$\begin{aligned}
Q_1 &= \frac{V r_0^2}{2g_s \ell_s^6} \sinh 2\alpha_1, \\
Q_5 &= \frac{r_0^2}{2g_s \ell_s^2} \sinh 2\alpha_5, \\
Q_p &= \frac{R^2 V r_0^2}{2g_s^2 \ell_s^8} \sinh 2\alpha_p.
\end{aligned} \tag{3.8}$$

The last charge is related to the momentum added in the S^1 direction by $p = Q_p/R$. These three charges are precisely the ones associated with the D-branes used in our black hole construction. As we explained in the previous section, the D-branes do not appear in our current discussion as higher-dimensional objects, but rather, only their charges are of interest to us because they allow us to write the desired supergravity solution.

Now, by following the standard procedure of dimensional reduction for our case $T^5 = T^4 \times S^1$, we can bring down the ten-dimensional solution (3.7) to five dimensions, where it takes the remarkably simple and symmetric form in the Einstein frame

$$ds_5^2 = -\lambda^{-2/3} h dt^2 + \lambda^{1/3} \left(\frac{dr^2}{h} + r^2 d\Omega_3^2 \right), \tag{3.9}$$

where

$$\lambda = \prod_{j=1,5,p} \left(1 + \frac{r_0^2 \sinh^2 \alpha_j}{r^2} \right) = \prod_{j=1,5,p} \left(1 + \frac{r_j^2}{r^2} \right) \quad (3.10)$$

and

$$h = 1 - \frac{r_0^2}{r^2}. \quad (3.11)$$

This is just the five-dimensional Schwarzschild metric with the time and space components rescaled by different powers of λ . It is obviously a static solution, since none of the metric components depends on time. Despite the fact that the coefficient of $d\Omega_3^2$ is not only r^2 (as it is in the Schwarzschild case, for example), this is still a spherically symmetric solution. In general, we can identify a d -dimensional, spherically symmetric metric if the unit $(d-2)$ -sphere $d\Omega_{d-2}^2$ appears explicitly.

The horizon structure of this solution can be directly read-off from the metric above. There is an event horizon located at $r = r_0$, but due to the choice of coordinates, there is also an inner horizon located at $r = 0$, given that all three charges are nonzero. If one of the charges is set to zero, the surface $r = 0$ becomes singular.

Now that we have this explicit solution, the relevant thermodynamical quantities of this black hole can be computed. For example, the Hawking temperature is given by (see [Appendix C](#) for a derivation of this result)

$$T_H = \frac{1}{2\pi r_0 \cosh \alpha_1 \cosh \alpha_5 \cosh \alpha_p}. \quad (3.12)$$

The Bekenstein-Hawking entropy can be calculated from geometrical arguments, by first finding the area of the five-dimensional black hole. It is easy to see from (3.9) that the radial size of the horizon is

$$r_h = r_0 [\lambda(r_0)]^{1/6},$$

so that the area of the black hole is that of a 3-sphere with radius r_h , given by

$$A_5 = 2\pi^2 r_h^3 = 2\pi^2 r_0^3 \cosh \alpha_1 \cosh \alpha_5 \cosh \alpha_p.$$

We now recall from (3.2) and (3.3) that the five-dimensional Newton constant is given by (in our case, the volume of the compactified space is just $(2\pi)^5 RV$)

$$G_5 = \frac{\pi g_s^2 \ell_s^8}{4RV}.$$

Then, the Bekenstein-Hawking entropy of the black hole is just

$$S_{bh} = \frac{A_5}{4G_5} = \frac{2\pi RV r_0^3}{g_s^2 \ell_s^8} \cosh \alpha_1 \cosh \alpha_5 \cosh \alpha_p. \quad (3.13)$$

Given that we want our supergravity approximation to remain valid everywhere, we must require that the geometry is slowly varying at the string scale. This implies that

$r_{1,5,p} \gg \ell_s$. In turn, these conditions become

$$g_s Q_1 \gg \frac{V}{\ell_s^4}, \quad g_s Q_5 \gg 1, \quad g_s^2 Q_p \gg \frac{R^2 V}{\ell_s^6}.$$

The above conditions for the charges and other parameters of the black hole solution are derived in the D-brane picture ($g_s \ll 1$). Therefore, given that the compactification sizes R and V are of the order of some powers of the string length ℓ_s , we see that the charges $Q_{1,5,p}$ must be large. This is true in general: black hole solutions always involve large values of the charges.

3.5.1 Special cases

The five-dimensional black hole with three charges (3.9) depends on α_1 , α_5 , α_p and r_0 . Let us now see what well-known black hole solutions can be obtained depending on the values that we assign to these parameters. We will also write their corresponding temperature and Bekenstein-Hawking entropy, which can be obtained from (3.12) and (3.13), respectively. We will only show black hole solutions, but we should mention that other black objects, such as black strings and black branes, can be obtained from (3.9) [21].

Schwarzschild solution

This case clearly corresponds to setting $\alpha_1 = \alpha_5 = \alpha_p = 0$, so that the metric (3.9) reduces to

$$ds_5^2 = -h dt^2 + h^{-1} dr^2 + r^2 d\Omega_3^2,$$

which is immediately recognized as the usual Schwarzschild black hole in five dimensions, with h given by (3.11). Note that it has exactly the form that we gave in (1.5) for the $(4+n)$ -dimensional Schwarzschild black hole, with $n = 1$. The relevant thermodynamical quantities in this case are given by

$$T_H = \frac{1}{2\pi r_0},$$

$$S_{bh} = \frac{2\pi R V r_0^3}{g_s^2 \ell_s^8}.$$

Reissner-Nordström solution

This case corresponds to $\alpha_1 = \alpha_5 = \alpha_p = \alpha$, so that (3.10) becomes

$$\lambda = \left(1 + \frac{r_0^2 \sinh^2 \alpha}{r^2}\right)^3$$

By defining a new coordinate as $\rho^2 = r^2 + r_0^2 \sinh^2 \alpha$, so that the horizons $r = 0$ and $r = r_0$ are now located at $\rho^2 = r_0^2 \sinh^2 \alpha$ and $\rho^2 = r_0^2 (1 + \sinh^2 \alpha)$ respectively, we can

bring the metric (3.9) to the following form

$$ds_5^2 = -h dt^2 + h^{-1} d\rho^2 + \rho^2 d\Omega_3^2,$$

where in this case, h is given by

$$h = \left(1 - \frac{r_0^2 (1 + \sinh^2 \alpha)}{\rho^2}\right) \left(1 - \frac{r_0^2 \sinh^2 \alpha}{\rho^2}\right).$$

Note that it has exactly the form that we gave in (1.14) for the $(4+n)$ -dimensional Reissner-Nordström black hole, with $n = 1$. The thermodynamical properties in this case are given by

$$T_H = \frac{1}{2\pi r_0 \cosh^3 \alpha},$$

$$S_{bh} = \frac{2\pi R V r_0^3}{g_s^2 \ell_s^8} \cosh^3 \alpha.$$

Extremal solution

This case corresponds to $r_0 \rightarrow 0$ with $\alpha_1, \alpha_5, \alpha_p \rightarrow \infty$, keeping R, V and the charges Q_1, Q_5 and Q_p fixed. The metric (3.9) becomes

$$ds_5^2 = -\lambda^{-2/3} dt^2 + \lambda^{1/3} (dr^2 + r^2 d\Omega_3^2),$$

with λ given by (3.10). A peculiar thing happens in this case, namely, as a consequence of α_j going to infinity, then $\cosh \alpha_j \rightarrow \infty$, which clearly makes the temperature of this black hole to vanish

$$T_H = 0.$$

However, the entropy is nonzero. Since $\alpha_j \rightarrow \infty$, we can use the approximation $\sinh 2\alpha_j \approx 2 \sinh^2 \alpha_j = 2 \cosh^2 \alpha_j$, with which the charges (3.8) can be written as

$$Q_1 = \frac{V r_0^2}{g_s \ell_s^6} \sinh^2 \alpha_1,$$

$$Q_5 = \frac{r_0^2}{g_s \ell_s^2} \sinh^2 \alpha_5,$$

$$Q_p = \frac{R^2 V r_0^2}{g_s^2 \ell_s^8} \sinh^2 \alpha_p. \quad (3.14)$$

In this case, it is easy to see that the entropy (3.13) can be written in terms of these charges as

$$S_{bh} = 2\pi \sqrt{Q_1 Q_5 Q_p}.$$

Near-extremal solution

Strictly speaking, (3.9) is already a non-extremal solution. However, we want to have a near-extremal solution, which is the limit where r_0 is small and $\alpha_1, \alpha_5, \alpha_p$ large.

Obviously, these conditions give a large range of possibilities for the near-extremal solution. To be more specific, we will be interested in the case when $\alpha_p \ll \alpha_1, \alpha_5$. That is, when the contribution to the mass of the black hole due to the D1- and D5-branes is much larger than the contribution due to the momentum excitations. This is known as the *dilute gas region* and it is defined by [22]

$$r_0, r_p \ll r_1, r_5, \quad (3.15)$$

which is equivalent to the condition on α_j given above and the r_j are defined as in (3.10).

Let us now give the thermodynamical properties of this black hole. Given that in this case $\alpha_p \ll \alpha_1, \alpha_5$, we can use the approximation yet again $\sinh 2\alpha_j \approx 2 \sinh^2 \alpha_j = 2 \cosh^2 \alpha_j$ for α_1 and α_5 , so that their corresponding charges are those given in (3.14). In this case, we get

$$T_H = \frac{\sqrt{V} r_0}{2\pi g_s \ell_s^4 \sqrt{Q_1 Q_5} \cosh \alpha_p},$$

$$S_{bh} = \frac{2\pi R \sqrt{V} r_0}{g_s \ell_s^4} \sqrt{Q_1 Q_5} \cosh \alpha_p.$$

However, there is a much more convenient form to write these two quantities, that will help us in understanding the D-brane description of this near-extremal black hole (we will do that in chapter 7). Using again (3.14) and recalling that $r_j^2 = r_0^2 \sinh^2 \alpha_j$, we can write

$$T_H = \frac{r_0}{2\pi r_1 r_5 \cosh \alpha_p},$$

$$S_{bh} = \frac{2\pi R V r_0 r_1 r_5}{g_s^2 \ell_s^8} \cosh \alpha_p. \quad (3.16)$$

The crucial step is to realize that we can write these two expressions as

$$\frac{1}{T_H} = \frac{1}{2} \left(\frac{1}{T_L} + \frac{1}{T_R} \right),$$

$$S_{bh} = S_L + S_R, \quad (3.17)$$

with

$$T_L = \frac{r_0}{2\pi r_1 r_5} e^{\alpha_p}, \quad T_R = \frac{r_0}{2\pi r_1 r_5} e^{-\alpha_p}, \quad (3.18)$$

and

$$S_L = \frac{\pi R V r_0 r_1 r_5}{g_s^2 \ell_s^8} e^{\alpha_p}, \quad S_R = \frac{\pi R V r_0 r_1 r_5}{g_s^2 \ell_s^8} e^{-\alpha_p}. \quad (3.19)$$

The subscripts L, R will become clear in our description of the D-brane bound state corresponding to this black hole. Furthermore, the entropies and the temperatures above are related by (where we use (3.14))

$$T_{L,R} = \frac{S_{L,R}}{2\pi^2 R Q_1 Q_5}. \quad (3.20)$$

Part II

Greybody Factors: Hawking Radiation in Disguise

Chapter 4

Klein-Gordon equation in black hole backgrounds

In this chapter, we present solutions of the Klein-Gordon equation for a massless scalar field in two types of black hole backgrounds. Namely, in four-dimensional, static and spherically symmetric black hole backgrounds and in the five-dimensional black hole background with three charges presented in [chapter 3](#). The results we obtain will constitute the starting point of the semiclassical computation of greybody factors.

4.1 $d = 4$ black hole backgrounds

Let us consider a static and spherically symmetric black hole background in four dimensions. In spherical coordinates (t, r, θ, ϕ) , the metric is given by

$$ds^2 = -f(r)dt^2 + f(r)^{-1}dr^2 + r^2 d\Omega_2^2, \quad (4.1)$$

with $d\Omega_2^2 = d\theta^2 + \sin^2\theta d\phi^2$ the metric on a unit 2-sphere S^2 . We want to solve the Klein-Gordon equation for a massless uncharged scalar field in this background, which reads (see [Appendix D](#) for a short reminder on how this equation comes about)

$$\nabla^\mu \partial_\mu \Phi = 0. \quad (4.2)$$

Recalling that the covariant derivative acting on a one-form is defined as $\nabla_\nu V_\mu = \partial_\nu V_\mu - \Gamma_{\nu\mu}^\lambda V_\lambda$, we can rewrite the Klein-Gordon equation as

$$g^{\mu\nu} \left(\partial_\mu \partial_\nu - \Gamma_{\mu\nu}^\lambda \partial_\lambda \right) \Phi = 0, \quad (4.3)$$

where $\Gamma_{\mu\nu}^\lambda$ are the usual Christoffel symbols defined as

$$\Gamma_{\mu\nu}^\lambda = \frac{g^{\lambda\rho}}{2} (\partial_\mu g_{\nu\rho} + \partial_\nu g_{\rho\mu} - \partial_\rho g_{\mu\nu}).$$

Given that the metric is diagonal, we only need to compute the nonzero Christoffel

symbols that have $\mu = \nu$. They are the following

$$\begin{aligned}\Gamma_{tt}^r &= \frac{f}{2}f' & \Gamma_{rr}^r &= -\frac{f^{-1}}{2}f' \\ \Gamma_{\theta\theta}^r &= -rf & \Gamma_{\phi\phi}^r &= -rf\sin^2\theta \\ \Gamma_{\phi\phi}^\theta &= -\sin\theta\cos\theta,\end{aligned}$$

with $f' = \partial_r f$. Putting all these expressions in (4.3), we obtain

$$\left[-f^{-1}\partial_t^2 + f\partial_r^2 + \frac{1}{r^2}\partial_\theta^2 + \frac{1}{r^2\sin^2\theta}\partial_\phi^2 + \left(f' + \frac{2}{r}f\right)\partial_r + \frac{\cos\theta}{r^2\sin\theta}\partial_\theta\right]\Phi = 0. \quad (4.4)$$

The symmetries of the black hole background allow us to simplify the above equation. First, because of the spherical symmetry, we can write the field as

$$\Phi = U(t, r)Y(\theta, \phi), \quad (4.5)$$

which, using the standard method of separation of variables, enables us to split (4.4) in two parts: one depending only on t and r and the other depending only on θ and ϕ . Each of these parts is a differential equation, which must be equal to a constant. In our case, we choose the $U(t, r)$ equation to be equal to k^2 , hence, the $Y(\theta, \phi)$ equation will be equal to $-k^2$. The two resulting equations are

$$\left[-f^{-1}\partial_t^2 + f\partial_r^2 + \left(f' + \frac{2}{r}f\right)\partial_r\right]U(t, r) = \frac{k^2}{r^2}U(t, r), \quad (4.6)$$

$$\left[\partial_\theta^2 + \frac{1}{\sin^2\theta}\partial_\phi^2 + \frac{\cos\theta}{\sin\theta}\partial_\theta\right]Y(\theta, \phi) = -k^2Y(\theta, \phi). \quad (4.7)$$

We still have to determine the constant k^2 . To do so, notice that (4.7) can be written as

$$\frac{1}{\sin\theta}\partial_\theta(\sin\theta\partial_\theta Y) + \frac{1}{\sin^2\theta}\partial_\phi^2 Y + k^2 Y = 0.$$

This is exactly the equation for the spherical harmonics Y_{lm} (hence our choice to name Y the angular dependent part in (4.5)) that one obtains from Laplace's equation in spherical coordinates on S^2 . Therefore, our constant k^2 is equal to $l(l+1)$, with l the eigenvalues of the Laplacian on the two-sphere.

Let us now make use of the translational symmetry of the black hole background. It allows us to write

$$U(t, r) = T(t)\phi(r),$$

with which we can split (4.6) in two parts: one depending only on t and the other depending only on r . We choose the $T(t)$ equation to be equal to ω^2 , hence, the $\phi(r)$ equation will be equal to $-\omega^2$. The two equations we get are

$$\partial_t^2 T(t) = -\omega^2 T(t), \quad (4.8)$$

$$\left[f^2\partial_r^2 + f\left(f' + \frac{2}{r}f\right)\partial_r\right]\phi(r) = \left[f\frac{l(l+1)}{r^2} - \omega^2\right]\phi(r). \quad (4.9)$$

Therefore, we have that $T = e^{i\omega t}$. We do not take into account solutions that go like $e^{-i\omega t}$ because we consider those to move in the negative time direction. Note that our choice to name the constant ω^2 was because ω will be the frequency of the wave. By making the following change of variable

$$\phi(r) = r^{-1}\psi(r),$$

we can simplify (4.9) to

$$[f^2\partial_r^2 + ff'\partial_r]\psi = \left\{ f \left[\frac{l(l+1)}{r^2} + \frac{f'}{r} \right] - \omega^2 \right\} \psi. \quad (4.10)$$

In order to simplify even more this equation, we define the so-called tortoise coordinate x as

$$x \equiv \int \frac{dr}{f(r)}, \quad (4.11)$$

so that $\partial_x = f\partial_r$ and $\partial_x^2 = f^2\partial_r^2 + ff'\partial_r$. Finally, the equation for the radial part of our scalar field becomes

$$\left(\frac{d^2}{dx^2} + \omega^2 - V(r) \right) \psi(r) = 0, \quad (4.12)$$

with $V(r)$ given by

$$V(r) = f(r) \left[\frac{l(l+1)}{r^2} + \frac{f'(r)}{r} \right]. \quad (4.13)$$

Of course, in order to solve the above equation, we still need to express $\psi(r)$ and r in terms of the tortoise coordinate x (4.11). The reason to name V this part of the expression will become clear in the next chapter.

4.1.1 Generalizations

Still in four dimensions, our result can be generalized for the case of fields of nonzero spin. For example, we might want to consider the propagation of an electromagnetic test-field ($j = 1$) or a linearized perturbation of the metric ($j = 2$). The resulting Schrödinger-like equation is exactly (4.12), but with the potential $V(r)$ given by [23, 24]

$$V(r) = f(r) \left[\frac{l(l+1)}{r^2} + \frac{f'(r)(1-j^2)}{r} \right]. \quad (4.14)$$

We should stress that this result is valid when the black hole under consideration does not carry any electric or magnetic charge. See Appendix F for a brief discussion on how it gets modified in the case of a charged black hole.

Futhermore, the case of the massless uncharged scalar field can be generalized to higher dimensions. In spherical coordinate $(t, r, \theta, \phi, \xi_1, \xi_2, \dots, \xi_{d-4})$, the metric of a static and spherically symmetric black hole background in d dimensions ($d \geq 4$) is given by

$$ds_d^2 = -f(r)dt^2 + f(r)^{-1}dr^2 + r^2 d\Omega_{d-2}^2. \quad (4.15)$$

The metric on a unit $(d-2)$ -sphere ($d > 4$) is given by the following relation

$$d\Omega_{d-2}^2 = d\xi_{d-4}^2 + \sin^2 \xi_{d-4} d\Omega_{d-3}^2 \quad (4.16)$$

with the well-known formula for a unit 2-sphere $d\Omega_2^2 = d\theta^2 + \sin^2 \theta d\phi^2$, so that

$$\begin{aligned} d\Omega_3^2 &= d\xi_1^2 + \sin^2 \xi_1 d\Omega_2^2, \\ d\Omega_4^2 &= d\xi_2^2 + \sin^2 \xi_2 d\Omega_3^2, \\ &\vdots \end{aligned}$$

When solving the Klein-Gordon equation in the background (4.15), there will be other non-vanishing Christoffel symbols, such as $\Gamma_{\xi_j \xi_j}^r$, $\Gamma_{\theta\theta}^{\xi_j}$, $\Gamma_{\phi\phi}^{\xi_j}$ and so on. After following a similar procedure to the one we explained for the four-dimensional case, we obtain again the Schrödinger-like equation, but with the scalar field decomposed as¹

$$\Phi = \phi(r) e^{i\omega t} Y_{lm\dots}(\Omega_{d-2}), \quad (4.17)$$

where

$$\phi(r) = r^{\frac{2-d}{2}} \psi(r) \quad (4.18)$$

and the potential $V(r)$ is given by [25]

$$V(r) = f(r) \left[\frac{l(l+d-3)}{r^2} + \frac{(d-2)(d-4)f(r)}{4r^2} + \frac{(d-2)f'(r)}{2r} \right]. \quad (4.19)$$

4.2 $d = 5$ black hole background with three charges

Let us now consider the five-dimensional black hole with three charges presented in chapter 3. In spherical coordinates $(t, r, \theta, \phi, \xi)$, the metric is given by

$$ds_5^2 = -\lambda^{-2/3} h dt^2 + \lambda^{1/3} \left(\frac{dr^2}{h} + r^2 d\Omega_3^2 \right), \quad (4.20)$$

with

$$d\Omega_3^2 = d\xi^2 + \sin^2 \xi (d\theta^2 + \sin^2 \theta d\phi^2)$$

the metric on a unit 3-sphere S^3 and $\lambda(r)$ and $h(r)$ defined as in (3.10) and (3.11). To solve the Klein-Gordon equation in this case, we need to compute the corresponding Christoffel symbols that have $\mu = \nu$. They are the following

$$\begin{aligned} \Gamma_{tt}^r &= -\frac{1}{3} \lambda^{-2} \lambda' h^2 + \frac{1}{2} \lambda^{-1} h h' & \Gamma_{rr}^r &= -\frac{1}{6} \lambda^{-1} \lambda' - \frac{1}{2} h^{-1} h' \\ \Gamma_{\phi\phi}^\theta &= -\sin \theta \cos \theta & \Gamma_{\theta\theta}^\xi &= -\sin \xi \cos \xi \end{aligned}$$

¹The following decomposition holds in general for higher-dimensional, spherically symmetric black holes. Of course, $Y_{lm\dots}(\Omega_{d-2})$ are just the higher-dimensional spherical harmonics on the S^{d-2} sphere.

$$\begin{aligned}\Gamma_{\phi\phi}^\xi &= -\sin\xi\cos\xi\sin^2\theta & \Gamma_{\xi\xi}^r &= -hr - \frac{1}{6}\lambda^{-1}\lambda'hr^2 \\ \Gamma_{\theta\theta}^r &= -\left(\frac{1}{6}\lambda^{-1}\lambda'hr^2 + hr\right)\sin^2\xi & \Gamma_{\phi\phi}^r &= -\left(\frac{1}{6}\lambda^{-1}\lambda'hr^2 + hr\right)\sin^2\xi\sin^2\theta,\end{aligned}$$

with $h' = \partial_r h$ and $\lambda' = \partial_r \lambda$. Putting all these expressions into the massless Klein-Gordon equation, we obtain

$$\begin{aligned}\left[-\lambda\partial_t^2 + h^2\partial_r^2 + \frac{h}{r^2\sin^2\xi}\partial_\theta^2 + \frac{h}{r^2\sin^2\xi\sin^2\theta}\partial_\phi^2 + \frac{h}{r^2}\partial_\xi^2 + \right. \\ \left. + \left(hh' + \frac{3h^2}{r} \right) \partial_r + \frac{h\cos\theta}{r^2\sin^2\xi\sin\theta}\partial_\theta + \frac{2h\cos\xi}{r^2\sin\xi}\partial_\xi \right] \Phi = 0.\end{aligned}\quad (4.21)$$

We now decompose the field as

$$\Phi = U(t, r)Y(\theta, \phi, \xi). \quad (4.22)$$

With this, we can split (4.21) in two parts: one depending only on t and r and the other depending on θ , ϕ and ξ . Each of these parts must be equal to a constant and we choose the U equation to be equal to k^2 , hence, the Y will be equal to $-k^2$. The two resulting equations are

$$\left[-\lambda\partial_t^2 + h^2\partial_r^2 + \left(hh' + \frac{3h^2}{r} \right) \partial_r \right] U = k^2 \frac{h}{r^2} U, \quad (4.23)$$

$$\left[\partial_\xi^2 + 2\frac{\cos\xi}{\sin\xi}\partial_\xi + \frac{1}{\sin^2\xi}\partial_\theta^2 + \frac{1}{\sin^2\xi\sin^2\theta}\partial_\phi^2 + \frac{\cos\theta}{\sin^2\xi\sin\theta}\partial_\theta \right] Y = -k^2 Y. \quad (4.24)$$

In order to determine the constant k^2 , note that (4.24) can be written as

$$\partial_\xi^2 Y + 2\frac{\cos\xi}{\sin\xi}\partial_\xi Y + \frac{1}{\sin^2\xi}\partial_\theta(\sin\theta\partial_\theta)Y + \frac{1}{\sin^2\xi\sin^2\theta}\partial_\phi^2 Y + k^2 Y = 0.$$

With $k^2 = l(l+2)$, this is exactly the equation for the spherical harmonics $Y_{lmm'}$ (hence our choice to name Y the angular dependent part) that one obtains from Laplace's equation in spherical coordinates on S^3 .

Now, just as in the four-dimensional case, let us write

$$U(t, r) = T(t)\phi(r),$$

with which we can split (4.23) in two parts: one depending only on t and the other depending only on r . We choose the $T(t)$ equation to be equal to ω^2 , hence, the $\phi(r)$ equation will be equal to $-\omega^2$. The two equations we get are

$$\partial_t^2 T(t) = -\omega^2 T(t), \quad (4.25)$$

$$\left[\frac{h^2}{\lambda}\partial_r^2 + \frac{1}{\lambda}\left(hh' + \frac{3h^2}{r} \right) \partial_r \right] \phi(r) = \left[\frac{h}{\lambda}\frac{l(l+2)}{r^2} - \omega^2 \right] \phi(r). \quad (4.26)$$

Again, we have that $T = e^{i\omega t}$. By making the following change of variable

$$\phi(r) = r^{-3/2}\psi(r),$$

we can simplify (4.26) to

$$[h^2\partial_r^2 + hh'\partial_r]\psi = \left[h\frac{l(l+2)}{r^2} + \frac{3h^2}{4}\frac{1}{r^2} + \frac{3hh'}{2}\frac{1}{r} - \lambda\omega^2 \right]\psi. \quad (4.27)$$

Furthermore, let us introduce the tortoise coordinate, defined for the black hole background (4.20) as

$$x \equiv \int \frac{dr}{h(r)}, \quad (4.28)$$

so that $\partial_x = h\partial_r$ and $\partial_x^2 = h^2\partial_r^2 + hh'\partial_r$. Finally, the equation for the radial part of our scalar field becomes

$$\left(\frac{d^2}{dx^2} + \lambda\omega^2 - V(r) \right) \psi(r) = 0, \quad (4.29)$$

with $V(r)$ given by

$$V(r) = h\frac{l(l+2)}{r^2} + \frac{3h^2}{4}\frac{1}{r^2} + \frac{3hh'}{2}\frac{1}{r}. \quad (4.30)$$

Again, in order to solve the above equation, we still need to express $\psi(r)$, $h(r)$, $\lambda(r)$ and r in terms of the tortoise coordinate x (4.28).

4.3 S-wave approximation

So far, we have not said anything about the frequency ω of the equations we derived in the two previous sections. That is, (4.12) and (4.29) are valid for *any* value of the frequency. However, we can further simplify our results if we consider the low frequency regime. Indeed, in [26], Unruh showed that in this limit, we can restrict to spherically symmetric solutions of the wave equation (known as *S-waves*), because higher angular momentum components will not be absorbed by the black hole. (We will explain in chapter 5 that the classical absorption cross-section is just equal to the greybody factor.) Therefore, in order to solve the Klein-Gordon equation for the massless scalar field $\nabla^\mu\partial_\mu\Phi = 0$ in the low frequency limit, the field decomposition that we need to consider is just

$$\Phi = e^{i\omega t}\phi(r)$$

In order to obtain the S-wave solution, we need not go through all the steps in the calculations. It suffices to take $l = 0$ in the formulas we derived in the previous two sections.

$d = 4$ black hole

For the four-dimensional black hole background (4.1), we can obtain the equation for $\phi(r)$ by setting $l = 0$ in (4.9). We get

$$\left[f^2 \partial_r^2 + f \left(f' + \frac{2}{r} f \right) \partial_r + \omega^2 \right] \phi(r) = 0. \quad (4.31)$$

Now, using the tortoise coordinate (4.11) and writing again

$$\phi(r) = r^{-1} \psi(r),$$

we can write the last equation as

$$\left(\frac{d^2}{dx^2} + \omega^2 - V(r) \right) \psi(r) = 0, \quad (4.32)$$

with $V(r)$ given by

$$V(r) = \frac{f(r)f'(r)}{r}. \quad (4.33)$$

 $d = 5$ black hole with three charges

For the five-dimensional black hole background with three charges (4.20), we can obtain the equation for $\phi(r)$ by setting $l = 0$ in (4.26). We get

$$\left[h^2 \partial_r^2 + \left(hh' + \frac{3h^2}{r} \right) \partial_r + \lambda \omega^2 \right] \phi(r) = 0, \quad (4.34)$$

which can be further simplified to

$$\left[\frac{h}{r^3} \frac{d}{dr} \left(hr^3 \frac{d}{dr} \right) + \lambda \omega^2 \right] \phi(r) = 0. \quad (4.35)$$

Now, using the tortoise coordinate (4.28) and writing again

$$\phi(r) = r^{-3/2} \psi(r),$$

we can write the last equation as

$$\left(\frac{d^2}{dx^2} + \lambda \omega^2 - V(r) \right) \psi(r) = 0, \quad (4.36)$$

with $V(r)$ given by

$$V(r) = \frac{3h^2}{4} \frac{1}{r^2} + \frac{3hh'}{2} \frac{1}{r}. \quad (4.37)$$

Chapter 5

Greybody factors

In this chapter, we introduce the concept of greybody factors and review some qualitative ideas about black hole scattering theory that will help us in the calculations that we will do in the next chapters. We also explain the important qualitative and quantitative differences between the computation of greybody factors in the low and high frequency regimes.

5.1 Modifying Hawking radiation

It should be clear by now that black holes are thermal systems: they have an associated temperature and entropy and therefore also radiate. The radiation that black holes emit is known as Hawking radiation, because in [7] he showed that exactly at the event horizon, the emission rate of a black hole in a mode with frequency ω is given by

$$\Gamma(\omega) = \frac{1}{e^{\beta\omega} \pm 1} \frac{d^3k}{(2\pi)^3},$$

where β is the inverse of the Hawking temperature and the minus (plus) sign is to be used when considering bosons (fermions). This formula is valid for massless and massive particles. Moreover, it is immediately generalized to d spacetime dimensions by replacing the exponents of 3 in the last term by $(d - 1)$. Therefore, at the event horizon, the spectrum of the radiation is that of a black body and perfectly thermal; as we saw in the previous chapter, this fact leads to the information loss paradox.

However, we are overlooking an important fact, namely that the geometry of the spacetime surrounding a black hole is non-trivial. Taking this into account, we might imagine that once Hawking radiation is emitted at the event horizon, it will get modified by this non-trivial geometry so that when an observer located very far away from the black hole measures the spectrum, this will no longer be that of a black body. This is indeed the case: the black hole geometry outside the event horizon acts as a potential barrier that filters Hawking radiation, i.e. part of it will be transmitted and will travel freely to infinity, whereas the rest will be reflected back into the black hole. In terms of formulas, we can summarize the previous statements by saying that the spectrum

emitted by a black hole that an observer at spatial infinity would measure is given by

$$\Gamma(\omega) = \frac{\gamma(\omega)}{e^{\beta\omega} \pm 1} \frac{d^3k}{(2\pi)^3}, \quad (5.1)$$

where $\gamma(\omega)$ is the so-called greybody factor, which depends on the frequency of the particles under consideration. As we can see, greybody factors get their name from the fact that they modify the spectrum emitted by a black hole so that it is no longer that of a black body, but that of a grey body.

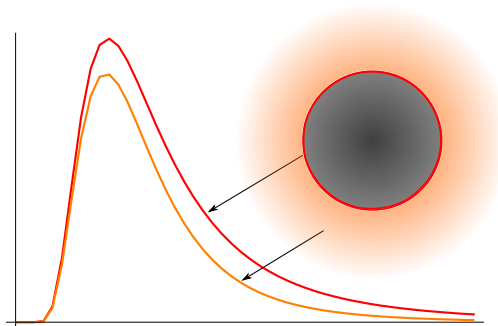


Figure 5.1: The purely thermal radiation emitted at the horizon (red) gets modified (orange) by the black hole geometry.

In order to quantify all the previous ideas about greybody factors, we will make use of the results obtained in [chapter 4](#). Let us recall the results we obtained when solving the Klein-Gordon equation for a massless scalar field in the four-dimensional black hole background (4.1). Given the scalar field

$$\Phi = r^{-1}\psi(r)e^{i\omega t}Y_{lm},$$

we found that the Klein-Gordon equation reduces to the following differential equation for the radial component of the field

$$\left(\frac{d^2}{dx^2} + \omega^2 - V(r) \right) \psi(r) = 0, \quad (5.2)$$

with $V(r)$ given by

$$V(r) = f(r) \left[\frac{l(l+1)}{r^2} + \frac{f'(r)}{r} \right]. \quad (5.3)$$

By simple inspection, we see that $V(r)$ acts as a potential in the Schrödinger-like equation (5.2). The scalar field will be filtered by this potential: part of it will tunnel through the potential and the rest will be reflected. In general, the explicit form of the potential depends on the black hole geometry and the spin j of the perturbation under study (in our case, it is a scalar field, so $j = 0$ and it does not appear in our formulas). Schrödinger-like equations like the one above, which we already obtained in [chapter 4](#), will be our starting point to compute greybody factors for different black holes.

The above discussion relates to the definition of greybody factors in the following way. Hawking radiation, as well as any other field propagating in the black hole back-

ground, will also be affected by the potential $V(r)$. This is natural, given that the potential depends only on the geometry of spacetime. Part of the radiation will tunnel through the potential barrier and part of it will be reflected back into the hole. Pictorially, we would have the following situation

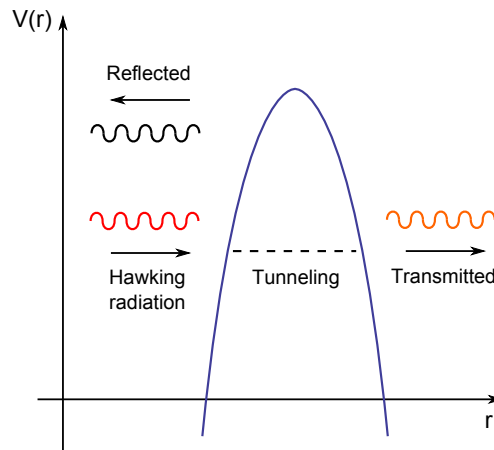


Figure 5.2: Once Hawking radiation is emitted, it will have to propagate in a non-trivial geometry, which is encoded in the potential $V(r)$. This will act as a filter: part of the radiation will be transmitted and will travel freely to infinity, whereas another part will be reflected back into the hole.

We can already anticipate that the specific form of the greybody factor will depend on some parameters related to the potential barrier. This is indeed the case: the greybody factor will be defined in terms of the transmission and reflection coefficients corresponding to the potential barrier. More details will follow in the next section.

5.2 Black hole scattering theory

Before going into the details of the computation of greybody factors for different black holes in asymptotically flat spacetime, we give a brief review of the basics of black hole scattering theory. This will allow us to give a quite general definition for greybody factors. To give a more general overview, let us consider a static, spherically symmetric d -dimensional black hole with metric

$$ds_d^2 = -f(r)dt^2 + f(r)^{-1}dr^2 + r^2 d\Omega_{d-2}^2, \quad (5.4)$$

which has an event horizon at r_0 . The goal is to study the wave equation for a propagating field in the exterior region $r_0 < r < +\infty$ of the above black hole. For simplicity, we take a massless uncharged scalar field ψ , but we could also consider an electromagnetic or gravitational field (e.g. a linearized perturbation of the metric). In the first section of [chapter 4](#), we mentioned that the field decomposition in this case is given by

$$\Phi = r^{\frac{2-d}{2}} \psi(r) e^{i\omega t} Y_{lm}, \quad (5.5)$$

with $\omega \in \mathbb{C}$ the complex frequency of the wave: the real part represents the actual frequency of oscillation of the wave and the imaginary part represents the damping.

Then, after introducing the tortoise coordinate x , defined as

$$x \equiv \int \frac{dr}{f(r)},$$

the radial part of the field obeys the following equation

$$\left(\frac{d^2}{dx^2} + \omega^2 - V(r) \right) \psi(r) = 0, \quad (5.6)$$

with the potential given by

$$V(r) = f(r) \left[\frac{l(l+d-3)}{r^2} + \frac{(d-2)(d-4)f(r)}{4r^2} + \frac{(d-2)f'(r)}{2r} \right]. \quad (5.7)$$

Here, $l(l+d-3)$, with $l \in \mathbb{N}$, are the eigenvalues of the Laplacian on S^{d-2} . In terms of the tortoise coordinate, the exterior region of the black hole is now $-\infty < x < +\infty$. Solutions of (5.6) describe the scattering of an incoming (originating at $x = +\infty$) or outgoing (originating at $x = -\infty$) wave, by the potential $V(r)$.

Note that since $V(r) \rightarrow 0$ as $x \rightarrow \pm\infty$, the solutions will behave as plane waves $\psi_\omega \sim e^{\pm i\omega x}$ in these limits. Let us recall the sign convention for the direction of propagation of a plane wave. Using our field decomposition (5.5), we have that (remember that in our units: $k = \omega$, with k being the wave number)

$$\begin{aligned} e^{\pm i(\omega x - \omega t)} &: \text{Wave travelling in the positive } x \text{ direction,} \\ e^{\pm i(\omega x + \omega t)} &: \text{Wave travelling in the negative } x \text{ direction.} \end{aligned} \quad (5.8)$$

Let us consider ψ_ω , a solution of the wave equation that describes the scattering of an incoming wave originating at $x = +\infty$, that satisfies the boundary conditions

$$\psi_\omega \sim \begin{cases} e^{i\omega x} + R e^{-i\omega x}, & x \rightarrow +\infty, \\ T e^{i\omega x}, & x \rightarrow -\infty, \end{cases} \quad (5.9)$$

where $R(\omega)$ and $T(\omega)$ are the reflection and transmission coefficients, respectively. We also have to consider $\psi_{-\omega}$, which also solves the wave equation, but with boundary conditions

$$\psi_{-\omega} \sim \begin{cases} e^{-i\omega x} + \tilde{R} e^{i\omega x}, & x \rightarrow +\infty, \\ \tilde{T} e^{-i\omega x}, & x \rightarrow -\infty, \end{cases} \quad (5.10)$$

for some other reflection and transmission coefficients, $\tilde{R}(-\omega)$ and $\tilde{T}(-\omega)$. We can now construct the conserved flux

$$\mathcal{F} = \frac{1}{2i} \left(\psi_{-\omega} \frac{d\psi_\omega}{dx} - \psi_\omega \frac{d\psi_{-\omega}}{dx} \right), \quad (5.11)$$

which does not depend on x , and evaluate it at $x \rightarrow \pm\infty$. Requiring that the flux must

be equal at both limits yields

$$R\tilde{R} + T\tilde{T} = 1. \quad (5.12)$$

This expression reduces to the familiar formula $|R|^2 + |T|^2$ for $\omega \in \mathbb{R}$.

Let us now consider ψ'_ω , a solution of the wave equation that describes the scattering of an outgoing wave originating at the black hole outer horizon $x = -\infty$, that satisfies the boundary conditions

$$\psi'_\omega \sim \begin{cases} T' e^{-i\omega x}, & x \rightarrow +\infty, \\ e^{-i\omega x} + R' e^{i\omega x}, & x \rightarrow -\infty. \end{cases}$$

Again, we also have to consider $\psi'_{-\omega}$, which also solves the wave equation, but with boundary conditions

$$\psi'_{-\omega} \sim \begin{cases} \tilde{T}' e^{i\omega x}, & x \rightarrow +\infty, \\ e^{i\omega x} + \tilde{R}' e^{-i\omega x}, & x \rightarrow -\infty. \end{cases}$$

The above solutions for an outgoing wave can be expressed as linear combinations of the solutions for an incoming wave

$$\begin{aligned} \psi'_\omega &= a \psi_\omega + b \psi_{-\omega}, \\ \psi'_{-\omega} &= c \psi_\omega + d \psi_{-\omega}. \end{aligned}$$

This is due to the fact that the space of solutions of (5.6) is two-dimensional. After some trivial manipulations, we find that the coefficients a, b, c and d are given by

$$\psi'_\omega = -\frac{\tilde{R}}{\tilde{T}} \psi_\omega + \frac{1}{\tilde{T}} \psi_{-\omega} \quad \text{and} \quad \psi'_{-\omega} = \frac{1}{T} \psi_\omega - \frac{R}{T} \psi_{-\omega}.$$

Moreover, as a consequence of the same manipulations, we find that the outgoing reflection and transmission coefficients can be expressed in terms of the incoming ones as

$$\begin{aligned} R' &= -\frac{T}{\tilde{T}} \tilde{R}, & \tilde{R}' &= -\frac{\tilde{T}}{T} R, \\ T' &= T, & \tilde{T}' &= \tilde{T}. \end{aligned} \quad (5.13)$$

We see that $T\tilde{T} = T'\tilde{T}'$ and $R\tilde{R} = R'\tilde{R}'$; therefore, we can define the greybody factor in terms of the incoming or outgoing transmission coefficients. We choose to define them in terms of the former. Thus, we can naturally define the greybody factor of the black hole (5.4), for generic frequency $\omega \in \mathbb{C}$, as

$$\gamma(\omega) = T(\omega)\tilde{T}(-\omega). \quad (5.14)$$

This formula generalizes the result for real frequencies $\gamma(\omega) = |T(\omega)|^2$.

5.2.1 Greybody factor = absorption cross section

It is important to stress the fact that, in view of (5.13), the greybody factor is the same for the incoming and outgoing wave scattering by the black hole. The equality $T\tilde{T} = T'\tilde{T}'$ implies that to calculate greybody factors, we can consider either the scattering of an incoming wave from infinity or the scattering of an outgoing wave originated at the black hole horizon. It is easy to see that if one considers the former case, the greybody factor is actually the *absorption cross section* σ_{abs} of the black hole, as it measures how much of the incident field is effectively transmitted through the potential barrier and “absorbed” by the hole.

If we choose to compute greybody factors as absorption cross sections, there is another natural way to define them. We can evaluate the flux (5.11) at the black hole horizon and compare it to the original flux coming from infinity. Then, the greybody factor, or absorption cross section, is obviously defined as

$$\gamma(\omega) = \sigma_{abs} = \frac{\mathcal{F}_{horizon}}{\mathcal{F}_{infinity}}. \quad (5.15)$$

On a side note, we should mention that the results derived above hold for asymptotically flat and asymptotically dS spacetimes. It is a little more subtle to obtain the results for asymptotically AdS spacetimes, because in that case the tortoise coordinate varies from $-\infty < x < C$, where C is a constant value that the coordinate takes at spatial infinity. The interested reader can see [27] for more details.

5.3 Frequency regimes: low versus high frequency

Up to now, we have not said anything about the frequency ω of the wave considered when computing greybody factors. Given that this is a key point for coming chapters, in which greybody factors for different black holes will be computed explicitly, let us take some time to explain how our calculations will depend on the frequency ω .

We will be interested in two frequency regimes: low ω and high ω . Of course, these are relative terms, so, we must specify low and high with respect to what. The natural choice is to consider the scales set by the black hole background. Therefore, we can define our two regimes of interest with two conditions; namely

$$\begin{aligned} \text{Low frequency regime:} & \quad \omega \ll T_H, \quad \omega r_0 \ll 1, \\ \text{High frequency regime:} & \quad |\omega| \gg T_H, \quad |\omega r_0| \gg 1, \end{aligned} \quad (5.16)$$

where T is the Hawking temperature of the black hole and r_0 the event horizon. These conditions specify the relative value of the energy of the wave with respect to the scale set by the black hole quantities, such as the Hawking temperature and the horizon radius. We take the absolute value in the high frequency case because, as we will see in chapter 9, the case of interest is when ω is very large and purely imaginary.

The greybody factor formula (5.14) does not depend on the frequency regime, because it was derived by considering only the *behavior* of the solutions to the wave equation (5.6) in the limits r_0 and $r \rightarrow \infty$. In practice, however, the methods used to

explicitly compute greybody factors will be different in both frequency regimes. Let us see how this comes about. When solving the wave equation (5.6), we will need to match the solutions that we will find in different regions of the spacetime around the black hole. More concretely, these regions are:

- Far region: The one between the asymptotic region (spatial infinity) and the event horizon.
- Near region: The one close to the event horizon.

The difference when computing greybody factors in both regimes will be the matching of the solutions found in each of these regions.

In the low frequency regime, the wavelength of the wave is much larger than the length scale set by the black hole. This allows us to match the solutions from different regions directly, much like we do in simple quantum mechanics problems. We will call this the *simple matching technique*.

In the high frequency regime, the wavelength of the wave becomes of the order of the length scale by the black hole. Therefore, in this case the wave will *see* the curvature of spacetime and we cannot simply match solutions found in different regions, as there would be an indeterminacy in doing so. Instead, we will use the *monodromy matching technique*.

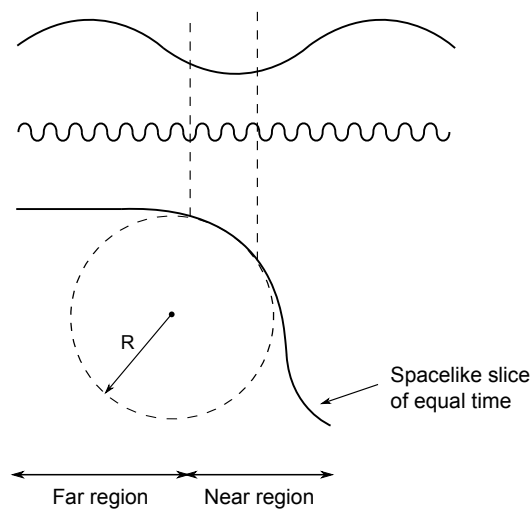


Figure 5.3: Low frequency (top) and high frequency (bottom) waves near the horizon of the black hole. R is the radius of curvature in some region of the spacelike slice. The relative size of the wavelength with respect to the length scale set by the background geometry will determine the matching technique to be used.

The main differences between the calculations of greybody factors at low and high frequency of the wave are summarized in [Table 5.1](#)

Table 5.1: Differences in the computation of greybody factors at low and high frequencies.

Low frequency	High frequency
S-wave approximation $\Phi = e^{i\omega t} r^{\frac{2-d}{2}} \psi(r)$	Full field decomposition $\Phi = e^{i\omega t} r^{\frac{2-d}{2}} \psi(r) Y_{lm\dots}(\Omega_{d-2})$
Simple matching technique	Monodromy matching technique

5.4 Motivating the study of greybody factors

One might ask why do we study greybody factors. The goal is twofold. First, the study of greybody factors allows us to increase our semiclassical gravity dictionary, i.e. to have a better and more complete understanding of black holes and Hawking radiation within this context. Also, and more importantly, it is thought that by studying greybody factors in different regimes, we will be able to gain insight into the quantum nature of black holes and, thus, of quantum gravity. That is, the deviation from pure black body radiation might carry information about the quantum degrees of freedom of the black hole. Indeed, the study of greybody factors in the low frequency regime led to a result that was one of the precursors of the AdS/CFT correspondence, one of the most profound ideas coming from string theory. We will review the computation that led to this insight in [chapter 6](#) and [chapter 7](#). In this thesis we will also study a different frequency regime and see if the results suggest something new about the quantum nature of black holes. If so, then greybody factors may help us in resolving the information loss paradox.

Part III

Greybody Factors: Computations

Chapter 6

Greybody factors at low frequency: Semiclassical computation

In this chapter we compute the greybody factor at low frequency for the five-dimensional black hole with three charges presented in [chapter 3](#). This calculation was first done by Maldacena and Strominger in [\[22\]](#). First, we show the explicit form of the wave equation and then proceed to use the simple matching technique outlined in [chapter 5](#) to obtain the absorption cross section, which is equal to the greybody factor.

6.1 The wave equation

We are interested in computing the greybody factor at low frequency for the five-dimensional black hole with three charges

$$ds_5^2 = -\lambda^{-2/3} h dt^2 + \lambda^{1/3} \left(\frac{dr^2}{h} + r^2 d\Omega_3^2 \right), \quad (6.1)$$

where

$$\lambda = \prod_{j=1,5,p} \left(1 + \frac{r_0^2 \sinh^2 \alpha_j}{r^2} \right) = \prod_{j=1,5,p} \left(1 + \frac{r_j^2}{r^2} \right), \quad (6.2)$$

$$h = 1 - \frac{r_0^2}{r^2}.$$

Given that we are in the low frequency regime, we will use the S-wave approximation found in [chapter 4](#). In this limit, we argued that the field decomposes as

$$\Phi = e^{i\omega t} \phi(r)$$

and that the equation for the radial part is given by

$$\left[\frac{h}{r^3} \frac{d}{dr} \left(hr^3 \frac{d}{dr} \right) + \lambda \omega^2 \right] \phi(r) = 0. \quad (6.3)$$

This time, we will need an explicit expression for the tortoise coordinate x . Using its definition, we find that

$$x \equiv \int \frac{dr}{h(r)} = r + \frac{r_0}{2} \ln \left| \frac{r - r_0}{r + r_0} \right|. \quad (6.4)$$

Now, after writing

$$\phi(r) = r^{-3/2} \psi(r),$$

we obtained the following Schrödinger-like equation

$$\left(\frac{d^2}{dx^2} + \lambda\omega^2 - V(r) \right) \psi(r) = 0, \quad (6.5)$$

with $V(r)$ given by (4.37). More explicitly

$$V(r) = \frac{3}{4r^2} \left(1 - \frac{r_0^2}{r^2} \right) \left(1 + 3\frac{r_0^2}{r^2} \right). \quad (6.6)$$

Now that we have the equation that we will use in our computation, let us give a physical picture of what we will do. We will study the propagation of a wave coming from infinity toward the black hole. The potential $V(r)$ will act as a potential barrier, which will filter the incoming wave: part of it will be reflected back to infinity and the rest will be transmitted into the black hole.

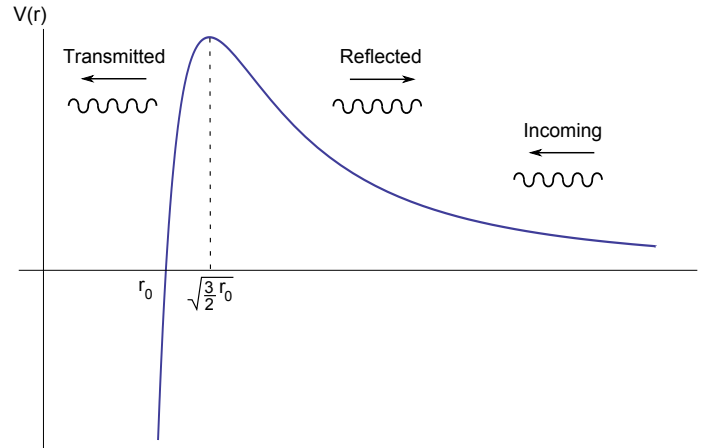


Figure 6.1: Potential corresponding to the five-dimensional black hole with three charges.

We will work in the dilute gas region (3.15)

$$r_0, r_p \ll r_1, r_5, \quad (6.7)$$

and restrict to low energies satisfying

$$\omega r_1 \ll 1, \quad \omega r_5 \ll 1. \quad (6.8)$$

Moreover, we will treat the ratios r_0/r_p and r_1/r_5 as order one.

Now, recall from (3.18) that we introduced two temperatures $T_{L,R}$. Given their definitions, note that due to (6.7), we have that $T_{L,R} \ll 1/r_1, 1/r_5$. Taking this and (6.8) into account, we impose an extra condition on the energy, which is

$$\omega \sim T_{L,R}, \quad (6.9)$$

so that the ratio $\omega/T_{L,R}$ is also of order one.

6.2 Computation using simple matching technique

It is readily seen that (6.5) cannot be solved analytically. Therefore, we will use the simple matching technique outlined in chapter 5. That is, we will divide space in two regions, namely, the far and near region, and find the solutions to the wave equation in each of them. Then, we will proceed to match the solutions at an intermediate point r_m .

$$\begin{aligned} \text{Far zone:} & \quad r > r_m \\ \text{Near zone:} & \quad r < r_m. \end{aligned}$$

The matching point is chosen so that

$$r_0, r_p \ll r_m \ll r_1, r_5, \quad \omega r_1 \frac{r_1}{r_m} \ll 1. \quad (6.10)$$

Taking these conditions into account together with (6.8), we also have that

$$\omega r_m \ll 1. \quad (6.11)$$

Far zone computation

First, note that in this region, the tortoise coordinate satisfies $x = r$, given that the ln term appearing in (6.4) goes to zero due to (6.10) and the far region condition $r > r_m$. Hence, we can write (6.5) as

$$\left(\frac{d^2}{dr^2} + \lambda \omega^2 - V(r) \right) \psi(r) = 0. \quad (6.12)$$

We now need to find explicit expressions for λ and $V(r)$ in the far zone region. Using (6.10) and the far region condition $r > r_m$, it is easy to check that the original expressions (6.2) and (6.6) reduce to

$$\lambda = 1 + \frac{(r_1^2 + r_5^2)}{r^2} + \frac{r_1^2 r_5^2}{r^4}$$

and

$$V(r) = \frac{3}{4r^2}.$$

Before putting these two expressions into the Schrödinger-like equation, we change the radial variable to $\rho = \omega r$. With this, (6.12) becomes

$$\frac{d^2\psi}{d\rho^2} + \left[1 + \frac{\omega^2(r_1^2 + r_5^2)}{\rho^2} + \frac{\omega^4 r_1^2 r_5^2}{\rho^4} - \frac{3}{4\rho^2} \right] \psi = 0.$$

Finally, using the conditions (6.8), we get a tractable form for the above equation. Namely

$$\frac{d^2\psi}{d\rho^2} + \left(1 - \frac{3}{4\rho^2} \right) \psi = 0. \quad (6.13)$$

The above equation is solved independently by $J_1(\rho)$ and $N_1(\rho)$, Bessel functions of the first and second kind. We can write a general solution as

$$\psi = \sqrt{\frac{\pi\rho}{2}} [A J_1(\rho) + B N_1(\rho)]. \quad (6.14)$$

Now, the Bessel functions above have in general complicated expressions. However, we will be interested in their asymptotic behavior. For very large r (or equivalently, very large ρ or far away from the black hole), we can write $J_1(\rho)$ and $N_1(\rho)$ as (see (E.3))

$$\begin{aligned} J_1(\rho) &= \sqrt{\frac{2}{\pi\rho}} \cos\left(\rho - \frac{3\pi}{4}\right) = \frac{1}{2} \sqrt{\frac{2}{\pi\rho}} \left(e^{i\rho} e^{-i3\pi/4} + e^{-i\rho} e^{i3\pi/4} \right) \\ N_1(\rho) &= \sqrt{\frac{2}{\pi\rho}} \sin\left(\rho - \frac{3\pi}{4}\right) = \frac{1}{2i} \sqrt{\frac{2}{\pi\rho}} \left(e^{i\rho} e^{-i3\pi/4} - e^{-i\rho} e^{i3\pi/4} \right). \end{aligned}$$

Given that $e^{\pm i3\pi/4} = \pm i e^{\pm i\pi/4}$, we get that our general solution (6.14) for very large r , and using the fact that $\phi = r^{-3/2}\psi$ and $\rho = \omega r$, is

$$\phi(r) = \frac{1}{2r^{3/2}} \left[e^{i\omega r} \left(A e^{-i3\pi/4} - B e^{-i\pi/4} \right) + e^{-i\omega r} \left(A e^{i3\pi/4} - B e^{i\pi/4} \right) \right]. \quad (6.15)$$

This will not be the solution that we will use to perform the matching. Instead, we will use it to compute the incoming flux from spatial infinity.

We now want to find the behavior of the solutions for $r \sim r_m$ or, equivalently, very small ρ . In this limit, we can write $J_1(\rho)$ and $N_1(\rho)$ as (see (E.4))

$$\begin{aligned} J_1(\rho) &= \frac{\rho}{2}, \\ N_1(\rho) &= -\frac{2}{\pi\rho} + \frac{\rho}{\pi} (\ln \rho + c), \end{aligned}$$

where $c = \ln 1/2$. Therefore, using $\phi = r^{-3/2}\psi$, the general solution (6.14) is given by

$$\phi(r) = \sqrt{\frac{\pi\omega^3}{2}} \left[\frac{A}{2} + \frac{B}{\pi} \left(-\frac{2}{\omega^2 r^2} + \ln(\omega r) + c \right) \right]. \quad (6.16)$$

This is the far-zone solution that we will use to perform the matching at $r = r_m$.

Near zone computation

In this zone, we have that $r < r_m$. Using this condition and (6.10), the expression for λ reduces to

$$\lambda = \frac{r_1^2 r_5^2}{r^4} \left(1 + \frac{r_p^2}{r^2} \right).$$

With this, the wave equation (6.3) reduces to

$$\left[\frac{h}{r^3} \frac{d}{dr} \left(hr^3 \frac{d}{dr} \right) + \frac{\omega^2 r_1^2 r_5^2}{r^4} \left(1 + \frac{r_p^2}{r^2} \right) \right] \phi(r) = 0. \quad (6.17)$$

We have chosen to write directly the equation for $\phi(r)$ instead of using the one for $\psi(r)$. This is a more complicated equation and we need to perform a series of steps to obtain the solutions. First, defining a new variable $v = r_0^2/r^2$, the above equation becomes

$$(1-v) \frac{d}{dv} (1-v) \frac{d\phi}{dv} + \left(D + \frac{C}{v} \right) \phi = 0, \quad (6.18)$$

where we have set

$$D = \left(\frac{\omega r_1 r_5 r_p}{2r_0^2} \right)^2, \quad C = \left(\frac{\omega r_1 r_5}{2r_0} \right)^2.$$

Note that now the horizon is located at $v = 1$ and the matching point r_m is in a region where v is small. The next change of variable happens close to the horizon, where we set $y = -\ln(1-v)$, with which it is easy to see that the equation becomes

$$\frac{d^2 \phi}{dy^2} + (C + D) \phi = 0.$$

Finally, we have an equation that is actually tractable, whose solutions are

$$\phi(v) \sim e^{\pm i\sqrt{C+D}y}$$

and we interpret them as ingoing (+) and outgoing (−) solutions at the horizon. We now use the fact that at the horizon, we should only have ingoing waves and so

$$\phi(v) = \tilde{A} e^{-i\sqrt{C+D} \ln(1-v)}, \quad (6.19)$$

where \tilde{A} is a constant that will be determined below. This will be the solution that we will use to find the flux absorbed by the hole.

Let us now find the solutions to (6.18), not restricting to the region close to the horizon. By making the following change of variables

$$z = 1 - v, \quad \phi = \tilde{A} z^{-i(a+b)/2} F,$$

the equation becomes

$$z(1-z) \frac{d^2 F}{dz^2} + [(1-ia-ib) - (1-ia-ib)z] \frac{dF}{dz} + abF = 0. \quad (6.20)$$

This is a hypergeometric differential equation, whose solutions are given by hypergeometric functions (see [Appendix E](#)). Note that the parameters appearing in the equation are related to the parameters of (6.18) by

$$(a + b)^2 = 4(C + D), \quad ab = C. \quad (6.21)$$

Using the definitions (3.18), it is straightforward to check that

$$a = \frac{\omega}{4\pi T_R}, \quad b = \frac{\omega}{4\pi T_L}. \quad (6.22)$$

Finally, the solution to the above equation is

$$\phi(r) = \tilde{A} z^{-i(a+b)/2} {}_2F_1(-ia, -ib; 1 - ia - ib; z), \quad (6.23)$$

with ${}_2F_1$ a hypergeometric function. We are interested in this solution at the matching point $r = r_m$, where due to (6.10), we have that $z = 1$. Hence, the solution we will use to perform the matching will be (6.23) with the hypergeometric function given by

$${}_2F_1(-ia, -ib; 1 - ia - ib; 1) = \frac{\Gamma(1 - ia - ib)}{\Gamma(1 - ia)\Gamma(1 - ib)}, \quad (6.24)$$

where Γ are just Gamma functions (again, see [Appendix E](#)).

Matching and greybody factor derivation

We have all we need to perform the matching of the far-zone and near-zone solutions found above. We will match (6.16) and (6.23), and their respective derivatives, at the matching point $r = r_m$, which satisfies $\omega r_m \ll 1$.

First, note that the term multiplying B in (6.16) is very large at the matching point. This will require B to be very small and we can ignore it in the solution.¹ Also, notice that at the matching point, we have that $z = 1$ in (6.23). Taking the above simplifications into account, the matching of the solutions gives

$$\sqrt{\frac{\pi\omega^3}{2}} \frac{A}{2} = \tilde{A} \frac{\Gamma(1 - ia - ib)}{\Gamma(1 - ia)\Gamma(1 - ib)}. \quad (6.25)$$

We now construct the conserved flux corresponding to the wave equation (6.3). It is

$$\mathcal{F} = \frac{1}{2i} \left(hr^3 \phi^* \frac{d\phi}{dr} - c.c. \right), \quad (6.26)$$

where *c.c.* stands for complex conjugate. To find the flux coming from infinity, we use (6.15) ignoring B for the reason explained above and get

$$\mathcal{F}_{infty} = -\omega \frac{|A|^2}{4}. \quad (6.27)$$

¹If the reader wants to be more rigorous, one can perform the matching without ignoring B and get that $B/A \ll 1$. See [22] for the details.

To find the flux absorbed by the black hole, i.e. that at the horizon, note that in this region we had that $v = r_0^2/r^2$ and $h = 1 - v$; hence, we can write the formula for the flux as

$$\mathcal{F} = \frac{1}{2i} \left(-2(1-v)r_0^2\phi^* \frac{d\phi}{dv} - c.c. \right).$$

So, using (6.19) we obtain

$$\mathcal{F}_{horizon} = -2r_0^2\sqrt{C+D}|\tilde{A}|^2 = -r_0^2(a+b)|\tilde{A}|^2, \quad (6.28)$$

where we used (6.21). Then, we finally get the absorption cross section using the formula introduced in chapter 5 and (6.25)

$$\sigma_{abs}^S = \frac{\pi}{2}r_0^2\omega^2(a+b) \left(\frac{\Gamma(1-ia)\Gamma(1-ib)}{\Gamma(1-ia-ib)} \right)^2.$$

Using the formulas in Appendix E, we finally get

$$\sigma_{abs}^S = \pi^2 r_0^2 \omega^2 ab \frac{e^{2\pi(a+b)} - 1}{(e^{2\pi a} - 1)(e^{2\pi b} - 1)}. \quad (6.29)$$

Notice the superscript S . It is because we have found the absorption cross section for the S-wave. However, we want that for the plane wave. They are related by [28]

$$\sigma_{abs} = \frac{4\pi}{\omega^3} \sigma_{abs}^S.$$

With this, we can finally get the desired result. Using the expressions for a, b given in (6.22) and the definitions (3.17) and (3.18), we get

$$\sigma_{abs}(\omega) = \pi^3 \omega r_1^2 r_5^2 \frac{e^{\omega/T_H} - 1}{(e^{\omega/2T_L} - 1)(e^{\omega/2T_R} - 1)}. \quad (6.30)$$

This is the result that Maldacena and Strominger obtained in [22]. It has a suggestive structure by itself: statistical factors in the denominator coming apparently from different systems (the subscripts L and R); a Bose-Einstein distribution factor in the denominator corresponding to that of the total black hole system and that cancels out the one appearing in the denominator of Hawking radiation for a massless scalar field. Therefore, the rate of emission by the five-dimensional black hole with three charges is

$$\Gamma_{bh}(\omega) = \pi^3 \omega r_1^2 r_5^2 \frac{1}{(e^{\omega/2T_L} - 1)(e^{\omega/2T_R} - 1)} \frac{d^4 k}{(2\pi)^4}. \quad (6.31)$$

However, even more surprising is that this result can be obtained from string theory. We will see how this comes about in the next chapter.

Chapter 7

Greybody factors at low frequency: String theory computation

We now present the calculation done by Das and Mathur for the decay rate of D-branes [28]. We begin by explaining basic concepts of statistical mechanics in two dimensions, which describes the thermodynamics of massless open string states moving on a D-brane. Then, we explain the long string configuration and finally show the result for the D-brane decay rate. We will see that it exactly reproduces the semiclassical result obtained in the previous chapter. Further references with pedagogical discussions on the subjects of this chapter are [29, 30].

7.1 Statistical mechanics in two dimensions

Let us consider an two-dimensional ideal gas at weak coupling, which is assumed to thermalize. It is composed of f flavors of massless bosons and fermions living on a circle of length L . If L is large, we can describe the system by a canonical ensemble with inverse temperature $\beta = 1/T$, conjugate to the energy, and with a chemical potential μ , conjugate to the momentum. Therefore, the partition function can be written as

$$\mathcal{Z} = \sum_{states} \exp \left(-\beta \sum_r n_r e_r - \mu \sum_r n_r p_r \right),$$

where n_r is the number of particles with energy e_r and momentum p_r . We immediately see that the total energy and momentum of the system are related to the inverse temperature and chemical potential by

$$E = -\frac{\partial \log \mathcal{Z}}{\partial \beta}, \quad P = -\frac{\partial \log \mathcal{Z}}{\partial \mu}.$$

The average number of particles n_r in a state characterized by (e_r, p_r) is given by the following thermal distribution function

$$\rho(e_r, p_r) = \frac{1}{e^{\beta e_r + \mu p_r} \pm 1}, \quad (7.1)$$

with $+$ for fermions and $-$ for bosons.

The entropy of the system is given by the usual thermodynamical relation

$$S = \log \mathcal{Z} + \mu P + \beta E.$$

We can evaluate the corresponding expressions appearing in this formula with the above definitions. Recalling that we are considering f flavors of particles, we get

$$\begin{aligned} P &= \frac{fL\pi}{8} \left[\frac{1}{(\beta + \mu)^2} - \frac{1}{(\beta - \mu)^2} \right], \\ E &= \frac{fL\pi}{8} \left[\frac{1}{(\beta + \mu)^2} + \frac{1}{(\beta - \mu)^2} \right], \\ S &= \frac{fL\pi}{4} \left[\frac{1}{\beta + \mu} - \frac{1}{\beta - \mu} \right]. \end{aligned}$$

Now, since they live in one spatial dimension, the particles we are considering can either be right-moving or left-moving and they satisfy in each case

$$\text{Right-movers: } e_r = p_r, \quad \text{Left-movers: } e_r = -p_r.$$

Plugging these two conditions into (7.1), we get the distribution functions for left- and right-moving particles

$$\rho_L = \frac{1}{e^{(\beta - \mu)e_r} \pm 1}, \quad \rho_R = \frac{1}{e^{(\beta + \mu)e_r} \pm 1}. \quad (7.2)$$

Hence, we see that the combinations $T_L = 1/(\beta - \mu)$ and $T_R = 1/(\beta + \mu)$, appearing in the exponents of the denominators, act as effective temperatures for the two subsystems. It is straightforward to check that the total temperature of the system is related to these two new temperatures as

$$\frac{1}{T} = \frac{1}{2} \left(\frac{1}{T_L} + \frac{1}{T_R} \right). \quad (7.3)$$

This is exactly the formula (3.17) that we found for the temperature of the five-dimensional black hole with three charges! The subscripts L, R introduced then have now a clear meaning.

Finally, we should note that all thermodynamical quantities mentioned above can be split into left- and right-moving parts as $E = E_L + E_R$, $P = P_L + P_R$ and $S = S_L + S_R$. In particular, we see that the entropy and temperature in each of the subsystems are related by

$$T_L = \frac{4S_L}{fL\pi}, \quad T_R = \frac{4S_R}{fL\pi}. \quad (7.4)$$

The upshot of this section is that we have found a dual description, that of an ideal gas composed of left- and right-movers, whose thermodynamical quantities are exactly those introduced in the very end of [chapter 3](#) for the near-extremal five-dimensional black hole with three charges. Therefore, in the D-brane picture of the hole, the thermodynamics of open strings moving on branes are precisely described by the system discussed in this section.

7.2 The long string model

The D-brane configuration that we have is a system of static Q_1 D1-branes, Q_5 D5-branes and Q_p units of momentum $1/R$. Recall that we are compactifying on $T^5 = T^4 \times S^1$ and V is the volume of the four-torus, while R is the radius of the circle. The low energy excitations of this system are more easily understandable when R is much larger than the other four directions of T^4 . In that case, the effective theory is a $(1+1)$ -dimensional supersymmetric gauge theory, whose modes are essentially those of the oscillations of the D1-branes.

Now, consider the case when all the D1-branes in our configuration are separate (think of them as a stack, with each of them on top of each other). If they tried to move away from the D5-branes, there would be a nonzero binding energy for the system. If there was a single D1-brane and a single D5-brane, the quantized waves that would appear in the process would be massless particles with four flavors (since the effective theory is supersymmetric, we would have four bosons and four fermions). Therefore, if we have many D1- and D5-branes like in our original configurations, the quantized waves that appear are massless particles with $4Q_1Q_5$ flavors.

However, we can also consider a different case. Namely, that of joining up several of our D1-branes in order to form a *long string*, which will now be multiply wound around S^1 . In fact, it was discovered in [\[31\]](#) that if one considers a number n_w of D1-branes without anything else wrapping a circle, the preferred configuration of the system would be to join into a long string of length $2\pi n_w R$. This implies that the long string configuration is the most entropically favorable.

For our system of D1- and D5-branes, it was found in [\[32\]](#) that the most entropically favorable configuration is indeed that of a long string winding around the S^1 , with an effective length of $L_{eff} = 2\pi R Q_1 Q_5$. Therefore, to study the low energy theory of our D-brane system, it will suffice to study the gauge theory of four bosons and four fermions living on the circle of length L_{eff} . At weak coupling, these particles form an ideal gas. Therefore, we can use our results from the previous section to describe its thermodynamical properties! Since the results obtained in this description must be equivalent to those obtained for the black hole, the relations between the entropies and the temperatures should be the same. Then, comparing [\(7.4\)](#) and [\(3.20\)](#), they are equal if

$$fL = 8\pi R Q_1 Q_5,$$

from where we identify for the long string configuration: $f = 4$ and $L = 2\pi R Q_1 Q_5$.

7.3 Decay rate of the D-brane bound state

Recall that our D-brane configuration is such that we have compactified five spatial dimensions on $T^5 = T^4 \times S^1$, adding momentum in the S^1 direction. The noncompact directions are labeled by coordinates x^μ , $\mu = 0, \dots, 4$, the compact directions of T^4 are labeled by x^i , $i = 6, \dots, 9$ and we choose the S^1 to be in the direction of x^5 . Let us now use the long string model to compute the decay rate for this system, which gives rise to the near-extremal five-dimensional black hole with three charges. This was done in [28].

As we saw in the previous section, the theory that describes the long string is a $(1+1)$ -dimensional massless supersymmetric gauge theory with four flavors of bosons ϕ^i and their corresponding fermionic partners. We will be interested in calculating the decay rate for massless minimal scalars, so, we only need to figure out how the bosonic fields of the long string couple to the bulk supergravity fields¹. First, the low-energy action that describes the coupling of the relevant long string fields to fluctuations of the four-torus metric is given by

$$S = \mathcal{T} \int d^2\xi \partial_\alpha \phi^i \partial^\alpha \phi^j g_{ij}. \quad (7.5)$$

The full action contains higher derivative terms, but we neglect those in the present energy regime. We are also not taking into account any dilaton field. Let us explain the terms appearing in this action. The coordinates ξ^α are those on the worldsheet of the long string, g_{ij} is the metric on T^4 and \mathcal{T} is just a constant representing the effective tension of the long string.

Now, we can expand the metric on the four-torus as

$$g_{ij} = \delta_{ij} + \sqrt{2}\kappa_{10} h_{ij}(\xi, \phi^i, x^\mu), \quad (7.6)$$

where x^μ are the coordinates transverse to the five-torus and h_{ij} is the ten-dimensional graviton (which is the traceless part of the deviation of the bulk metric from the flat metric). From this equation, we can read-off the coupling of the long string with h_{ij} . It is given by κ_{10} , which is related to the ten-dimensional Newton constant by $\kappa_{10}^2 = 8\pi G_{10}$. Using (3.2), we get

$$\kappa_{10}^2 = 64\pi^7 g_s^2 \ell_s^8.$$

Then, plugging (7.6) into (7.5), we get the part of the action that will be relevant for our discussion

$$S_{int} = \sqrt{2}\kappa_{10} \int d^2\xi \partial_\alpha \phi^i \partial^\alpha \phi^j h_{ij}. \quad (7.7)$$

Note that the constant \mathcal{T} has disappeared from the action. This is because it can be absorbed in the normalization of the bosonic fields ϕ^i , given that the interaction is quadratic.

Using (7.7), we are interested in studying the decay of a near-extremal state of our D-brane system, using the long string model, into the mode h_{ij} . This decay is

¹Remember that in the D-brane description, these live in ten-dimensional flat spacetime, which we refer to as the bulk.

dominated by the process of annihilation of a pair of modes of the long string, a left and a right mover travelling in opposite directions, giving rise to a closed string mode. The latter is regarded as the quanta of Hawking radiation (see Figure 7.1). Note that

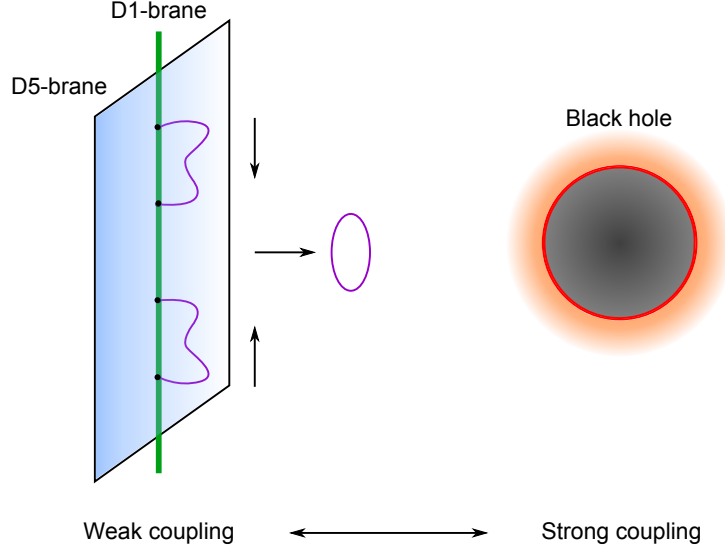


Figure 7.1: Realization of Hawking radiation in the D-brane bound state picture at weak coupling. Left- and right-movers interact and emit a closed string, regarded as the quanta of Hawking radiation.

since we are working in the limit where R is much larger than the directions of T^4 , we can ignore the dependence of h_{ij} on the fields ϕ^i . Furthermore, if one considers S-wave decay, the dependence on the transverse coordinates on (7.6) will be only through the radial variable. In fact, we will consider a closed string mode that does not carry any momentum along the S^1 (x^5 direction) and that is an S-wave in the transverse space.

Let us now proceed with the actual computation. Consider two long string modes, corresponding to ϕ^i and ϕ^j in (7.7), moving in the x^5 direction. They have momenta p and q given by

$$\begin{aligned} p &= (p^0, 0, 0, 0, 0, p^5, 0, 0, 0, 0), \\ q &= (q^0, 0, 0, 0, 0, q^5, 0, 0, 0, 0). \end{aligned}$$

These two long open string modes will collide to give rise to a closed string mode with momentum k given by

$$k = (k^0, k^1, k^2, k^3, k^4, 0, 0, 0, 0, 0).$$

One can write the decay rate for this process in the usual QFT way as

$$\Gamma(p, q; k) = (2\pi)^2 L \delta(p^0 + q^0 - k^0) \delta(p^5 + q^5) \frac{2\kappa_{10}^2 (p \cdot q)^2}{(2p^0 L) (2q^0 L) (2k^0 V L V_4)} \frac{V_4 d^4 k}{(2\pi)^4}. \quad (7.8)$$

The delta functions are there to impose conservation of energy and conservation of

momentum in the x^5 direction. The terms in the denominator come from normalization of the open and closed string modes: the former are normalized on L , the length of the long string introduced in the previous section, and the latter are normalized in the entire space with volume VLV_4 , with V_4 the volume of the non-compact directions.

The total decay rate for the emission of the closed string mode is obtained by averaging (7.8) over all possible initial open string states. Now, recall that in the first section of this chapter, we found that the thermodynamics of open string moving on a D-brane are exactly those of an ideal gas composed of left- and right-movers. Therefore, the initial open string states are drawn from a thermal ensemble and their distributions are given by (7.2). Then, the total decay rate is given by

$$\Gamma(k) = \left(\frac{L}{2\pi}\right)^2 \int_{-\infty}^{+\infty} dp^5 \int_{-\infty}^{+\infty} dq^5 \rho(p^0, p^5) \rho(q^0, q^5) \Gamma(p, q; k).$$

Naturally, one of the distribution functions is that of a left-mover and the other that of a right-mover. Which one is which is conventional. Note that since $L = 2\pi RQ_1Q_5$, we can write it in terms of the charges for the near-extremal black hole that we gave at the end of chapter 3. Doing that and using the explicit form of the distributions to evaluate the integrals above and obtain the final result

$$\Gamma(k) = \pi^3 \omega r_1^2 r_5^2 \frac{1}{(e^{\omega/2T_L} - 1)(e^{\omega/2T_R} - 1)} \frac{d^4k}{(2\pi)^4}. \quad (7.9)$$

Furthermore, since this is the decay rate into a massless scalar field, we can write the absorption cross-section of the D-brane configuration by multiplying the above result by a Bose-Einstein distribution factor for the whole system and get²

$$\sigma(k) = \pi^3 \omega r_1^2 r_5^2 \frac{e^{\omega/T} - 1}{(e^{\omega/2T_L} - 1)(e^{\omega/2T_R} - 1)} \frac{d^4k}{(2\pi)^4}. \quad (7.10)$$

The two formulas above precisely agree with the results (6.30) and (6.31) derived in the semiclassical picture of the black hole.

7.4 Surprising agreement

It is quite remarkable that the result obtained for the D-brane decay rate exactly agrees with the semiclassical computation of the Hawking emission rate modified by the corresponding greybody factor. Let us quote part of [22]: “The black hole emits blackbody radiation from the horizon. Potential barriers outside the horizon act as a frequency-dependent filter, reflecting some of the radiation back into the black hole and transmitting some to infinity. The filtering acts in just such a way that the black hole spectroscopy mimics the excitation spectrum of the string. Hence to the observer at infinity the black hole, masquerading in its greybody cloak, looks like the string, for en-

²Note that the process we have considered is symmetric under time reversal. Therefore, the result (7.9) can be regarded as the absorption rate of the D-brane system. Hence, multiplying it by a distribution factor for the whole system gives the absorption cross section.

ergies small compared to the inverse Schwarzschild radius of the black hole.” Somehow, the greybody factor, at least at low frequency, seems to “know” about the quantum structure of the black hole so that it precisely modifies Hawking radiation to make it look like the radiation coming from fundamental constituents of the hole.

Historically, the D-brane decay rate computation was done first. However, imagine it had been the other way around. If the semiclassical computation had been done first, people might have suspected from the structure of the result that it was telling us something about the quantum structure of the black hole. The Boltzmann terms corresponding to the left- and right-movers would have pointed to microscopic degrees of freedom related to the black hole. As we have seen, that is indeed the case: the superconformal field theory that describes the degrees of freedom of the D-brane construction has left- and right-moving oscillations.

The bottom line is that the study of greybody factors at low frequency played an important role in our understanding of black holes and their quantum nature. This was the main motivation to pursue the topic of this thesis: we want to motivate the study of greybody factors in a different frequency regime that will perhaps lead to further advances in our understanding of black holes in the string theory context.

Chapter 8

Monodromy technique

Before going into the explicit calculations of greybody factors at high frequency, we explain in this chapter the monodromy technique, first introduced in this context by Motl and Neitzke [33].

8.1 Preliminaries

Up to now we have been studying the behavior of the radial part of a field $\Phi = r^{-1}\psi(r)e^{i\omega t}Y_{lm}(\Omega_2)$ propagating in a black hole background using the following equation

$$\left(-\frac{d}{dx^2} + V(r)^2 - \omega^2\right)\psi(r) = 0 \quad (8.1)$$

in the physical range $r_0 < r < +\infty$, where r_0 is the black hole horizon (the outer horizon in the case of Reissner-Nordström black holes). That is, $r \in \mathbb{R}$. We have also seen that in terms of the tortoise coordinate, the physical range is $-\infty < x < +\infty$. As we said in [chapter 5](#), the equation holds for $\omega \in \mathbb{C}$, with the real part being the actual frequency of oscillation and the imaginary part being the damping. However, the calculation at low frequency that we showed in the previous chapters only considered $\omega \in \mathbb{R}$. We are now interested in considering a special case for the frequency, namely, that of a wave of very high imaginary frequency (more on this below).

However, to do so, we need cannot use the simple matching technique used before; instead, we will use the monodromy matching technique that we mentioned in [chapter 5](#). First, we need to analytically continue (8.1) to the complex r -plane (of course, the tortoise coordinate will also be such that $x \in \mathbb{C}$). The reason behind is that we will need to study the behavior of the solutions to the wave equations as we travel around some contours that enclose some of the singular points of the equation. Obviously, that cannot be done if r is restricted to the real line. Let us now explain the idea behind the technique.

First, recall that the asymptotic behavior of the solutions to (8.1) for an incoming

wave, for r and x real, is

$$\psi_\omega \sim \begin{cases} e^{i\omega x} + R e^{-i\omega x}, & x \rightarrow +\infty, \\ T e^{i\omega x}, & x \rightarrow -\infty. \end{cases} \quad (8.2)$$

Therefore, we see that if we were to keep the radial coordinates in the real line, in the limit of high frequency, we would have the problem that the solutions contain terms that are exponentially growing and terms that are exponentially vanishing. This would result in an indeterminacy in the definition of the asymptotic solutions. To remediate this, we will restrict our solutions to contours in the r -plane that have $\text{Im } \omega x = 0$. By doing so, we see that the terms $e^{i\omega x}$ and $e^{-i\omega x}$ are now purely oscillatory: the problem of having exponentially growing and vanishing terms has disappeared. This, in turn, will allow us to match solutions to the wave equation along the contour $\text{Im } \omega x = 0$, even when these were found in very different physical regions.

Now, let us say something about the frequency regime that we will consider. First, note that since we have chosen the time-dependent part of our field to be $e^{i\omega t}$, in order to have stable solutions, we need to require that $\text{Im } \omega > 0$, otherwise the solutions would grow exponentially in time. Moreover, numerical studies show that for the type of black holes that we will consider, the frequency of the waves is such that $\text{Im } \omega \gg \text{Re } \omega$. In fact, we will be interested in the regime where $\text{Im } \omega \rightarrow +\infty$. This implies that our condition for the contour mentioned above becomes

$$\text{Im } \omega x = 0 \quad \longrightarrow \quad \text{Re } x = 0. \quad (8.3)$$

We will have to draw the contour that satisfies the above condition for each of the black holes that we will consider in the next chapter. This contour is called the Stokes line.

In our computations, we will also consider the case $\text{Im } \omega \rightarrow -\infty$, since it is necessary to get the greybody factor. There is nothing contradictory here: in that case, the time-dependent part of our field is $e^{-i\omega t}$, which implies using the same reasoning as above, that $\text{Im } \omega < 0$. Moreover, the Stokes line is the same as before.¹

Finally, since we are in the high frequency regime, we impose the following energy condition

$$|\omega r_h| \gg 1, \quad (8.4)$$

with r_h each of the horizons of the black holes we will consider. This condition will be handy when finding the expressions for the potential.

8.2 Monodromy of the tortoise coordinate and plane waves

In our computations, we will be interested in finding how do our solutions behave as they run around a horizon of a black hole of the form

$$ds_2^2 = -f(r)dt^2 + f(r)^{-1}dr^2 + r^2 d\Omega_2^2.$$

¹There are some differences regarding the sign of ωx , but we will address them in the next chapter for each of the black holes we will consider.

Naturally, the horizons of the black hole are found by solving $f(r) = 0$. Let us consider one of the horizons r_h and expand $f(r)$ around it. Then, the tortoise coordinate will be

$$x = \int \frac{dr}{f(r)} = \int \frac{dr}{(r - r_h)f'(r_h)} = \frac{\beta}{4\pi} \log(r - r_h), \quad (8.5)$$

where we have used the fact that the surface gravity is defined as $\kappa = (1/2)f'(r_h)$ and its well-known relation to the Hawking temperature of the black hole.

Now, recall that the logarithm of a complex number $z = |z|e^{i\theta}$ is given by

$$\log z = \ln |z| + i(\theta + 2\pi m),$$

with $m = 0, 1, 2, \dots$. That is, the complex logarithm is a multivalued function. Therefore, so will our tortoise coordinate around a horizon. This multivaluedness plays a crucial role in the current method: it will allow us to define the monodromy of the tortoise coordinate. For example, suppose we have a horizon r_h and we travel around it along C (see figure below). Then, using (8.5), it is easy to see that the tortoise coordinate will change as

$$x \rightarrow x - i\frac{\beta}{2}. \quad (8.6)$$

This is the monodromy of x around a black hole horizon.

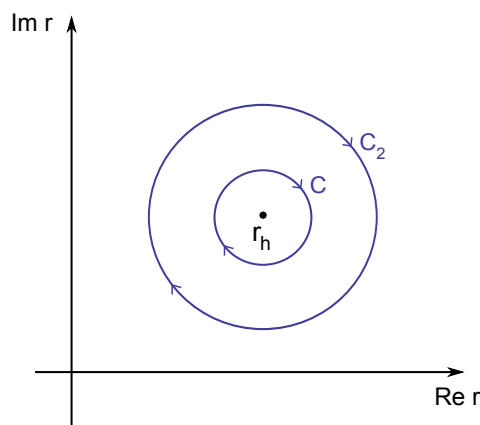


Figure 8.1: Monodromy of the tortoise coordinate along a path C around a black hole horizon in the r -plane. The monodromy does not change if we deform the contour and make it into a bigger one, C_2 .

Now, we can readily find the monodromy of the plane wave solutions that will appear in our asymptotic solutions to the wave equation. Using the equation above, it is easy to see that as one takes $e^{\pm i\omega x}$ around a contour C enclosing a horizon, their monodromies will be given by

$$\mathcal{M}_{C, r_h} [e^{\pm i\omega x}] = e^{\pm \frac{\beta\omega}{2}}. \quad (8.7)$$

This result will be one of the main ingredients in the computation of greybody factors at high frequencies.

Before concluding this chapter, let us comment on a crucial point. We have found the

monodromy of the tortoise coordinate and the plane waves around a black hole horizon. If we deform the initial contour C , making it larger and larger (without crossing any singularity!), until we obtain another contour C_2 around the horizon, the monodromy of the tortoise coordinate and of the plane wave around this final contour has to be the same as that around the initial contour.

We have now all the general tools and definitions of the monodromy technique to start our computations. The details explained in this chapter will hold for all the black hole cases we will consider. The only exception is the one considered in [chapter 10](#), but we will explain the minor differences there.

Chapter 9

Greybody factors at high frequency

In this chapter we use the monodromy technique to compute the greybody factors at high frequency for two four-dimensional black holes in asymptotically flat spacetime. In the case of the Reissner-Nordström black hole, the computation has not been presented explicitly in the literature. Further references for this chapter are [34, 35, 27].

9.1 $d = 4$ Schwarzschild black hole

Before embarking on the actual greybody factor computation, we still need to specify some other subtleties regarding the form of the tortoise coordinate, of the solutions and the explicit construction of the Stokes lines. We will be more explicit in this section in order to explain thoroughly the steps involved in the computation.

9.1.1 Constructing the Stokes line

Recall that the Stokes line is the one that satisfies $\text{Re } x = 0$ in the r -plane. First, note that the only singular point of the Stokes line will be at $r = 0$. Then, let us see its behavior near that point. Going back for a moment to $r, x \in \mathbb{R}$, the Schwarzschild tortoise coordinate is given by

$$x = r + r_0 \log \left| \frac{r}{r_0} - 1 \right|, \quad (9.1)$$

so that for $r < r_0$, we can write it as

$$x = r + r_0 \log \left(1 - \frac{r}{r_0} \right).$$

Then, to find the behavior of x around the origin, we expand the logarithm near $r = 0$ and get

$$x = r + r_0 \left(-\frac{r}{r_0} - \frac{r^2}{2r_0^2} \right) = -\frac{r^2}{2r_0}. \quad (9.2)$$

Note that we only expand the log term to second order because that suffices to give us a non-trivial result. This will change for other black holes, where we will need to expand up to third order to get a non-trivial result. Of course, the event horizon r_0 is located on the real line in the r -plane.

Now, back to $r, x \in \mathbb{C}$. We use the above relation with $r = |r|e^{i\theta}$, so that

$$x = -\frac{|r|^2}{2r_0} \cos 2\theta - i\frac{|r|^2}{2r_0} \sin 2\theta.$$

Hence, the condition $\text{Re } x = 0$ for the Stokes line implies that

$$\theta = \left(m + \frac{1}{2}\right) \frac{\pi}{2}. \quad (9.3)$$

Therefore, the Stokes line around the origin behaves as

$$r = |r|e^{i\frac{\pi}{2}(m+\frac{1}{2})}, \quad (9.4)$$

with $m = 0, 1, 2, 3$. These are just half-lines in the complex r -plane, separated by an angle of $\frac{\pi}{2}$. The first is at $\frac{\pi}{4}$ (see figure below).

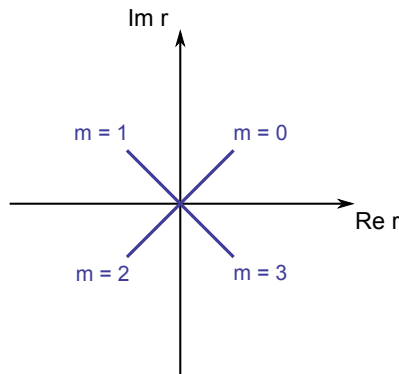


Figure 9.1: Behavior of the Stokes line very close to the origin for the Schwarzschild black hole.

We will be interested in knowing the sign of ωx in each of the branches of the Stokes line. It will be sufficient to know the sign of x by looking at equations (9.2) and (9.4). For $m = 0, 2$ x is negative, while for $m = 1, 3$, x is positive. Since $\text{Im } \omega \rightarrow +\infty$, then the sign of ωx is such that

$$\text{Sign } \omega x = (-1)^m. \quad (9.5)$$

It is easy to see that if when we consider a wave with frequency $\text{Im } \omega \rightarrow -\infty$, the formula would be $\text{Sign } \omega x = (-1)^{m+1}$.

Now, remember that x is a multivalued function near to the horizon. Therefore, the horizon is a branch point. Also, from (9.1), we see that the Stokes line must intersect the real line in a point greater than r_0 . Moreover, as $r \rightarrow +\infty$, it is easy to see from the definition of the tortoise coordinate that $x \rightarrow +\infty$, or equivalently, $x \sim r$. Then, very far away from the origin, the Stokes line $\text{Re } x = 0$ will be approximately parallel

to $\text{Re } r = 0$. With these last remarks, we have all the information needed to draw the Stokes line below.

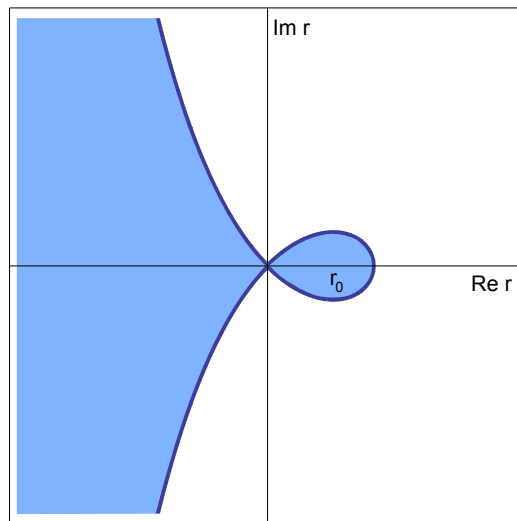


Figure 9.2: Stokes line for the Schwarzschild black hole. The colored region corresponds to $\text{Re } x < 0$. It will prove to be useful in our computation to know the sign of x in different regions.

9.1.2 Asymptotics of the solutions

Now, we need to know how our solutions behave in the limits of our physical region. These will be the solutions that will be matched along the Stokes line constructed above. We will be interested in the solutions as $r \rightarrow +\infty$ and $r \rightarrow 0$. The reader might be puzzled of why we are interested in studying the solutions to the wave equation near the singularity $r = 0$, since that point has nothing to do with greybody factors and their modification of Hawking radiation. This is not a problem: we are just using the monodromy technique to study the behavior of the solutions in the r -plane. There is nothing unphysical here.

Just for convenience, recall that the wave equation in this case was found to be

$$\left(\frac{d^2}{dx^2} + \omega^2 - V(r) \right) \psi(r) = 0. \quad (9.6)$$

To keep things more general, we will use the potential given in [chapter 4](#)

$$V(r) = f(r) \left[\frac{l(l+1)}{r^2} + \frac{f'(r)(1-j^2)}{r} \right],$$

with j the spin of the perturbation. We should, however, make an important remark. How analysis below will depend on the term with $f'(r)$ being dominant, so that the potential falls rapidly to zero far away from the black hole. Therefore, the results we will obtain will *not* hold for $j = 1$. Hence, we will only take $j = 0, 2$ in our final results, for scalar and gravitational perturbations, respectively.

Solutions as $r \rightarrow +\infty$

In this limit, the potential $V(r)$ goes to zero and we will have that the solutions behave as

$$\psi(x) \sim A_+ e^{i\omega x} + A_- e^{-i\omega x}.$$

Of course, when we study, for example, the scattering of an incoming wave, one of the coefficients will be replaced by a reflection coefficient R and the other will simply be one.

Solutions as $r \rightarrow 0$

Now, we turn to the task of finding the reduced expression for the potential in this case. Near $r = 0$, it reduces to (see [Appendix F](#))

$$V = \frac{j^2 - 1}{4x^2}. \quad (9.7)$$

Therefore, after performing the change of variable $\rho = \omega x$, the wave equation in this region is

$$\frac{d^2\psi}{d\rho^2} + \left(1 - \frac{j^2 - 1}{4\rho^2}\right)\psi = 0, \quad (9.8)$$

with solutions given by

$$\psi(x) \sim B_+ \sqrt{2\pi\omega x} J_{\frac{j}{2}}(\omega x) + B_- \sqrt{2\pi\omega x} J_{-\frac{j}{2}}(\omega x), \quad (9.9)$$

where J_n are Bessel functions of first kind.

Given that we will be interested in the regime where $\omega x \gg 1$ (no need to take the absolute value, because remember that we will use these solutions in the contour where $\text{Im } \omega x = 0$), we can use the asymptotic expression for a Bessel function of first kind as a cosine function, given in [Appendix E](#). It is a simple exercise to check that the solution to the wave equation reduces to

$$\psi(x) \sim (-\mathbf{1})_B e^{i\omega x} + (\mathbf{1})_B e^{-i\omega x}, \quad (9.10)$$

where we have borrowed the shorthand notation introduced in [\[33\]](#)

$$(\mathbf{m})_B = B_+ e^{i\frac{m\pi}{4}(1+j)} + B_- e^{i\frac{m\pi}{4}(1-j)}. \quad (9.11)$$

9.1.3 Rotating the tortoise coordinate and the solutions

Finally, recall that we will travel along contours in the r -plane to know the monodromy of our solutions. Therefore, we will also need to know how does the tortoise coordinate change as we travel from one branch of the Stokes line to another near $r = 0$ in the r -plane. Of course, due to [\(9.4\)](#), these rotations will happen as multiples of $\frac{\pi}{2}$. Then, by looking at [\(9.2\)](#), it is easy to see that

$$\text{Rotation of } \frac{\pi}{2} \text{ in } r \quad \rightarrow \quad \text{Rotation of } \pi \text{ in } x. \quad (9.12)$$

For convenience, let us see what happens to the solution (9.10) as we rotate an angle of $\frac{n\pi}{2}$ near $r = 0$ in the r -plane. This is equivalent to a rotation of $n\pi$ in x . With these, the terms appearing in (9.9) will get modified as

$$\begin{aligned}\sqrt{2\pi\omega}e^{in\pi}xJ_{\pm\frac{j}{2}}(\omega e^{in\pi}x) &= e^{i\frac{n\pi}{2}(1\pm j)}\sqrt{2\pi\omega}xJ_{\pm\frac{j}{2}}(\omega x) \\ &= 2e^{i\frac{n\pi}{2}(1\pm j)}\cos\left(\omega x - \frac{\pi}{4}(1\pm j)\right).\end{aligned}$$

So, the solution will take the form

$$\begin{aligned}\psi \sim &\left[B_+e^{i\frac{(2n-1)\pi}{4}(1+j)} + B_-e^{i\frac{(2n-1)\pi}{4}(1-j)}\right]e^{i\omega x} \\ &+ \left[B_+e^{i\frac{(2n+1)\pi}{4}(1+j)} + B_-e^{i\frac{(2n+1)\pi}{4}(1-j)}\right]e^{-i\omega x},\end{aligned}$$

which, using notation (9.11), can be written as

$$\psi \sim (\mathbf{2n-1})_B e^{i\omega x} + (\mathbf{2n+1})_B e^{-i\omega x}. \quad (9.13)$$

This equation will be handy when moving from one branch of the Stokes line to another. However, when doing so, we will need to keep track of what the sign of ωx is in each of the branches (9.5).

Finally, let us stress that most of what we have said in this and the previous subsection, have assumed that $\text{Im}\omega \rightarrow +\infty$. The above formulas are easily modified if one considers $\text{Im}\omega \rightarrow -\infty$ and we will show how below, when computing the greybody factor.

9.1.4 Greybody factor computation

We now have all the necessary tools to perform the explicit calculation of the greybody factor. In some sense, what we will do is study the behavior of the solutions as we go around a given contour in the r -plane and also study the monodromy of the solutions around the horizon. These two steps will give us enough information to find explicit expressions for the transmission and reflection coefficients associated to the potential barrier. We will consider an incoming wave. The setup for the calculation is shown below.

Incoming wave with positive frequency

First, let us consider an incoming wave with positive frequency $\text{Im}\omega \rightarrow +\infty$. We start in the branch $m = 2$ of the Stokes line, at point 1, where $r \rightarrow \infty$, so that the solution there is given by

$$\psi(x) \sim e^{i\omega x} + R e^{-i\omega x}.$$

Note that in this branch ωx is positive. Then, we approach $r = 0$, up to point 2, where the solution is given by

$$\psi(x) \sim (-\mathbf{1})_B e^{i\omega x} + (\mathbf{1})_B e^{-i\omega x}.$$

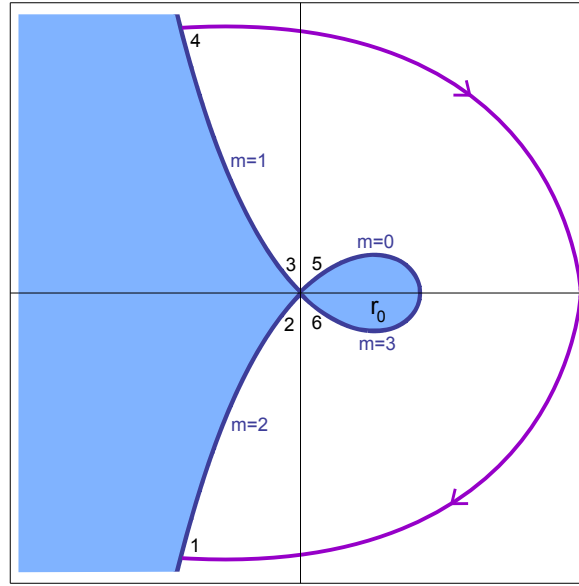


Figure 9.3: Setup for our computation in the Schwarzschild case. Note that the sign of ωx will change in each branch of the Stokes lines depending on the sign of the frequency of the wave.

Given that we are on the Stokes line, we can match these two solutions. Therefore, we get

$$\begin{aligned} (\mathbf{1})_B &= R \\ (-\mathbf{1})_B &= 1. \end{aligned} \quad (9.14)$$

Now, we rotate near $r = 0$ from point 2 to 3, which are separated by an angle of $\frac{3\pi}{2}$. Then, using (9.13), we get that our solution at point 3 is

$$\psi(x) \sim (\mathbf{7})_B e^{i\omega x} + (\mathbf{5})_B e^{-i\omega x}.$$

Note that we have used the fact that in the branch with $m = 1$, ωx is negative. Then, we take this solutions and move along the Stokes line up to point 4. To close the contour, we take big clockwise trip until we reach our initial point 1. Note that as we approach it, we are in the region where $\text{Re } x > 0$, and since $\text{Im } \omega \rightarrow \infty$, the term $e^{i\omega x}$ in the solution is exponentially small and we cannot take its coefficient into account because there will be inherent indeteterminacy in its value. Therefore, we only take into account the term $e^{-i\omega x}$, whose coefficient after travelling around the contour has changed by

$$\frac{(\mathbf{5})_B}{(\mathbf{1})_B}.$$

Moreover, we have to remember that $e^{-i\omega x}$ has a monodromy of $e^{-\frac{\beta\omega}{2}}$, so that its coefficient after the trip effectively changes by

$$\frac{(\mathbf{5})_B}{(\mathbf{1})_B} e^{-\frac{\beta\omega}{2}}. \quad (9.15)$$

One can deform the contour considered above and reduce it to a contour very close to the horizon r_0 . There, the solution goes as $e^{i\omega x}$, because we are considering an incoming wave with positive frequency. In this case, the monodromy of the solution as we travel along the new small contour is $e^{\frac{\beta\omega}{2}}$. The crucial step is to realize that the monodromy must be the same in both cases: either if we travel around the big contour or if we choose to go close to the horizon. Therefore, we get

$$\frac{(\mathbf{5})_B}{(\mathbf{1})_B} e^{-\frac{\beta\omega}{2}} = e^{\frac{\beta\omega}{2}}. \quad (9.16)$$

Finally, one can take our initial solution at point 2 and rotate until we reach the branch $m = 0$ of the Stokes line at point 5. Using (9.13), we find that the solution there is given by

$$\psi(x) \sim (\mathbf{3})_B e^{i\omega x} + (\mathbf{5})_B e^{-i\omega x}.$$

Again, note that in that branch, ωx is positive. We could also take our solution at point 2 and rotate until we reach the branch $m = 3$ at point 6, where ωx is negative, and get

$$\psi(x) \sim (\mathbf{3})_B e^{i\omega x} + (\mathbf{1})_B e^{-i\omega x}.$$

With this information, let us do the following. If we take the trip along the Stokes line from point 5 to 6, we see that we are very close to the horizon and so, the solution there is given by (5.9) as

$$\psi(x) \sim T e^{i\omega x}.$$

Comparing this equation with the two above, we immediately realize that

$$(\mathbf{3})_B = T. \quad (9.17)$$

Equations (9.14), (9.16) and (9.17) form the following linear system for the four variables B_+ , B_- , R , T

$$\begin{pmatrix} e^{i\frac{\pi}{4}(1+j)} & e^{i\frac{\pi}{4}(1-j)} & 0 & -1 \\ e^{-i\frac{\pi}{4}(1+j)} & e^{-i\frac{\pi}{4}(1-j)} & 0 & 0 \\ e^{i\frac{5\pi}{4}(1+j)} & e^{i\frac{5\pi}{4}(1-j)} & 0 & -e^{\beta\omega} \\ e^{i\frac{3\pi}{4}(1+j)} & e^{i\frac{3\pi}{4}(1-j)} & -1 & 0 \end{pmatrix} \begin{pmatrix} B_+ \\ B_- \\ T \\ R \end{pmatrix} = \begin{pmatrix} 0 \\ 1 \\ 0 \\ 0 \end{pmatrix}$$

We now take a moment to thank Stephen Wolfram for inventing Mathematica. Recalling that j is an integer and it cannot be 1 for the reasons we explained in the beginning of the previous subsection, the solutions we get for the transmission and reflection coefficients are given by

$$\begin{aligned} T(\omega) &= \frac{e^{\beta\omega} - 1}{e^{\beta\omega} + 1 + 2 \cos \pi j}, \\ R(\omega) &= \frac{2i \cos \frac{\pi j}{2}}{e^{\beta\omega} + 1 + 2 \cos \pi j}. \end{aligned} \quad (9.18)$$

Incoming wave with negative frequency

Now, let us consider an incoming wave with negative frequency, so that $\text{Im } \omega \rightarrow -\infty$. Recall that in this case the time dependent part of the field is $e^{-i\omega t}$. The computation proceeds exactly as before, except that the frequency being now negative changes the plane wave terms and the sign of ωx in each of the branches of the Stokes line. At point 1, far away from the black hole, the solution is now given by¹

$$\psi(x) \sim e^{i\omega x} + \tilde{R}e^{-i\omega x}.$$

Recall that in this branch ωx is negative. To find the solution near $r = 0$, at point 2, notice that it will not be the solution (9.10) that we used in the positive frequency case. More explicitly, the solution to the wave equation there is of the form

$$\psi(x) \sim \tilde{B}_+ \sqrt{2\pi\omega x} J_{\frac{j}{2}}(\omega x) + \tilde{B}_- \sqrt{2\pi\omega x} J_{-\frac{j}{2}}(\omega x),$$

but now with $\omega x \ll -1$. This fact changes the sign of the first term in the argument of the cosine in the asymptotic expression for the Bessel function (E.3). It is a simple exercise to check that the solution at point 2 reduces to

$$\psi(x) \sim (\mathbf{1})_{\tilde{B}} e^{i\omega x} + (-\mathbf{1})_{\tilde{B}} e^{-i\omega x}, \quad (9.19)$$

where $(\mathbf{m})_{\tilde{B}}$ has exactly the same form as (9.11), but with different coefficients. Matching the two solutions above, we get

$$\begin{aligned} (-\mathbf{1})_{\tilde{B}} &= \tilde{R} \\ (\mathbf{1})_{\tilde{B}} &= 1. \end{aligned} \quad (9.20)$$

Equation (9.13) also needs to be modified in this case. It is straightforward to check that after rotating an angle $\frac{n\pi}{2}$ in the r -plane near $r = 0$, solution (9.19) becomes

$$\psi \sim (\mathbf{2n+1})_{\tilde{B}} e^{i\omega x} + (\mathbf{2n-1})_{\tilde{B}} e^{-i\omega x}. \quad (9.21)$$

Then, rotating from point 2 to 3, where ωx is now positive, the solution there becomes

$$\psi(x) \sim (\mathbf{5})_{\tilde{B}} e^{i\omega x} + (\mathbf{7})_{\tilde{B}} e^{-i\omega x}.$$

We move it to point 4 and then close the contour back to our initial point 1. In this case, as we close the path, the term $e^{-i\omega x}$ is exponentially small and its coefficient does not enter the analysis. Then, the coefficient of $e^{i\omega x}$ as we travel along the contour changes by (including also its monodromy)

$$\frac{(\mathbf{5})_{\tilde{B}}}{(\mathbf{1})_{\tilde{B}}} e^{\frac{\beta\omega}{2}}.$$

¹At first sight, this equation seems to be in contradiction with the boundary conditions for an incoming wave with negative frequency that we gave in chapter 5. However, we have to realize that we are starting in a branch of the Stokes line where $\omega x < 0$, so that the change of signs in the exponents from (5.9) to (5.10) is now redundant and not necessary for our discussion.

Again, we can deform the contour to one very close to the horizon, where the solution in this case behaves as $e^{i\omega x}$, whose monodromy is $e^{\frac{\beta\omega}{2}}$. Then, we finally get

$$\frac{(\mathbf{5})_{\tilde{B}}}{(\mathbf{1})_{\tilde{B}}} = 1. \quad (9.22)$$

Finally, we take our initial solution at point 2 and rotate until we reach the branch $m = 0$ of the Stokes line at point 5, where the solution is given by

$$\psi(x) \sim (\mathbf{5})_{\tilde{B}} e^{i\omega x} + (\mathbf{3})_{\tilde{B}} e^{-i\omega x}.$$

Again, note that in that branch, ωx is negative. We could also take our solution at point 2 and rotate until we reach the branch $m = 3$ at point 6, where ωx is positive, and get

$$\psi(x) \sim (\mathbf{1})_{\tilde{B}} e^{i\omega x} + (\mathbf{3})_{\tilde{B}} e^{-i\omega x}.$$

With this information, let us do the following. If we take the trip along the Stokes line from point 5 to 6, we see that we are very close to the horizon and so, the solution there is given by

$$\psi(x) \sim \tilde{T} e^{i\omega x}.$$

Comparing this equation with the two above, we immediately realize that

$$(\mathbf{5})_{\tilde{B}} = (\mathbf{1})_{\tilde{B}} = \tilde{T}. \quad (9.23)$$

We now have a linear system for the four variables \tilde{B}_+ , \tilde{B}_- , \tilde{T} , \tilde{R} , given by equations (9.20), (9.22) and (9.23). It is

$$\begin{pmatrix} e^{i\frac{\pi}{4}(1+j)} & e^{i\frac{\pi}{4}(1-j)} & 0 & 0 \\ e^{-i\frac{\pi}{4}(1+j)} & e^{-i\frac{\pi}{4}(1-j)} & 0 & -1 \\ e^{i\frac{\pi}{4}(1+j)} & e^{i\frac{\pi}{4}(1-j)} & -1 & 0 \\ e^{i\frac{5\pi}{4}(1+j)} & e^{i\frac{5\pi}{4}(1-j)} & 0 & 0 \end{pmatrix} \begin{pmatrix} \tilde{B}_+ \\ \tilde{B}_- \\ \tilde{T} \\ \tilde{R} \end{pmatrix} = \begin{pmatrix} 1 \\ 0 \\ 0 \\ 1 \end{pmatrix}.$$

Solving it, we obtain

$$\begin{aligned} \tilde{T}(-\omega) &= 1 \\ \tilde{R}(-\omega) &= -2i \cos \frac{\pi j}{2}. \end{aligned} \quad (9.24)$$

Results

Now that we have the transmission coefficients for an incoming wave of both positive and negative frequency, we can use (5.14) to obtain the final expression for the greybody factor at high frequency for the four-dimensional Schwarzschild black hole. It is given by

$$\gamma(\omega) = \frac{e^{\beta\omega} - 1}{e^{\beta\omega} + 1 + 2 \cos \pi j}, \quad (9.25)$$

for $j = 0$ or $j = 2$ the spin of the particle under consideration.

Let us now restrict to the case of a massless scalar field, for which the greybody factor becomes

$$\gamma(\omega) = \frac{e^{\beta\omega} - 1}{e^{\beta\omega} + 3}, \quad (9.26)$$

so that the original emission rate originated at the black hole horizon gets modified to (see (5.1))

$$\Gamma(\omega) = \frac{1}{e^{\beta\omega} + 3} \frac{d^3k}{(2\pi)^3}. \quad (9.27)$$

9.2 $d = 4$ Reissner-Nordström black hole

Having explained carefully the steps involved for the Schwarzschild black hole, let us be more concise in the discussion of this section. All steps are essentially the same as before.

9.2.1 Constructing the Stokes line

Again, the only singular point of the Stokes line will be at $r = 0$. Going back for a moment to $r, x \in \mathbb{R}$, the tortoise coordinate in this case is given by

$$x = r + \frac{r_+^2}{r_+ - r_-} \log \left| \frac{r}{r_+} - 1 \right| - \frac{r_-^2}{r_+ - r_-} \log \left| \frac{r}{r_-} - 1 \right|, \quad (9.28)$$

where r_+ and r_- are the outer and inner horizon, respectively. So, for $r < r_0$, we can write the tortoise coordinate as

$$x = r + \frac{r_+^2}{r_+ - r_-} \log \left(1 - \frac{r}{r_+} \right) - \frac{r_-^2}{r_+ - r_-} \log \left(1 - \frac{r}{r_-} \right).$$

Then, to find the behavior of x around the origin, we expand the logarithm near $r = 0$. In this case, it is necessary to expand to third order in order to get a non-trivial answer. We find that

$$x = \frac{r^3}{3r_+r_-}. \quad (9.29)$$

Now, back to $r, x \in \mathbb{C}$. We use the above relation with $r = |r|e^{i\theta}$, so that the condition $\text{Re } x = 0$ for the Stokes line implies that

$$\theta = \left(m + \frac{1}{2} \right) \frac{\pi}{3}. \quad (9.30)$$

Therefore, the Stokes line around the origin behaves as

$$r = |r|e^{i\frac{\pi}{3}(m+\frac{1}{2})}, \quad (9.31)$$

with $m = 0, 1, 2, 3, 4, 5$. These are just half-lines in the complex r -plane, separated by an angle of $\frac{\pi}{3}$. The first is at $\frac{\pi}{6}$ (see figure below).

We will be interested in knowing the sign of ωx in each of the branches of the Stokes line. Following the same reasoning as for the Schwarzschild case, when $\text{Im } \omega \rightarrow +\infty$, we

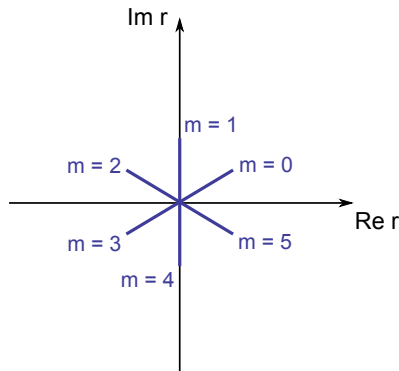


Figure 9.4: Behavior of the Stokes line very close to the origin for the Reissner-Nordström black hole.

get

$$\text{Sign } \omega x = (-1)^{m+1}. \tag{9.32}$$

When $\text{Im } \omega \rightarrow -\infty$, it is easy to check that the above formula changes to $\text{Sign } \omega x = (-1)^m$.

Now, remember that x is a multivalued function near the horizons r_+, r_- . Therefore, the two horizons are branch points. Also, in this case the Stokes line should intersect the real line in two points: one between r_- and r_+ and the other between r_+ and $+\infty$. Moreover, as $r \rightarrow +\infty$, it is easy to see from the definition of the tortoise coordinate that $x \rightarrow +\infty$, or equivalently, $x \sim r$. Then, very far away from the origin, the Stokes line $\text{Re } x = 0$ will be approximately parallel to $\text{Re } r = 0$. With these last remarks, we have all the information needed to draw the Stokes line below.

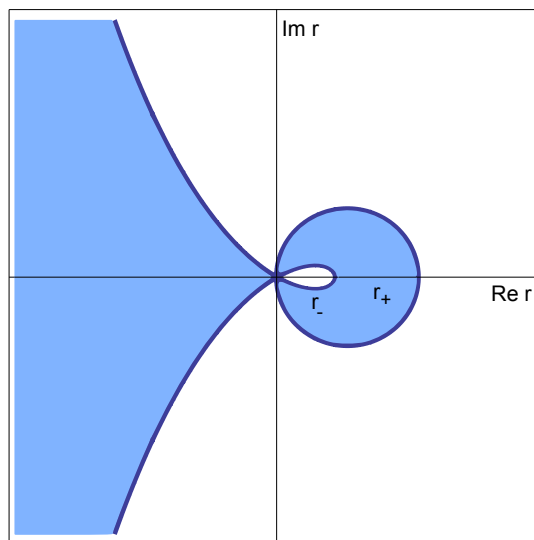


Figure 9.5: Stokes line for the Reissner-Nordström black hole. The colored region corresponds to $\text{Re } x < 0$. It will prove to be useful in our computation to know the sign of x in different regions.

9.2.2 Asymptotics of the solutions

The wave equation is the same as before, but the potential term must be modified. This is because we are considering a charged black hole, whose electromagnetic field will of course interact with a spin $j = 1$ or $j = 2$ particle. We briefly mention in [Appendix F](#) the modifications to the potential entering the wave equation. Let us now use those results to see the form of the solutions for this black hole.

Solutions as $r \rightarrow +\infty$

In this limit, the potential $V(r)$ still goes to zero and we will have that the solutions behave as

$$\psi(x) \sim A_+ e^{i\omega x} + A_- e^{-i\omega x}.$$

Again, for an incoming wave, one of the coefficients will be replaced by the reflection coefficient R and the other will simply be one.

Solutions as $r \rightarrow 0$

Near $r = 0$, the potential reduces again to

$$V = \frac{j^2 - 1}{4x^2}, \quad (9.33)$$

with $j = \frac{1}{3}$ for spin-0 and spin-2 particles and $j = \frac{5}{3}$ for spin-1 particles (see [Appendix F](#) for the details). Therefore, after performing the change of variable $\rho = \omega x$, the wave equation in this region is again

$$\frac{d^2\psi}{d\rho^2} + \left(1 - \frac{j^2 - 1}{4\rho^2}\right)\psi = 0, \quad (9.34)$$

with solutions given by

$$\psi(x) \sim B_+ \sqrt{2\pi\omega x} J_{\frac{j}{2}}(\omega x) + B_- \sqrt{2\pi\omega x} J_{-\frac{j}{2}}(\omega x), \quad (9.35)$$

where J_n are Bessel functions of first kind. Therefore, using again the asymptotic form for the Bessel function, our solutions are exactly [\(9.10\)](#). That is

$$\psi(x) \sim (-\mathbf{1})_B e^{i\omega x} + (\mathbf{1})_B e^{-i\omega x}, \quad (9.36)$$

with the notation [\(9.13\)](#).

9.2.3 Rotating the tortoise coordinate and the solutions

Finally, recall that we will travel along contours in the r -plane to know the monodromy of our solutions. Therefore, we will also need to know how does the tortoise coordinate change as we travel from one branch of the Stokes line to another near $r = 0$ in the r -plane. Of course, due to [\(9.31\)](#), these rotations will happen as multiples of $\frac{\pi}{3}$. Then,

by looking at (9.29), it is easy to see that

$$\text{Rotation of } \frac{\pi}{3} \text{ in } r \rightarrow \text{Rotation of } \pi \text{ in } x. \quad (9.37)$$

Just as before, we want to know how the solutions change as we rotate an angle of $\frac{n\pi}{3}$ near $r = 0$ in the r -plane. This is equivalent to a rotation of $n\pi$ in x . Therefore, our solutions will change just as in the Schwarzschild case (9.13)

$$\psi \sim (\mathbf{2n-1})_B e^{i\omega x} + (\mathbf{2n+1})_B e^{-i\omega x}. \quad (9.38)$$

Again, when using this formula in our computations, we need to keep track of what the sign of ωx is in each of the branches of the Stokes line.

9.2.4 Greybody factor computation

We now have all the necessary tools to perform the explicit calculation of the greybody factor. The steps are basically the same as before, except that we now have two physical horizons and we have to be more careful when choosing the contour. We will explain how to do it below. First, we present the setup for our calculation.

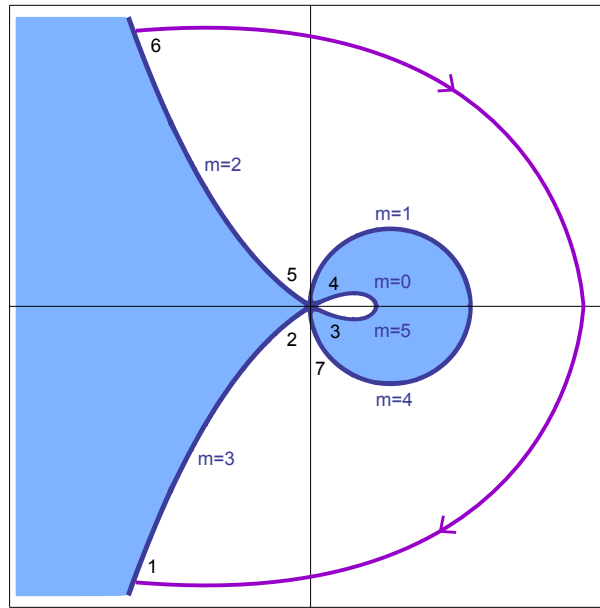


Figure 9.6: Setup for our computation in the Reissner-Nordström case. Note that the sign of ωx will change in each branch of the Stokes lines depending on the sign of the frequency of the wave.

Incoming wave with positive frequency

Again, let us first consider an incoming wave with positive frequency $\text{Im } \omega \rightarrow +\infty$. We start in the branch $m = 3$ of the Stokes line, at point 1, where $r \rightarrow \infty$, so that the solution there is given by

$$\psi(x) \sim e^{i\omega x} + R e^{-i\omega x}.$$

Note that in this branch ωx is positive. Then, we approach $r = 0$, up to point 2, where the solution is given by

$$\psi(x) \sim (-\mathbf{1})_B e^{i\omega x} + (\mathbf{1})_B e^{-i\omega x}. \quad (9.39)$$

Given that we are on the Stokes line, we can match these two solutions. Therefore, we get

$$\begin{aligned} (\mathbf{1})_B &= R \\ (-\mathbf{1})_B &= 1. \end{aligned} \quad (9.40)$$

We now rotate from point 2 to 3, where, using (9.13), the solution is given by

$$\psi(x) \sim (\mathbf{3})_B e^{i\omega x} + (\mathbf{5})_B e^{-i\omega x}. \quad (9.41)$$

Note that point 3 is in a branch where ωx is positive. The reader might wonder why we chose to move to point 3, instead of point 7. As we said above, given that there are two horizons, we have to be more careful when choosing the contour, which will *only* enclose the outer event horizon r_+ . Now that we are at point 3, we will travel along the Stokes line around the inner horizon r_- until we reach point 4. When doing, recall from (8.6) that the tortoise coordinate will change as $x \rightarrow x - i\frac{\beta}{2}$. Therefore, our plane wave terms appearing in the solution will have monodromies already defined in (8.7) and in this case they are

$$\mathcal{M}_{C,r_-} [e^{\pm i\omega x}] = e^{\pm \frac{\beta-\omega}{2}}$$

Then, the solution at point 4 is

$$\psi(x) \sim (\mathbf{1})_C e^{\frac{\beta-\omega}{2}} e^{i\omega x} + (-\mathbf{1})_C e^{-\frac{\beta-\omega}{2}} e^{-i\omega x}. \quad (9.42)$$

Let us make some remarks about this solution. We *have not* obtained it by using our rotation formula with the solution from point 3, because our trip between these two points did not take place near the origin. However, the plane wave terms will still be in the solution with their corresponding monodromies. Then, the solution at point 4 will be just like (9.39), but with different coefficients: there is no reason why they would be the same. Finally, to obtain the form of the solution written above, notice that in the branch of point 4, ωx is negative. By matching the solutions at points 3 and 4, we obtain

$$\begin{aligned} (\mathbf{3})_B &= (\mathbf{1})_C e^{\frac{\beta-\omega}{2}} \\ (\mathbf{5})_B &= (-\mathbf{1})_C e^{-\frac{\beta-\omega}{2}}. \end{aligned} \quad (9.43)$$

We now want to rotate from point 4 to 5. It is important to note that we cannot use the formula (9.13) with the solution (9.42): the former is only valid with solutions of the form we had at point 2, for example. Instead, we will make use of the rotation formula (9.21) that we obtained in the negative frequency case for the Schwarzschild black hole, which applies to solutions of the form we have at point 4. Then, at point 5

we have

$$\psi(x) \sim (\mathbf{5})_C e^{\frac{\beta_- \omega}{2}} e^{i\omega x} + (\mathbf{3})_C e^{-\frac{\beta_- \omega}{2}} e^{-i\omega x}. \quad (9.44)$$

We move the above solution along the Stokes line up to point 6 and then close the contour along the big clockwise trip until we reach point 1. As we approach it, we are in the region where $\text{Re } x > 0$, so that the term $e^{i\omega x}$ is exponentially small and will not be taken into account. Hence, we are only interested in the change in the coefficient of the term $e^{-i\omega x}$. Comparing (9.39) and (9.44), and including its monodromy as it travels around the outer horizon, the change of the coefficient of $e^{-i\omega x}$ is

$$\frac{(\mathbf{3})_C e^{-\frac{\beta_- \omega}{2}}}{(\mathbf{1})_B} e^{-\frac{\beta_+ \omega}{2}}.$$

Again, by deforming our contour to a small one around the outer horizon, we require that the monodromy remains the same. Close to the horizon, the solution behaves as $e^{i\omega x}$, which has monodromy $e^{\frac{\beta_+ \omega}{2}}$. Therefore, we obtain

$$\frac{(\mathbf{3})_C e^{-\frac{\beta_- \omega}{2}}}{(\mathbf{1})_B} e^{-\frac{\beta_+ \omega}{2}} = e^{\frac{\beta_+ \omega}{2}}. \quad (9.45)$$

Finally, to get an equation involving the transmission coefficient, take our solution at point 2 and rotate it to point 7, where ωx is negative. There, the solution will be

$$\psi(x) \sim (\mathbf{3})_B e^{i\omega x} + (\mathbf{1})_B e^{-i\omega x}. \quad (9.46)$$

Now, imagine we started a trip at point 3, traveled along the Stokes line around the inner horizon to point 4, then move to the part of the Stokes line that goes around the outer horizon to point 7 and go back to our initial point 3. In this trip, we are moving close to r_+ , where the solution is

$$\psi(x) \sim T e^{i\omega x}.$$

Then, comparing (9.41) and (9.46) with the equation above, we get

$$(\mathbf{3})_B = T. \quad (9.47)$$

Equations (9.40), (9.43), (9.45) and (9.47) form a linear system $M \cdot v = z$, with the two column vectors $z = (0; 1; 0; 0; 0; 0; 0)$ and $v = (B_+; B_-; C_+; C_-; T; R)$ and M given by

$$\begin{pmatrix} e^{i\frac{\pi}{4}(1+j)} & e^{i\frac{\pi}{4}(1-j)} & 0 & 0 & 0 & -1 \\ e^{-i\frac{\pi}{4}(1+j)} & e^{-i\frac{\pi}{4}(1-j)} & 0 & 0 & 0 & 0 \\ e^{i\frac{3\pi}{4}(1+j)} & e^{i\frac{3\pi}{4}(1-j)} & -e^{\frac{\beta_- \omega}{2}} e^{i\frac{\pi}{4}(1+j)} & -e^{\frac{\beta_- \omega}{2}} e^{i\frac{\pi}{4}(1-j)} & 0 & 0 \\ e^{i\frac{5\pi}{4}(1+j)} & e^{i\frac{5\pi}{4}(1-j)} & -e^{\frac{-\beta_- \omega}{2}} e^{-i\frac{\pi}{4}(1+j)} & -e^{\frac{-\beta_- \omega}{2}} e^{-i\frac{\pi}{4}(1-j)} & 0 & 0 \\ e^{\beta_+ \omega} e^{i\frac{\pi}{4}(1+j)} & e^{\beta_+ \omega} e^{i\frac{\pi}{4}(1-j)} & -e^{\frac{-\beta_- \omega}{2}} e^{i\frac{3\pi}{4}(1+j)} & -e^{\frac{-\beta_- \omega}{2}} e^{i\frac{3\pi}{4}(1-j)} & 0 & 0 \\ e^{i\frac{3\pi}{4}(1+j)} & e^{i\frac{3\pi}{4}(1-j)} & 0 & 0 & -1 & 0 \end{pmatrix}$$

Solving the system, we obtain

$$\begin{aligned} T(\omega) &= \frac{e^{\beta+\omega} - 1}{e^{\beta+\omega} + 2e^{-\beta-\omega}(\cos \pi j + 1) + 2 \cos \pi j + 1}, \\ R(\omega) &= \frac{2i \cos \frac{\pi j}{2} (1 + e^{-\beta-\omega})}{e^{\beta+\omega} + 2e^{-\beta-\omega}(\cos \pi j + 1) + 2 \cos \pi j + 1}. \end{aligned} \quad (9.48)$$

Incoming wave with negative frequency

Let us now consider the case of negative frequency. The reasoning here is the same as in the Schwarzschild case. Yet again, at point 1, far away from the black hole, the solution is given by

$$\psi(x) \sim e^{i\omega x} + \tilde{R}e^{-i\omega x}.$$

Note that in this branch, ωx is now negative. Therefore, at point 2, the solution is given by (9.19)

$$\psi(x) \sim (\mathbf{1})_{\tilde{B}} e^{i\omega x} + (-\mathbf{1})_{\tilde{B}} e^{-i\omega x}.$$

Matching these two solutions, we get

$$\begin{aligned} (-\mathbf{1})_{\tilde{B}} &= \tilde{R} \\ (\mathbf{1})_{\tilde{B}} &= 1. \end{aligned} \quad (9.49)$$

Now, rotating from point 2 to 3 using (9.21), the solution there is given by

$$\psi(x) \sim (\mathbf{5})_{\tilde{B}} e^{i\omega x} + (\mathbf{3})_{\tilde{B}} e^{-i\omega x}. \quad (9.50)$$

Again, we take the trip around the inner horizon and end up in point 4, where ωx is now positive. By the same reasoning than in the positive frequency case, the solution there is given by²

$$\psi(x) \sim (-\mathbf{1})_{\tilde{C}} e^{\frac{\beta-\omega}{2}} e^{i\omega x} + (\mathbf{1})_{\tilde{C}} e^{-\frac{\beta-\omega}{2}} e^{-i\omega x}.$$

Matching the solutions at points 3 and 4 yields

$$\begin{aligned} (\mathbf{5})_{\tilde{B}} &= (-\mathbf{1})_{\tilde{C}} e^{\frac{\beta-\omega}{2}} \\ (\mathbf{3})_{\tilde{B}} &= (\mathbf{1})_{\tilde{C}} e^{-\frac{\beta-\omega}{2}}. \end{aligned} \quad (9.51)$$

We now use (9.13) and rotate from point 4 to 5, where the solution becomes

$$\psi(x) \sim (\mathbf{3})_{\tilde{C}} e^{\frac{\beta-\omega}{2}} e^{i\omega x} + (\mathbf{5})_{\tilde{C}} e^{-\frac{\beta-\omega}{2}} e^{-i\omega x}.$$

Move this solution to point 6 and then close to contour back to point 1. When approaching it, now the term that will be exponentially small will be $e^{-i\omega x}$, so that we only need to see how the coefficient of $e^{i\omega x}$ change as we traveled along the contour. Comparing the solutions at points 2 and 6, it is easy to see that the coefficient changed

²Since point 4 is in a branch where ωx is positive, the solution there is of the form (9.36).

by, including its monodromy around the outer horizon

$$\frac{(\mathbf{3})_{\tilde{C}} e^{\frac{\beta-\omega}{2}}}{(\mathbf{1})_{\tilde{B}}} e^{\frac{\beta+\omega}{2}}.$$

However, this change should be equal to the monodromy of the solution around a contour very close to the horizon, where it behaves as $e^{i\omega x}$. Therefore, we get

$$\frac{(\mathbf{3})_{\tilde{C}} e^{\frac{\beta-\omega}{2}}}{(\mathbf{1})_{\tilde{B}}} = 1. \quad (9.52)$$

To get an equation for the transmission coefficient, let us rotate the solution at point 2 to point 7 using (9.21). Since at point 7 ωx is positive, the solution there will be

$$\psi(x) \sim (\mathbf{1})_{\tilde{B}} e^{i\omega x} + (\mathbf{3})_{\tilde{B}} e^{-i\omega x}. \quad (9.53)$$

Now, imagine we started a trip at point 3, traveled along the Stokes line around the inner horizon to point 4, then move to the branch of the Stokes line with $m = 1$ and travel around the outer horizon until we get to point 7 and go back to our initial point 3. In this trip, we are moving close to r_+ , where the solution is yet again

$$\psi(x) \sim \tilde{T} e^{i\omega x}.$$

Then, comparing (9.50) and (9.53) with the equation above, we immediately realize that

$$\begin{aligned} (\mathbf{1})_{\tilde{B}} &= (\mathbf{5})_{\tilde{B}} = \tilde{T} \\ (\mathbf{3})_{\tilde{B}} &= 0. \end{aligned} \quad (9.54)$$

Note that from (9.49) and (9.54), we immediately get $\tilde{T} = (\mathbf{5})_{\tilde{B}} = 1$. Then, using (9.49), (9.51), (9.52) and (9.54) we solve the linear system $M \cdot v = z$, with the two column vectors $z = (0; 1; 1; 0; 1; 0)$ and $v = (\tilde{B}_+; \tilde{B}_-; \tilde{C}_+; \tilde{C}_-; \tilde{T}; \tilde{R})$ and M given by

$$\begin{pmatrix} e^{-i\frac{\pi}{4}(1+j)} & e^{-i\frac{\pi}{4}(1-j)} & 0 & 0 & 0 & -1 \\ e^{i\frac{\pi}{4}(1+j)} & e^{i\frac{\pi}{4}(1-j)} & 0 & 0 & 0 & 0 \\ 0 & 0 & e^{\frac{\beta-\omega}{2}} e^{-i\frac{\pi}{4}(1+j)} & e^{\frac{\beta-\omega}{2}} e^{-i\frac{\pi}{4}(1-j)} & 0 & 0 \\ e^{i\frac{3\pi}{4}(1+j)} & e^{i\frac{3\pi}{4}(1-j)} & -e^{\frac{-\beta-\omega}{2}} e^{i\frac{\pi}{4}(1+j)} & -e^{\frac{-\beta-\omega}{2}} e^{i\frac{\pi}{4}(1-j)} & 0 & 0 \\ 0 & 0 & e^{\frac{\beta-\omega}{2}} e^{i\frac{3\pi}{4}(1+j)} & e^{\frac{\beta-\omega}{2}} e^{i\frac{3\pi}{4}(1-j)} & 0 & 0 \\ e^{i\frac{\pi}{4}(1+j)} & e^{i\frac{\pi}{4}(1-j)} & 0 & 0 & -1 & 0 \end{pmatrix}.$$

Solving the system, we obtain

$$\begin{aligned} \tilde{T}(-\omega) &= 1, \\ \tilde{R}(-\omega) &= \frac{-2i e^{i\frac{\pi j}{2}} (1 + \cos \pi j)}{1 + e^{i\pi j}}. \end{aligned} \quad (9.55)$$

Results

The final expression for the greybody factor at high frequency for the four-dimensional Reissner-Nordström black hole is given by

$$\gamma(\omega) = \frac{e^{\beta+\omega} - 1}{e^{\beta+\omega} + 2e^{-\beta-\omega} (\cos \pi j + 1) + 2 \cos \pi j + 1}, \quad (9.56)$$

where $j = \frac{1}{3}$ if considering a spin-0 or spin-2 particle and $j = \frac{5}{3}$ if considering a spin-1 particle.

Therefore, the result for a massless scalar field is

$$\gamma(\omega) = \frac{e^{\beta+\omega} - 1}{e^{\beta+\omega} + 3e^{-\beta-\omega} + 2}, \quad (9.57)$$

so that the original emission rate originated at the black hole outer horizon gets modified to

$$\Gamma(\omega) = \frac{1}{e^{\beta+\omega} + 3e^{-\beta-\omega} + 2} \frac{d^3k}{(2\pi)^3}. \quad (9.58)$$

9.3 Suggestive results

As we can see, the results we have obtained in the previous sections are highly suggestive. Focusing on the results for a massless scalar field, the greybody factors at high frequency that we found have the characteristic Bose-Einstein statistics term in the numerator, which exactly cancels the one appearing in the formula for the Hawking radiation rate. The resulting emission rates as measured far away from the black hole have peculiar forms. In the case of the Schwarzschild black hole, the denominator looks like a modified Fermi-Dirac statistics term. In [36], the author coined the name *tripled Pauli statistics* to refer to this term.³ In the case of the Reissner-Nordström black hole, the denominator involves Boltzmann factors for both the outer and inner horizons.

We have already shown in [chapter 6](#) and [chapter 7](#) that for the five-dimensional black hole with three charges, the greybody factor computed at low frequency in the semiclassical picture admitted a realization in string theory. Drawing on these results, Motl and Neitzke [33, 34] proposed that the results obtained above for the greybody factors at high frequency should admit a dual description. If so, the degrees of freedom in the dual gauge theory must have rather exotic statistics, as the ones appearing in the greybody factors (9.26) and (9.57). In the case of the charged black hole, it is rather strange that there is a term involving the inverse temperature of the inner horizon. It appears that the geometry outside the black hole that modifies the initial Hawking radiation somehow “knows” about the inner horizon, although they are causally disconnected by the outer event horizon.

³Historically, Pascual Jordan was the first to find the Fermi-Dirac statistics, which he named Pauli statistics.

Chapter 10

An attempt

In this chapter, we present an attempt of an original computation. We will apply the monodromy technique to compute the greybody factor at high frequency for the five-dimensional black hole with three charges introduced in [chapter 3](#). We restrict to the case of a massless scalar field. We choose this specific black hole because it has a well-known D-brane description; therefore, the results in this case might be more easily realized in the context of string theory.

10.1 Setup

The metric of the five-dimensional black hole with three charges is

$$ds_5^2 = -\lambda^{-2/3} h dt^2 + \lambda^{1/3} \left(\frac{dr^2}{h} + r^2 d\Omega_3^2 \right),$$

where

$$\lambda = \prod_{j=1,5,p} \left(1 + \frac{r_j^2}{r^2} \right) \quad (10.1)$$

and

$$h = 1 - \frac{r_0^2}{r^2}. \quad (10.2)$$

We will restrict to the case of a propagating massless scalar field in the above background. Recall that the equation we found in [chapter 4](#) for the radial part of this field $\Phi = r^{-3/2} \psi(r) e^{i\omega t} Y_{lmm'}$ was

$$\left(\frac{d^2}{dx^2} + \lambda\omega^2 - V \right) \psi = 0,$$

with the potential given by

$$V(r) = h \frac{l(l+2)}{r^2} + \frac{3h^2}{4} \frac{1}{r^2} + \frac{3hh'}{2} \frac{1}{r}. \quad (10.3)$$

Note that since we are not in the low frequency regime, we cannot simply use the S-wave approximation to set $l = 0$ in the formula for the potential. Just as in the previous

chapter, the goal will be to analytically continue r to the complex plane and study the behavior of our solutions to compute the greybody factors. Therefore, the first thing to notice is that we will have two horizons r_0 and $-r_0$, which are solutions of $h(r) = 0$. Obviously, the physical horizon is still r_0 , but we will need to position of the other one to draw the Stokes line. Finally, the tortoise coordinate for this black hole is defined as

$$x \equiv \int \frac{dr}{h(r)} = r + \frac{r_0}{2} \log \left| \frac{r - r_0}{r + r_0} \right| \quad (10.4)$$

Now, let us give the assumptions that we will make in order to perform our calculations. We will work in the dilute gas regime, so that

$$r_0, r_p \ll r_1, r_5$$

and we will treat the ratios r_0/r_p and r_1/r_5 as order one. Furthermore, since we will be considering high (imaginary) frequencies, we define our energy conditions as

$$|\omega r_1| \gg 1, \quad |\omega r_5| \gg 1, \quad |\omega r_0| \gg 1.$$

10.2 Monodromy of the tortoise coordinate and plane waves

We want to find the monodromy of the tortoise coordinate around the two horizons of the black hole. As we did before, let us expand $h(r)$ around a horizon r_n and see its behavior. We get

$$x = \int \frac{dr}{(r - r_n)h'(r_n)} = \frac{\beta_n}{4\pi} \log(r - r_n),$$

where we have used that the surface gravity at the horizon r_n is just $\kappa_n = (1/2)h'(r_n)$ and its relation to the Hawking temperature. Then, we find that the monodromy of x , as we take it around a contour C enclosing a horizon, is just

$$x \rightarrow x - i \frac{\beta_n}{2}. \quad (10.5)$$

Hence, the monodromy of the plane waves appearing in our solutions will be

$$\mathcal{M}_{C, r_n} [e^{\pm i\omega x}] = e^{\pm \frac{\beta_n \omega}{2}} \quad (10.6)$$

10.3 Constructing the Stokes line

In a similar fashion to what was done previously, let us begin by find the behavior of the tortoise coordinate around the origin. Going back to $r, x \in \mathbb{R}$ for a while, near $r = 0$, the tortoise coordinate (10.4) can be written as

$$x = r + \frac{r_0}{2} \log \left(\frac{1 - \frac{r}{r_0}}{1 + \frac{r}{r_0}} \right).$$

Now, we need to expand the logarithm up to third order to get a non-trivial answer. Doing that, we get

$$x = -\frac{r^3}{3r_0^2}. \quad (10.7)$$

Back to $r, x \in \mathbb{C}$. Again, by writing $r = |r|e^{i\theta}$, the above equation becomes

$$x = -\frac{|r|^3}{3r_0^2} \cos 3\theta - i\frac{|r|^3}{3r_0^2} \sin 3\theta.$$

Then, the condition $\operatorname{Re} x = 0$ for the Stokes line implies that

$$\theta = \left(m + \frac{1}{2}\right) \frac{\pi}{3},$$

so that near the origin, we have

$$r = |r|e^{i\frac{\pi}{3}(m+\frac{1}{2})},$$

with $m = 0, 1, 2, 3, 4, 5$. These are just half-lines in the complex plane, separated by an angle of $\frac{\pi}{3}$ (see figure below).

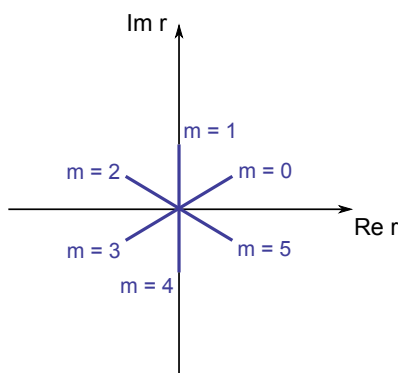


Figure 10.1: Behavior of the Stokes line very close to the origin for the five-dimensional black hole with three charges.

The sign of ωx will be determined by that of x . From the equation above, we can see that for $m = 0, 2, 4$, x is negative, while for $m = 1, 3, 5$, it is positive. Therefore, since $\operatorname{Im} \omega \rightarrow +\infty$, we have that

$$\operatorname{Sign} \omega x = (-1)^m. \quad (10.8)$$

It is easy to check that if we consider a wave with negative frequency $\operatorname{Im} \omega \rightarrow -\infty$, the formula becomes

$$\operatorname{Sign} \omega x = (-1)^{m+1}. \quad (10.9)$$

To finally construct the Stokes line, note that the two horizons will be branch points and, again, as $r \rightarrow +\infty$, $r \sim x$. Then, the Stokes line $\operatorname{Re} x = 0$ will be approximately parallel to $\operatorname{Re} r = 0$ in that limit. We have all the information needed to draw the Stokes line below.

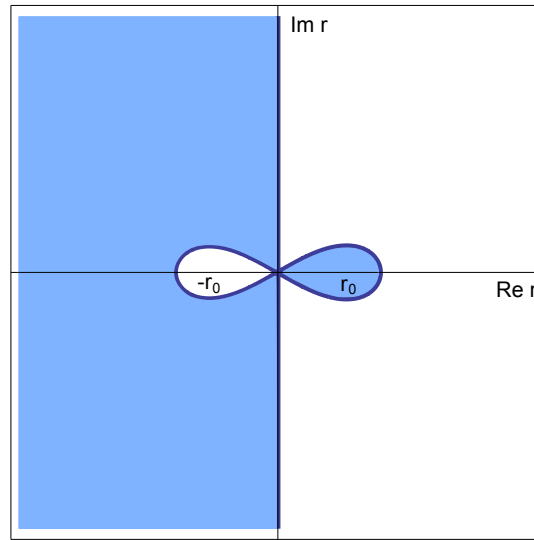


Figure 10.2: Stokes line for the five-dimensional black hole with three charges. Again, the colored region corresponds to $\text{Re } x < 0$.

10.4 Asymptotics of the solutions

Again, we will be interested in the solutions as $r \rightarrow +\infty$ and $r \rightarrow 0$.

10.4.1 Solutions as $r \rightarrow +\infty$

In this limit, we immediately see that $\lambda = 1$ and $V(r) = 0$. So, the solutions of our wave equation are just of the form

$$\psi(x) \sim A_+ e^{i\omega x} + A_- e^{-i\omega x}. \quad (10.10)$$

Again, the coefficients above will be replaced either by 1 or R , the reflection coefficient of the potential barrier, in the case of an incoming wave.

10.4.2 Solutions as $r \rightarrow 0$

To find the solutions in this limit, we first need to express V and λ in terms of the tortoise coordinate and see if the equation reduces to a simple form. This is not an easy task because what we are looking for is a resulting equation that has plane wave terms in its solution, so that we can match them to the solution at $r \rightarrow +\infty$. That is the approach we used in the previous chapter. Let us try to do the same here.

First, we use (10.7) to find r in terms of x in this region. We get

$$r = \begin{cases} i^{1/3} (3x)^{1/3} r_0^{2/3} \\ -i^{2/3} (3x)^{1/3} r_0^{2/3} \\ -(3x)^{1/3} r_0^{2/3}. \end{cases} \quad (10.11)$$

We will work with the real solution. Now, let us write the explicit expression for the

potential (9.10) keeping *all* terms in $h(r)$, $h^2(r)$ and $h'(r)$ appearing in the formula. At first sight it might seem like we could neglect the 1 terms appearing in h and h^2 compared to the r^{-n} terms. However, we choose to keep them because it might prove to be useful later on when we will try to make some clever approximations. The full potential as a function of r is

$$V(r) = \frac{\frac{3}{4} + l(l+2)}{r^2} + \frac{r_0^2 \left[\frac{3}{2} - l(l+2) \right]}{r^4} - \frac{9r_0^4}{4r^6}. \quad (10.12)$$

Using the real solution from (10.11), we can write the potential as a function of the tortoise coordinate as

$$V(x) = \frac{\frac{3}{4} + l(l+2)}{9^{1/3} r_0^{4/3} x^{2/3}} + \frac{\frac{3}{2} - l(l+2)}{81^{1/3} r_0^{2/3} x^{4/3}} - \frac{1}{4x^2}. \quad (10.13)$$

Following the same idea, keeping all terms in $\lambda(r)$, its formula is explicitly

$$\lambda(r) = 1 + \frac{r_1^2 + r_5^2 + r_p^2}{r^2} + \frac{r_1^2 r_5^2 + r_1^2 r_p^2 + r_5^2 r_p^2}{r^4} + \frac{r_1^2 r_5^2 r_p^2}{r^6}, \quad (10.14)$$

which in terms of the tortoise coordinate is

$$\lambda(x) = 1 + \frac{r_1^2 + r_5^2 + r_p^2}{9^{1/3} r_0^{4/3} x^{2/3}} + \frac{r_1^2 r_5^2 + r_1^2 r_p^2 + r_5^2 r_p^2}{81^{1/3} r_0^{2/3} x^{4/3}} + \frac{r_1^2 r_5^2 r_p^2}{9r_0^4 x^2}. \quad (10.15)$$

Let us now make the first attempt to solve the wave equation. To do so, we will neglect all the terms of 1 appearing in the formulas (10.1) and (10.2) for λ and h and also in h^2 . Given that we are near $r = 0$, this seems like a plausible thing to do. Doing that, the formulas (10.13) and (10.15) simplify to

$$V(x) = \frac{\frac{3}{2} - l(l+2)}{81^{1/3} r_0^{2/3} x^{4/3}} - \frac{1}{4x^2} \quad (10.16)$$

and

$$\lambda(x) = \frac{r_1^2 r_5^2 r_p^2}{9r_0^4 x^2}. \quad (10.17)$$

Note that we can use the fact that we are taking the ratio r_0/r_p as order one and the temperatures defined in (3.18) to further simplify the expression for λ to

$$\lambda(x) = \frac{1}{36\pi^2 T_L T_R x^2} \quad (10.18)$$

We plug the two expressions above into the wave equation and make the following change of variable $\rho = \omega x$ and divide everything by ω^2 . Doing this, we get

$$\left(\frac{d^2}{d\rho^2} + \frac{\omega^2}{36\pi^2 T_L T_R \rho^2} - \frac{\frac{3}{2} - l(l+2)}{81^{1/3} (\omega r_0)^{2/3} \rho^{4/3}} + \frac{1}{4\rho^2} \right) \psi(x) = 0.$$

However, due to the high energy conditions that we gave in the previous section, we

can neglect the third term, so that the equation reduces to

$$\left(\frac{d^2}{d\rho^2} + \frac{\omega^2}{36\pi^2 T_L T_R \rho^2} + \frac{1}{4\rho^2} \right) \psi(\rho) = 0.$$

This is a rather simple equation, whose solution is given by

$$\psi(x) = C_1(\omega x)^{\frac{1}{4}(2-4\sqrt{-A})} + C_2(\omega x)^{\frac{1}{4}(2+4\sqrt{-A})},$$

for some constants C_1 and C_2 and where we have set $A = 1/(36\pi^2 T_L T_R)$. The problem with this solution is that, as we said in the beginning of this subsection, we are looking for a solution that has plane wave terms in order to be able to match it with the one at $r \rightarrow +\infty$. So, our approximation has not worked in this case.

Another possibility is to rescale the solution itself. For example, one can make $\psi = \lambda\varphi$ and assume the same reduced expressions for V and λ as above. In that case, we obtain an equation whose solutions are also linear combinations of some powers of x . Therefore, that does not help either.

Recall that in the previous chapter, we could obtain a wave equation that looked like a Bessel differential equation due to the presence of a single term of $\psi(x)$ in the equation (see e.g. (9.8)). Apparently, the only way to obtain an equation similar to that one is to *not* drop the terms of 1 appearing in the original expression for λ (10.1). That means that we have to consider the full expression for our computation. That seems rather complicated and we can anticipate that the resulting differential equation will probably be hard to solve. Nevertheless, let us see if you can simplify it enough to make it solvable.

First let us simplify the expression for λ using the dilute gas regime conditions mentioned in our setup. With them, some of the terms in (10.14) will get simplified as follow:

$$\begin{aligned} \frac{r_1^2 + r_5^2 + r_p^2}{r^2} &\rightarrow \frac{r_1^2 + r_5^2}{r^2}, \\ \frac{r_1^2 r_5^2 + r_1^2 r_p^2 + r_5^2 r_p^2}{r^4} &\rightarrow \frac{r_1^2 r_5^2}{r^4}. \end{aligned}$$

Note that to obtain the second simplification we also made use of the fact that we mentioned in our setup that we would take the ratio r_1/r_5 as order one. Furthermore, we can again use the temperatures (3.18), with which the second term above becomes

$$\frac{r_1^2 r_5^2}{r^4} = \frac{r_0^2}{4\pi^2 T_L T_R r^4}.$$

Recall also the the last term in (10.14) can be written in terms of the temperatures, as we did in our previous attempt.

Then, the formula for λ that we will work with is

$$\lambda(r) = 1 + \frac{r_1^2 + r_5^2}{r^2} + \frac{r_0^2}{4\pi^2 T_L T_R r^4} + \frac{r_0^2 r_p^2}{4\pi^2 T_L T_R r^6}. \quad (10.19)$$

The formula for V that we will use is just its full expression (10.12). Now, we write them both in terms of the tortoise coordinate and plug them into the wave equation. We get

$$\left[\frac{d^2}{dx^2} + \omega^2 + \frac{\omega^2 (r_1^2 + r_5^2)}{9^{1/3} r_0^{4/3} x^{2/3}} + \frac{\omega^2}{4(81)^{1/3} \pi^2 T_L T_R r_0^{2/3} x^{4/3}} + \frac{\omega^2}{36\pi^2 T_L T_R x^2} - \frac{\frac{3}{4} + l(l+2)}{9^{1/3} r_0^{4/3} x^{2/3}} - \frac{\frac{3}{2} - l(l+2)}{81^{1/3} r_0^{2/3} x^{4/3}} + \frac{1}{4x^2} \right] \psi(x) = 0. \quad (10.20)$$

Imagine we would use the same method that proved to be successful for in the previous chapter. That is, make the change $\rho = \omega x$ and divide everything by ω^2 . Then, the two first terms of the potential could again be neglected because they would have powers of ωr_0 in their denominators. Therefore, the resulting equation would be

$$\left[\frac{d^2}{d\rho^2} + 1 + \frac{\omega^2 (r_1^2 + r_5^2)}{9^{1/3} (\omega r_0)^{4/3} \rho^{2/3}} + \frac{\omega^2}{4(81)^{1/3} \pi^2 T_L T_R (\omega r_0)^{2/3} \rho^{4/3}} + \frac{\omega^2}{36\pi^2 T_L T_R \rho^2} + \frac{1}{4\rho^2} \right] \psi(\rho) = 0. \quad (10.21)$$

Note that the second and third term of λ cannot be neglected like we did with the two first terms of the potential. That is because even though they also have powers of ωr_0 in their denominators, they also have powers of ωr_1 and ωr_5 in their numerators, which due to the conditions on the energy and of the dilute gas regime, must be dominant. Therefore, these two terms of λ spoil the desired Bessel form for our differential equation. Without them, we would have solutions that would have plane wave terms and we would be ready to carry on the computation of the greybody factor. Trying to solve the above equation directly using some software does not help either, as it does not return any solution.

Apparently, if one wants to use the monodromy technique for the stringy black hole that we have considered in this chapter, the crucial step is to be able to reduce the wave equation in the limit $r \rightarrow 0$ to a form for which the solution can be matched to the solution at $r \rightarrow +\infty$. As we have seen above, it is not a trivial task, but rather a tricky one. There should be some clever change of variable or rescale of ψ that brings the equation to the desired form. Once that is done, the computation should be straightforward: it would proceed much like in the Schwarzschild case, with the choice of contour sketched below.

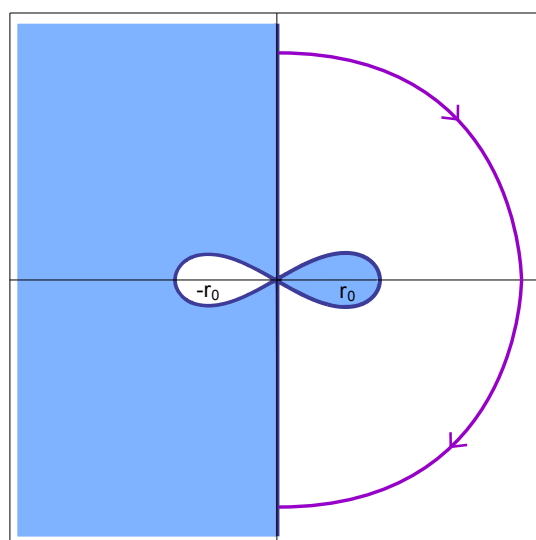


Figure 10.3: Sketch of the contour choice for the computation.

Chapter 11

Conclusions

We have given a pedagogical and thorough review of greybody factors for black holes in asymptotically flat spacetimes. Again, our goal was to publicize the subject as a possible way to learn new quantum features of black holes. As a motivation, we presented the computation in the low frequency regime for a stringy black hole. In the high frequency regime, we reviewed the monodromy technique and used it to compute the greybody factors for the Schwarzschild and Reissner-Nordström black holes. The latter had not been done explicitly in the literature. The reader might wonder how is it that greybody factors at large frequencies might teach us new things about the quantum structure of black holes. Pictorially, if we take a very high frequency wave, we could expect that it will be able to “probe” smaller length scales in the black hole geometry. One could then imagine that new degrees of freedom will make themselves manifest.

Let us conclude by discussing some subtleties of the computations at high frequency. We also comment on some recent developments in the subject and give some suggestions that should be taken into account for further work in the subject.

Corrections to the potential

The careful reader might have noticed that we omitted some terms in the approximation we made to find the form of the potentials as $r \rightarrow +\infty$. These terms are of order $\mathcal{O}(\omega r_h)^{-n}$, with r_h the horizons of the black holes we considered. Given that we worked in the high frequency limit, the energy condition is given by $\omega r_h \gg 1$. Therefore, the fact that we did not take those terms into account seems perfectly reasonable. However, it would be interesting to compute the greybody factors considering, at least, the first-order correction to the potentials. Perhaps the suggestive form of our results would get modified in such a way that it would either invalidate or strengthen the conjecture of a dual description. We should note that the first-order correction to the potentials was considered in [37], but in the context of quasinormal frequencies, which can be regarded as the poles of the denominator of the greybody factor. Nevertheless, it would be good to compute directly the greybody factors, as their numerators also contain important information.

Stringy black hole

Finally, let us stress that it would be interesting to continue the computation we started for the five-dimensional black hole with three charges. As we said previously, the problem boils down to finding the wave equation near $r = 0$. Once that is done, the computation should be straightforward using the Stokes line and contour shown in [chapter 10](#). Perhaps the way to solve the equation is to go back to the one written for $\phi(r)$, instead of solving the one for $\psi(r)$. Granted that the latter was more useful because it had a simple Schrödinger-like form, but in the case of the stringy black hole there is apparently no way out if we use the steps that proved to be useful in the case of the Schwarzschild and Reissner-Nordström black holes. Finally, let us say that the setup for our attempt relied heavily on the dilute gas regime assumptions. One could also speculate that by taking other conditions, the wave equation can be brought to a solvable form.

Non-asymptotically flat spacetimes

In this thesis, we have only considered black holes in asymptotically flat spacetimes. However, the reader might be wondering that happens in the case of asymptotically de Sitter and Anti de Sitter spacetimes. In [\[27\]](#), the authors worked out a full study for this cases in both the low and high frequency regimes. They also considered the cases presented in this thesis, but only mentioned the results by taking a special limit of de Sitter spacetime. In that sense, we hope that our presentation of the monodromy technique and its application to the computation of greybody factors at high frequency provides a good reference for anyone interested in this subject.

When considering black holes in asymptotically de Sitter spacetimes, the main difference is that spatial infinity is replaced by the cosmological horizon r_c . The formula for the greybody factor [\(5.14\)](#), the range of the tortoise coordinate, the form of the wave equation and its solutions far away from the hole and near $r = 0$ are the same. The results also have suggestive Boltzmann and statistics factors.

There are more differences in the case of asymptotically Anti de Sitter spacetimes. The range of the tortoise coordinate and the definition [\(5.14\)](#) of the greybody factor will vary. Remarkably, in this case the result for greybody factors obtained in [\[27\]](#) is universal: it is always equal to 1. This is quite a puzzling result and one can imagine that further investigation can be made in the context of the AdS/CFT correspondence.

Rotating black holes

We have only considered static and spherically symmetric black holes, where one needs to study the simple Klein-Gordon equation in a background. In the case of rotating black holes, things are more complicated due to the lack of the symmetries one has in the cases we have considered. To study the propagation of a particle in this kind of background, one uses Teukolsky's equation. Recently, Keshet and Neitzke [\[38\]](#) solved the problem of finding the quasinormal modes and greybody factor at high frequency for a four-dimensional Kerr black hole using the monodromy technique. Let us just mention their results, as they seem to give new hints to a possible dual description. The

greybody factor they obtained is given by

$$\gamma(\omega) = \frac{e^{\varepsilon(\omega-m\Omega)/T_H} \pm 1}{e^{\varepsilon(\omega-\tilde{\omega}_o)/2T_o} + 1} e^{-\varepsilon(\omega-m\Omega)/T_H},$$

with the minus (plus) sign for bosons (fermions). With this, the emission rate as measured far away from the black hole is

$$\Gamma(\omega) = \frac{e^{-\varepsilon(\omega-m\Omega)/T_H}}{e^{\varepsilon(\omega-\tilde{\omega}_o)/2T_o} + 1} \frac{d^3k}{(2\pi)^3}.$$

Here, T_H is the Hawking temperature of the hole, Ω is the angular velocity of the event horizon, while m and s are the azimuthal quantum number and spin of the particle under consideration. The variable ε is just the relative sign between two parameters in the problem, which we should not care about here. The punch line is that the relation between the quasinormal modes (QNMs) and total-transmission modes (TTMs) of the black hole¹ resembles the relation between quantities of two sectors of a dual CFT. Of course, this is very much what happened in the case at low frequency considered in [chapter 6](#) and [chapter 7](#). More specifically, the temperatures that one can associate with QNMs and TTMs are related by an equation like (7.3). Keshet and Neitzke speculate that the dual description should involve two distinct sets of degrees of freedom, somehow related to QNMs and TTMs. However, as we can see from the formulas written above, both sectors do not enter into the final answer, only the QNMs sector. The authors speculate that perhaps the correct dual picture here involves a single excitation associated with QNMs decaying into two quanta, one of which enters the subsystem associated with TTMs while the other emerges as Hawking radiation. It would be interesting to further investigate the case for rotating black hole in the high frequency limit.

Backreaction

As we said in [chapter 5](#), if we have a wave propagating in a black hole background with sufficiently high frequency, it can effectively “see” the curvature of spacetime. Therefore, the obvious, but very non-trivial step, is to include the effect of backreaction in the analysis. Of course one may say that the results obtained in this thesis are not valid because they do not include the effect of backreaction. However, we believe they are still interesting as a first step toward the full computation of greybody factors in the high frequency regime. The monodromy technique introduced is quite robust and it should hold when taking backreaction into account. The real problem is how to include this effect in the analysis. One possibility would be to consider shockwave geometries [39], which describe the geometry that a high energy particle produces as it propagates in spacetime. That is, one could study how a particle propagates in a shockwave geometry produced by a preceding particle and see what kind of equation one obtains.

¹These are just different resonances of the holes. The subscript o appearing in the formula for the greybody factor corresponds to QNMs.

Part IV

Appendices

Appendix A

Penrose diagrams

We mentioned and showed some Penrose diagrams in [chapter 1](#). In this appendix, we will quickly explain what they are and why we included them in this thesis. In general, a spacetime metric may be very intricate and complicated, which may hide some of its symmetries and hence does not allow to have an easy visualization of its global properties. It is therefore useful and convenient to represent spacetimes in a way that easily reproduces their causal structure, i.e. the relation between past and future events as determined by their respective light cones. This is accomplished by drawing Penrose diagrams.

In order to obtain the Penrose diagram for a given spacetime, we need to perform a series of coordinate transformations such that in the end, timelike and spacelike coordinates have finite ranges and the lightcones form angles of 45° . The initial metric will be related to an “unphysical” metric by a conformal transformation

$$\tilde{d}s^2 = \omega^2 ds^2 \tag{A.1}$$

To illustrate the procedure, let us use the simplest example: Minkowski spacetime. In polar coordinates (t, r, θ, ϕ) , it is given by

$$ds^2 = -dt^2 + dr^2 + r^2 d\Omega_2^2, \tag{A.2}$$

with $d\Omega_2^2 = d\theta^2 + \sin^2 \theta d\phi^2$ the metric on a unit 2-sphere. In this case, the lightcones already form angles of 45° , but the coordinate t and r have infinite ranges

$$-\infty < t < \infty, \quad 0 \leq r < \infty.$$

Let us first switch to null coordinates, defined by

$$u = t - r, \quad v = t + r,$$

so that $u \leq v$ and whose ranges are given by

$$-\infty < u < \infty, \quad -\infty \leq v < \infty.$$

In [Figure A.1](#), each point represents a 2-sphere of radius $r = \frac{1}{2}(v - u)$. In these null

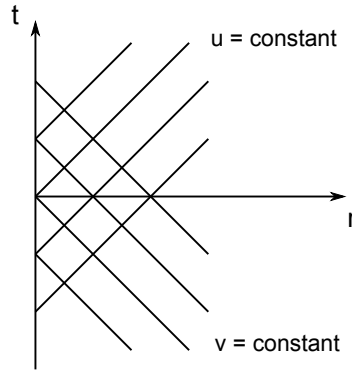


Figure A.1: Null coordinates for the Minkowski metric.

coordinates, the Minkowski metric reads

$$ds^2 = -\frac{1}{2}(dudv + dvdu) + \frac{1}{4}(v - u)^2 d\Omega_2^2. \quad (\text{A.3})$$

Our new coordinates still have infinite ranges. Therefore, our next coordinate transformation needs to bring an infinite value to a finite one. Let us recall that the function arctan exactly exhibits this behavior, given that

$$\arctan(\pm\infty) = \pm\frac{\pi}{2}.$$

So, we now define our new coordinates as

$$\begin{aligned} U &= \arctan u, \\ V &= \arctan v, \end{aligned}$$

so that $U \leq V$ and their finite ranges are given by

$$-\frac{\pi}{2} < U < \frac{\pi}{2}, \quad -\frac{\pi}{2} < V < \frac{\pi}{2}.$$

In terms of these new coordinates, the metric (A.3) becomes

$$ds^2 = \frac{1}{4 \cos^2 U \cos^2 V} [-2(dUdV + dVdU) + \sin^2(V - U) d\Omega_2^2]. \quad (\text{A.4})$$

Lastly, let us transform back to a timelike coordinate T and a radial coordinate R by making

$$\begin{aligned} T &= V + U, \\ R &= V - U, \end{aligned}$$

with ranges

$$0 \leq R < \pi, \quad |T| + R < \pi. \quad (\text{A.5})$$

In terms of these new coordinates, the metric (A.4) reads

$$ds^2 = \frac{1}{(\cos T + \cos R)^2} (-dT^2 + dR^2 + \sin^2 R d\Omega_2^2). \quad (\text{A.6})$$

We have finally arrived to our desired result: the original metric ds^2 is now related to an “unphysical” metric \tilde{ds}^2 via a conformal transformation. That is

$$\tilde{ds}^2 = \omega^2 ds^2, \quad (\text{A.7})$$

with

$$\begin{aligned} \omega &= \cos T + \cos R, \\ \tilde{ds}^2 &= -dT^2 + dR^2 + \sin^2 R d\Omega_2^2. \end{aligned} \quad (\text{A.8})$$

The metric \tilde{ds}^2 describes the manifold $\mathbb{R} \times S^3$, where we see that the 3-sphere is purely spacelike. Of course, this metric has curvature, unlike in Minkowski spacetime. This is not a problem: the real, physical metric is still flat spacetime, which is recovered by performing the conformal transformation. If we have curvature in our result it is because our choice of coordinates implies so.

We are one step away from getting the Penrose diagram for the Minkowski metric. First, let us draw $\mathbb{R} \times S^3$ on a cylinder, where each circle of constant T represents a 3-sphere. The shaded region in Figure A.2 corresponds to Minkowski spacetime, which in this case is the subspace defined by (A.5). Finally, we can unroll the shaded region

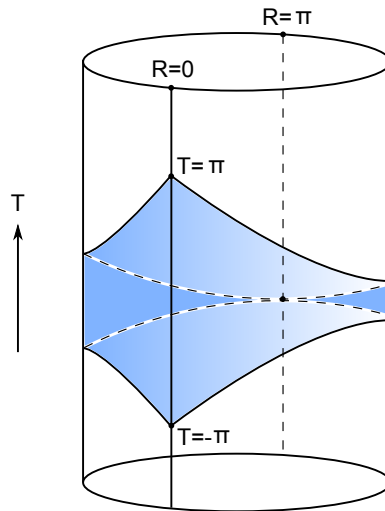


Figure A.2: Entire manifold $\mathbb{R} \times S^3$. Each circle of constant T represents a 3-sphere. The shaded region corresponds to Minkowski spacetime.

to obtain a triangular diagram that represents Minkowski spacetime. This is precisely the corresponding Penrose diagram, depicted in Figure A.3. Each point in the diagram represents a 2-sphere.

The boundaries of the Penrose diagram, except $R = 0$, do not correspond to the

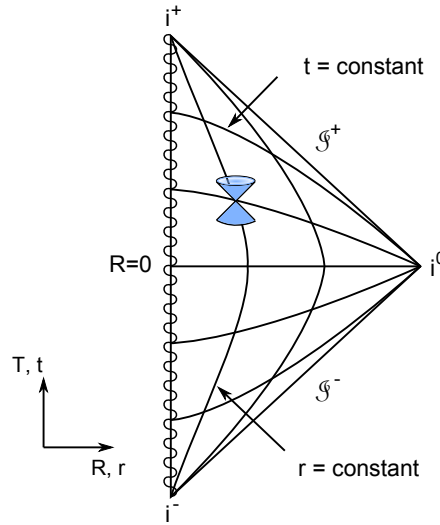


Figure A.3: Penrose diagram of Minkowski spacetime. Note that our initial requirements have been met: lightcones form angles of 45° and our time and radial coordinates have finite ranges.

original spacetime. They are referred to as *conformal infinity* and the union of the spacetime with conformal infinity is the *conformal compactification*. From the structure of the Penrose diagram, we see that conformal infinity is subdivided into different regions:

$$\begin{aligned}
 i^+ &: \text{future timelike infinity } (T = \pi, R = 0), \\
 i^- &: \text{past timelike infinity } (T = -\pi, R = 0), \\
 i^0 &: \text{spatial infinity } (T = 0, R = \pi), \\
 \mathcal{I}^+ &: \text{future null infinity } (T = \pi - R, 0 < R < \pi), \\
 \mathcal{I}^- &: \text{past null infinity } (T = -\pi + R, 0 < R < \pi),
 \end{aligned}$$

where \mathcal{I} is pronounced as “scri”. Note that i^+ , i^- and i^0 are points, whereas \mathcal{I}^+ and \mathcal{I}^- are null surfaces with the topology of $\mathbb{R} \times S^2$.

We now have a clear picture of the causal structure of Minkowski spacetime, which was the main goal of drawing the Penrose diagram. Radial null geodesics are at $\pm 45^\circ$, as expected from the inclination of the lightcones. All timelike geodesics begin at i^- and end at i^+ . All null geodesics begin at \mathcal{I}^- and end at \mathcal{I}^+ . Lastly, spacelike geodesics both begin and end at i^0 . Note that a singularity is indicated by a wavy line, as in the examples of [chapter 1](#).

For a more general spacetime, it is not trivial to find the series of transformations that allow us to draw the corresponding Penrose diagram. Fortunately, most of them can be found in the literature. The important thing about Penrose diagrams is to be able to “read” them, i.e. to understand the causal structure of spacetime by looking at the diagram. This is the reason why we included them in [chapter 1](#): to have a clear idea of what is going on with waves as they propagate in a given black hole background.

Appendix B

Euclidean derivation of the Hawking temperature

We will derive the Hawking temperature for any given d -dimensional metric that can be brought to the form

$$ds_d^2 = -F(r)C(r) dt^2 + \frac{1}{C(r)} dr^2 + H(r) r^2 d\Omega_{d-2}^2. \quad (\text{B.1})$$

This metric has an horizon at $r = r_0$ and the functions $F(r)$, $C(r)$ and $H(r)$ are such that

$$\begin{aligned} C(r_0) &= 0 \\ F(r), H(r) &> 0, \text{ for } r \geq r_0 \\ F(r), C(r), H(r) &\xrightarrow{r \rightarrow \infty} 1. \end{aligned}$$

The goal of this method is to use the analogy between path integrals with periodic time and systems at finite temperature. Since path integrals are only defined in Euclidean spacetime, let us first perform a standard Wick rotation $t \rightarrow i\tau$, so that the above metric can be written as

$$ds_d^2 = F(r)C(r) d\tau^2 + \frac{1}{C(r)} dr^2 + H(r) r^2 d\Omega_{d-2}^2,$$

which now describes the spacetime between $r = \infty$ and $r = r_0$. Due to rotational symmetry, we can set $d\Omega_{d-2}^2 = 0$, so that

$$ds_d^2 = F(r)C(r) d\tau^2 + \frac{1}{C(r)} dr^2. \quad (\text{B.2})$$

We now go very close to the horizon by writing $r = r_0 + \epsilon$, such that $0 < \epsilon \ll 1$ and $dr^2 = d\epsilon^2$. Taylor expanding the functions $F(r)$ and $C(r)$ around $r = r_0$, we get

$$\begin{aligned} C(r) &= C(r_0) + \epsilon C'(r_0) + \mathcal{O}(\epsilon^2) \\ F(r) &= F(r_0) + \epsilon F'(r_0) + \mathcal{O}(\epsilon^2). \end{aligned}$$

Then, using the fact that $C(r_0) = 0$ and keeping terms to first order in ϵ the metric (B.2) can be written as

$$ds_d^2 = \epsilon F(r_0) C'(r_0) d\tau^2 + \frac{1}{\epsilon C'(r_0)} d\epsilon^2. \quad (\text{B.3})$$

Let us now introduce a new coordinate defined as

$$u = \frac{2\sqrt{\epsilon}}{\sqrt{C'(r_0)}},$$

so that

$$du = \frac{d\epsilon}{\sqrt{\epsilon}\sqrt{C'(r_0)}},$$

in terms of which, the metric (B.3) can be written as

$$ds_d^2 = du^2 + u^2 \frac{F(r_0) C'^2(r_0)}{4} d\tau^2. \quad (\text{B.4})$$

This last equation has the form $dr^2 + r^2 d\phi^2$, which is a smooth Euclidean space if ϕ is a periodic variable such that $0 \leq \phi \leq 2\pi$. Therefore, in the case of the metric (B.4), we can write

$$\frac{F(r_0) C'^2(r_0)}{4} d\tau^2 = d\left(\frac{\sqrt{F(r_0) C'(r_0)}}{2} \tau\right)^2$$

which gives us a periodic time condition given by

$$0 \leq \frac{\sqrt{F(r_0) C'(r_0)}}{2} \tau \leq 2\pi \quad \longrightarrow \quad 0 \leq \tau \leq \frac{4\pi}{\sqrt{F(r_0) C'(r_0)}}.$$

Finally, recall that a path integral with periodic time $0 \leq \tau \leq \tau_{max}$ is equivalent to a system with finite temperature T and these quantities are related by

$$\beta = \frac{1}{T} = \tau_{max}.$$

Therefore, we have found that the Hawking temperature associated with the metric (B.1), which has a horizon at $r = r_0$, is

$$T_H = \frac{C'(r_0) \sqrt{F(r_0)}}{4\pi}. \quad (\text{B.5})$$

Appendix C

Hawking temperature of the five-dimensional black hole

To exemplify the utility of the result derived in the previous appendix, let us compute the temperature of the five-dimensional black hole with three charges (3.9). Let us first rewrite the corresponding metric

$$ds_5^2 = -\lambda^{-2/3} h dt^2 + \lambda^{1/3} \left(\frac{dr^2}{h} + r^2 d\Omega_3^2 \right), \quad (\text{C.1})$$

Comparing this metric with (B.1), we see that in this case $C(r) = h\lambda^{-1/3}$ and $F(r) = \lambda^{-1/3}$; that is:

$$C(r) = \left(1 - \frac{r_0^2}{r^2} \right) \prod_{j=1,5,p} \left(1 + \frac{r_0^2 \sinh^2 \alpha_j}{r^2} \right)^{-1/3} \quad (\text{C.2})$$

and

$$F(r) = \prod_{j=1,5,p} \left(1 + \frac{r_0^2 \sinh^2 \alpha_j}{r^2} \right)^{-1/3}. \quad (\text{C.3})$$

In order to calculate the Hawking temperature given by (B.5), we need $C'(r_0)$ and $\sqrt{F(r_0)}$. It is a simple exercise to find that

$$C'(r_0) = 2r_0^{-1} (1 + \sinh^2 \alpha_1)^{-1/3} (1 + \sinh^2 \alpha_5)^{-1/3} (1 + \sinh^2 \alpha_p)^{-1/3}$$

and

$$\sqrt{F(r_0)} = (1 + \sinh^2 \alpha_1)^{-1/6} (1 + \sinh^2 \alpha_5)^{-1/6} (1 + \sinh^2 \alpha_p)^{-1/6}.$$

We thus find that

$$C'(r_0)\sqrt{F(r_0)} = 2r_0^{-1} (1 + \sinh^2 \alpha_1)^{-1/2} (1 + \sinh^2 \alpha_5)^{-1/2} (1 + \sinh^2 \alpha_p)^{-1/2},$$

but since $1 + \sinh^2 x = \cosh^2 x$, this last equation can be written as

$$C'(r_0)\sqrt{F(r_0)} = 2r_0^{-1} \cosh^{-1} \alpha_1 \cosh^{-1} \alpha_5 \cosh^{-1} \alpha_p.$$

Finally, replacing this expression in (B.5), we get the Hawking temperature of the five-dimensional black hole with three charges (3.9) is given by

$$T_H = \frac{1}{2\pi r_0 \cosh \alpha_1 \cosh \alpha_5 \cosh \alpha_p}. \quad (\text{C.4})$$

Appendix D

Klein-Gordon equation in curved spacetime

In quantum field theory, the Klein-Gordon equation is the equation of motion of a scalar field (spin zero). In flat spacetime, it is obtained by considering the Lagrangian

$$\mathcal{L} = -\frac{1}{2}\eta^{\mu\nu}\partial_\mu\Phi\partial_\nu\Phi - \frac{1}{2}m^2\Phi^2,$$

with $\eta^{\mu\nu}$ being the Minkowski metric. After using the action principle with this Lagrangian, we obtain

$$(\square - m^2)\Phi = 0. \quad (\text{D.1})$$

This is the Klein-Gordon equation in flat spacetime. The operator \square is known as the d'Alembert operator and it is defined as

$$\square \equiv \partial^\mu\partial_\mu = \eta^{\mu\nu}\partial_\mu\partial_\nu = -\partial_t^2 + \nabla^2,$$

with $\nabla^2 = \partial_x^2 + \partial_y^2 + \partial_z^2$ being the usual Laplacian operator in three dimensions.

This equation can be generalized to curved spacetime. Consider a spacetime with metric $g_{\mu\nu}$; the first thing we need to do is the standard change from the normal derivative ∂_μ to the covariant derivative ∇_μ , defined by

$$\begin{aligned}\nabla_\mu V^\nu &= \partial_\mu V^\nu + \Gamma_{\mu\lambda}^\nu V^\lambda, \\ \nabla_\mu W_\nu &= \partial_\mu W_\nu - \Gamma_{\mu\nu}^\lambda W_\lambda,\end{aligned}$$

when acting on a vector and a one-form, respectively. Again, $\Gamma_{\mu\nu}^\lambda$ are the Christoffel symbols mentioned in [chapter 4](#). Then, the Lagrangian we need to consider is

$$\mathcal{L} = -\frac{1}{2}\sqrt{-g}(g^{\mu\nu}\nabla_\mu\Phi\nabla_\nu\Phi + m^2\Phi^2), \quad (\text{D.2})$$

where we have also included the standard measure $\sqrt{-g}$. Then, a natural step is to define the d'Alembert operator in a curved spacetime with metric $g^{\mu\nu}$ as

$$\square \equiv \nabla^\mu\nabla_\nu = g^{\mu\nu}\nabla_\mu\nabla_\nu.$$

Then, the Klein-Gordon equation in curved spacetime that one obtains by using the action principle with (D.2) is

$$(\nabla^\mu \nabla_\nu - m^2) \Phi = 0.$$

However, recall that the action of the covariant derivative on a scalar is the same as the action of the normal derivative, i.e. $\nabla_\nu \Phi = \partial_\nu \Phi$. Therefore, we can rewrite the last equation as

$$(\nabla^\mu \partial_\nu - m^2) \Phi = 0. \tag{D.3}$$

The Klein-Gordon equation for a massless scalar field is then

$$\nabla^\mu \partial_\nu \Phi = 0, \tag{D.4}$$

which we used as the starting point in our calculations of [chapter 4](#).

Appendix E

Some useful formulas

Let us give some formulas that are used for some computations in the body of the thesis.

Bessel functions

Bessel's differential equation is given by

$$\frac{d^2y}{dx^2} + \frac{1}{x} \frac{dy}{dx} + \left(1 - \frac{n^2}{x^2}\right) y = 0,$$

with n an arbitrary real or complex number. The solutions to the above equation are known as Bessel functions and n is the so-called order of the function. They come in two types: Bessel functions of first kind $J_n(x)$ and Bessel functions of second kind $N_n(x)$. Their general expressions are

$$J_n(x) = \sum_{j=0}^{\infty} \frac{(-1)^j}{j! \Gamma(j+n+1)} \left(\frac{x}{2}\right)^{2j+n} \quad (\text{E.1})$$

and

$$N_n(x) = \frac{J_n(x) \cos n\pi - J_{-n}(x)}{\sin n\pi}. \quad (\text{E.2})$$

Given that it is a second-order differential equation, it must have two independent solutions. When n is an integer, the following identity holds $J_{-n}(x) = (-1)^n J_n(x)$, meaning that they are not independent solutions. So, in this case the general solution is given by

$$y(x) = C_1 J_n(x) + C_2 N_n(x),$$

for some constants $C_{1,2}$. However, when n is non-integer, $J_n(x)$ and $J_{-n}(x)$ are linearly independent, so that the solution in that case is

$$y(x) = D_1 J_n(x) + D_2 J_{-n}(x)$$

What is more useful for our computations is to know the asymptotic behavior of the Bessel functions as the argument take large or small values. For large x , we have the

following asymptotic expressions

$$\begin{aligned} J_n(x) &= \sqrt{\frac{2}{\pi x}} \cos\left(x - \frac{n\pi}{2} - \frac{\pi}{4}\right), \\ N_n(x) &= \sqrt{\frac{2}{\pi x}} \sin\left(x - \frac{n\pi}{2} - \frac{\pi}{4}\right), \end{aligned} \quad (\text{E.3})$$

whereas for small x , we have

$$\begin{aligned} J_n(x) &= \frac{1}{\Gamma(n+1)} \left(\frac{x}{2}\right)^n, \\ N_1(z) &= -\frac{2}{\pi z} + \frac{z}{\pi} (\ln z + c). \end{aligned} \quad (\text{E.4})$$

Finally, the Bessel functions of first kind have the following property

$$\lambda^{-n} J_n(\lambda x) = \sum_{j=0}^{\infty} \frac{1}{j!} \left[\frac{(1-\lambda^2)x}{2} \right]^j J_{n+j}(x). \quad (\text{E.5})$$

Hypergeometric functions

The hypergeometric differential equation is

$$z(1-z)\frac{d^2y}{dx^2} + [c - (a+b+1)z]\frac{dy}{dx} - aby = 0$$

and has regular singular points at $x = 0, 1, \infty$. The solutions to the above equation are hypergeometric functions ${}_pF_q(a_1, \dots, a_p; b_1, \dots, b_q; x)$, which can be defined as a series for which the ratio of two successive terms can be written as

$$\frac{c_{k+1}}{c_k} = \frac{(k+a_1)(k+a_2)\dots(k+a_p)}{(k+b_1)(k+b_2)\dots(k+b_p)}. \quad (\text{E.6})$$

The function ${}_2F_1(a, b; c; x)$ is the first to be studied and its expression is given by

$${}_2F_1(a, b; c; x) = \sum_{n=0}^{\infty} \frac{(a)_n (b)_n}{(c)_n} \frac{x^n}{n!},$$

where $(a)_n = a(a+1)(a+2)\dots(a+n-1)$ is the Pochhammer symbol. In the body of the thesis, we are interested in knowing the value of the above function when $x = 1$. Its expression is

$${}_2F_1(a, b; c; 1) = \frac{\Gamma(c)\Gamma(c-a-b)}{\Gamma(c-a)\Gamma(c-b)},$$

where Γ are the usual Gamma functions. Furthermore, we make use of the following identity

$$|\Gamma(1-ix)|^2 = \frac{\pi x}{\sinh \pi x}.$$

Appendix F

Asymptotics of the potential

In this appendix, we will find the expressions for the potential $V(r)$ near the origin for the four-dimensional Schwarzschild and Reissner-Nordström black hole, which both have the form

$$ds^2 = -f(r)dt^2 + f(r)^{-1}dr^2 + r^2 d\Omega_2^2, \quad (\text{F.1})$$

$d = 4$ Schwarzschild potential

In this case, the general formula for the potential is given by

$$V(r) = f(r) \left[\frac{l(l+1)}{r^2} + \frac{f'(r)(1-j^2)}{r} \right]. \quad (\text{F.2})$$

Of course, as $r \rightarrow +\infty$, the potential simply vanishes.

$$f(r) = 1 - \frac{r_0}{r}, \quad f'(r) = \frac{r_0}{r^2}. \quad (\text{F.3})$$

To find how the potential behaves near $r = 0$, we use the form of the tortoise coordinate near that point, given by (9.2) and get

$$r = \pm i\sqrt{2xr_0}.$$

Plugging this expression into (F.2), we get the potential in terms of the tortoise coordinate

$$V(x) = \frac{j^2 - 1}{4x^2} - \frac{l(l+1)}{2xr_0} \pm i \left[\frac{(1-j^2) - l(l+1)}{2x\sqrt{2xr_0}} \right]. \quad (\text{F.4})$$

Now, we make the following change of variable $\rho = \omega x$, so that

$$V(\rho) = \omega^2 \frac{j^2 - 1}{4\rho^2} - \omega \frac{l(l+1)}{2\rho r_0} \pm i\omega^{3/2} \left[\frac{(1-j^2) - l(l+1)}{2\rho^{3/2}\sqrt{2r_0}} \right].$$

Then, it is straightforward to see that

$$\frac{V(\rho)}{\omega^2} = \frac{j^2 - 1}{4\rho^2} - \mathcal{O}\left(\frac{1}{(\omega r_0)^n}\right)$$

Hence, due to the high energy condition (8.4), we can effectively neglect the last terms. This allows us to just consider the first term of (F.4). That is the form of V that we use in the main body of the thesis

$$V(x) = \frac{j^2 - 1}{4x^2}. \quad (\text{F.5})$$

$d = 4$ Reissner-Nordström potential

The form of the wave equation we derived in chapter 4 and have been using up to now, holds for any static, spherically symmetric black hole in four dimensions and for *any* type of propagating particle. However, as we briefly mentioned in chapter 9, when considering a charged black hole, the potential term entering the equation will change. This is because the electromagnetic field of the hole will interact with, for example, an external electromagnetic field or a linearized perturbation of the metric. In [40], the authors found how the potential needs to be modified. Since it is not the specific subject of this thesis and we only want to know the form of the potential to use it in our monodromy technique, we follow the discussion in [35], which is more straightforward. We restrict our discussion to four-dimensional black holes.

Spin $j = 0$ particles

In this case, the potential is given by

$$V_0(r) = f(r) \left[\frac{l(l+1)}{r^2} + \frac{f'(r)}{r} \right], \quad (\text{F.6})$$

which is just the same as in the Schwarzschild case with $j = 0$. This is expected because these particles do not interact with the electromagnetic field of the charged black hole.

Spin $j = 1$ particles

In this case, the potential is given by

$$V_{1\pm}(r) = f(r) \left[\frac{l(l+1)}{r^2} - \frac{3G_4 M}{r^3} \pm \frac{\sqrt{9G_4^2 M^2 + 4G_4 Q^2 (l(l+1) - 2)}}{r^3} + \frac{4G_4 Q^2}{r^4} \right]. \quad (\text{F.7})$$

Note that the plus sign (minus) corresponds to the equation that gives the coupling of the particle to the electromagnetic (gravitational) field of the hole. Both obey the same Schrödinger-like equation that we have been using in this thesis.

Spin $j = 2$ particles

In this case, the formula for the potential involve some nasty expressions. It has the form

$$V_{2\pm}(r) = \frac{f(r) U_{\pm}(r)}{64r^2 H_{\pm}^2(r)}, \quad (\text{F.8})$$

where

$$H_+(r) = 1 + \frac{6G_4M(1 - \Upsilon)}{2[l(l+1) - 2]r},$$

$$H_-(r) = l(l+1) - 2 + \frac{3G_4M(1 + \Upsilon)}{r},$$

with

$$\Upsilon = \sqrt{1 + \frac{4Q^2[l(l+1) - 2]}{9G_4M^2}}.$$

The functions U_{\pm} are given by huge expressions, which we will not write down here, but refer the reader to [35] to have a look at them. Fortunately, all we need to know about them are their expressions when $r \rightarrow 0$. These are given by

$$U_+(r \rightarrow 0) = 64[l(l+1) - 2] + 128,$$

$$U_-(r \rightarrow 0) = 64[l(l+1) - 2]^3 + 128[l(l+1) - 2]^2,$$

Reduction of the potentials

In this case, the tortoise coordinate near $r = 0$ is given by (9.29). By following a similar procedure to the one for the Schwarzschild black hole, we arrive at the following expressions for the potentials near $r = 0$

$$V_0(x) = -\frac{2}{9x^2} = \frac{\left(\frac{1}{3}\right)^2 - 1}{4x^2}, \quad (\text{F.9})$$

$$V_{1\pm}(x) = \frac{4}{9x^2} = \frac{\left(\frac{5}{3}\right)^2 - 1}{4x^2}, \quad (\text{F.10})$$

$$V_{2\pm}(x) = -\frac{2}{9x^2} = \frac{\left(\frac{1}{3}\right)^2 - 1}{4x^2}. \quad (\text{F.11})$$

We see that these formulas are exactly like (F.5), but with $j = \frac{1}{3}$ or $j = \frac{5}{3}$. Therefore, when considering a spin-0 or spin-2 particle, the potential near the origin reduces to

$$V(x) = \frac{j^2 - 1}{4x^2}, \quad (\text{F.12})$$

with a “modified” spin entering the equation, given by $j = \frac{1}{3}$. And when considering a spin-1 particle, the potential near the origin also reduces to

$$V(x) = \frac{j^2 - 1}{4x^2}, \quad (\text{F.13})$$

but with a modified spin of $j = \frac{5}{3}$.

Bibliography

- [1] S. M. Carroll, “Spacetime and geometry: An introduction to general relativity,” San Francisco, USA: Addison-Wesley (2004) 513 p.
- [2] R. M. Wald, “General Relativity,” Chicago, USA: Univ. Pr. (1984) 491p.
- [3] R. Emparan and H. S. Reall, “Black Holes in Higher Dimensions,” [arXiv:0801.3471 \[hep-th\]](#).
- [4] J. D. Bekenstein, “Black holes and entropy,” *Phys. Rev.* **D7** (1973) 2333–2346.
- [5] S. W. Hawking, “Black holes in general relativity,” *Commun. Math. Phys.* **25** (1972) 152–166.
- [6] J. M. Bardeen, B. Carter, and S. W. Hawking, “The Four laws of black hole mechanics,” *Commun. Math. Phys.* **31** (1973) 161–170.
- [7] S. W. Hawking, “Particle Creation by Black Holes,” *Commun. Math. Phys.* **43** (1975) 199–220.
- [8] G. ’t Hooft, “Dimensional reduction in quantum gravity,” [arXiv:gr-qc/9310026](#).
- [9] J. M. Maldacena, “The large N limit of superconformal field theories and supergravity,” *Adv. Theor. Math. Phys.* **2** (1998) 231–252, [arXiv:hep-th/9711200](#).
- [10] A. Strominger and C. Vafa, “Microscopic Origin of the Bekenstein-Hawking Entropy,” *Phys. Lett.* **B379** (1996) 99–104, [arXiv:hep-th/9601029](#).
- [11] S. D. Mathur, “The fuzzball proposal for black holes: An elementary review,” *Fortsch. Phys.* **53** (2005) 793–827, [arXiv:hep-th/0502050](#).
- [12] K. Skenderis and M. Taylor, “The fuzzball proposal for black holes,” [arXiv:0804.0552 \[hep-th\]](#).
- [13] J. M. Maldacena, “Black holes in string theory,” [arXiv:hep-th/9607235](#).
- [14] A. W. Peet, “TASI lectures on black holes in string theory,” [arXiv:hep-th/0008241](#).
- [15] T. Mohaupt, “Black holes in supergravity and string theory,” *Class. Quant. Grav.* **17** (2000) 3429–3482, [arXiv:hep-th/0004098](#).

- [16] G. T. Horowitz, “Quantum states of black holes,” [arXiv:gr-qc/9704072](#).
- [17] J. Polchinski, “Dirichlet-Branes and Ramond-Ramond Charges,” *Phys. Rev. Lett.* **75** (1995) 4724–4727, [arXiv:hep-th/9510017](#).
- [18] R. Haag, J. T. Lopuszanski, and M. Sohnius, “All Possible Generators of Supersymmetries of the s Matrix,” *Nucl. Phys.* **B88** (1975) 257.
- [19] L. Susskind, “Some speculations about black hole entropy in string theory,” [arXiv:hep-th/9309145](#).
- [20] G. T. Horowitz and J. Polchinski, “A correspondence principle for black holes and strings,” *Phys. Rev.* **D55** (1997) 6189–6197, [arXiv:hep-th/9612146](#).
- [21] G. T. Horowitz, J. M. Maldacena, and A. Strominger, “Nonextremal Black Hole Microstates and U-duality,” *Phys. Lett.* **B383** (1996) 151–159, [arXiv:hep-th/9603109](#).
- [22] J. M. Maldacena and A. Strominger, “Black hole greybody factors and D-brane spectroscopy,” *Phys. Rev.* **D55** (1997) 861–870, [arXiv:hep-th/9609026](#).
- [23] T. Regge and J. A. Wheeler, “Stability of a Schwarzschild Singularity,” *Phys. Rev.* **108** (1957) 1063–1069.
- [24] J. A. Wheeler, “Geons,” *Phys. Rev.* **97** (1955) 511–536.
- [25] V. Cardoso, O. J. C. Dias, and J. P. S. Lemos, “Gravitational radiation in D-dimensional spacetimes,” *Phys. Rev.* **D67** (2003) 064026, [arXiv:hep-th/0212168](#).
- [26] W. G. Unruh, “Absorption Cross-Section of Small Black Holes,” *Phys. Rev.* **D14** (1976) 3251–3259.
- [27] T. Harmark, J. Natario, and R. Schiappa, “Greybody Factors for d-Dimensional Black Holes,” [arXiv:0708.0017 \[hep-th\]](#).
- [28] S. R. Das and S. D. Mathur, “Comparing decay rates for black holes and D-branes,” *Nucl. Phys.* **B478** (1996) 561–576, [arXiv:hep-th/9606185](#).
- [29] S. R. Das and S. D. Mathur, “The quantum physics of black holes: Results from string theory,” *Ann. Rev. Nucl. Part. Sci.* **50** (2000) 153–206, [arXiv:gr-qc/0105063](#).
- [30] J. M. Maldacena, “Black holes and D-branes,” *Nucl. Phys. Proc. Suppl.* **61A** (1998) 111–123, [arXiv:hep-th/9705078](#).
- [31] S. R. Das and S. D. Mathur, “Excitations of D-strings, Entropy and Duality,” *Phys. Lett.* **B375** (1996) 103–110, [arXiv:hep-th/9601152](#).
- [32] J. M. Maldacena and L. Susskind, “D-branes and Fat Black Holes,” *Nucl. Phys.* **B475** (1996) 679–690, [arXiv:hep-th/9604042](#).

- [33] L. Motl and A. Neitzke, “Asymptotic black hole quasinormal frequencies,” *Adv. Theor. Math. Phys.* **7** (2003) 307–330, [arXiv:hep-th/0301173](#).
- [34] A. Neitzke, “Greybody factors at large imaginary frequencies,” [arXiv:hep-th/0304080](#).
- [35] J. Natario and R. Schiappa, “On the Classification of Asymptotic Quasinormal Frequencies for d-dimensional Black Holes and Quantum Gravity,” *Adv. Theor. Math. Phys.* **8** (2004) 1001–1131, [arXiv:hep-th/0411267](#).
- [36] L. Motl, “An analytical computation of asymptotic Schwarzschild quasinormal frequencies,” *Adv. Theor. Math. Phys.* **6** (2003) 1135–1162, [arXiv:gr-qc/0212096](#).
- [37] F.-W. Shu and Y.-G. Shen, “Perturbative calculation of quasinormal modes of d-dimensional black holes,” *JHEP* **08** (2006) 087, [arXiv:hep-th/0605128](#).
- [38] U. Keshet and A. Neitzke, “Asymptotic Spectroscopy of Rotating Black Holes,” [arXiv:0709.1532 \[hep-th\]](#).
- [39] T. Dray and G. 't Hooft, “The Gravitational Shock Wave of a Massless Particle,” *Nucl. Phys.* **B253** (1985) 173.
- [40] H. Kodama and A. Ishibashi, “Master equations for perturbations of generalized static black holes with charge in higher dimensions,” *Prog. Theor. Phys.* **111** (2004) 29–73, [arXiv:hep-th/0308128](#).